# Role of Six transmembrane Protein of prostate 2 (Stamp2) in Experimental Pulmonary Hypertension

Inaugural Dissertation

zur

Erlangung des Doktorgrades
Dr. nat. med.

der Medizinischen Fakultät
und
der Mathematisch-Naturwissenschaftlichen Fakultät
der Universität zu Köln

vorgelegt von

*Mehreen Batool*

aus *Islamabad*

*Printhaus, Offenbach*

2024

Betreuer/in: Prof. Dr. Stephan Rosenkranz

Referent/in: Prof. Dr. Sabine Eming

Prof. Dr. Günter Schwarz

Datum der mündlichen Prüfung: 04.10.2023

# Table of Contents

## List of Figures

# List of Tables

# List of abbreviations

| | |
|---|---|
| ApoE | Apolipoprotein E |
| ATP | Adenosintriphosphate |
| bp | Base pairs |
| BSA | Bovin serum albumin |
| cDNA | Copy DNA |
| CO | Cardiac output |
| DMSO | Dimethyl sulfoxid |
| ECs | Endothelial cells |
| ELISA | Enzyme linked immunosorbent assay |
| ET-1 | Endothelin 1 |
| FCS | Fetal calf serum |
| HIF-1α | Hypoxia-inducible factor 1α |
| HMVECs | Human microvascular endothelial cells |
| HR | Heart rate |
| kDa | kilo Dalton |
| KO | Knock out |
| LVEDP | Left ventricular end diastolic pressure |
| MCT | Monocrotaline |
| mRNA | Messenger Ribonucleic acid |
| NAB | Neutralizing antibody |
| NO | Nitric oxide |
| P AKT | Protein kinase B |
| PAGE | Polyacryamide gel electrophoresis |
| PAH | Pulmonary arterial hypertension |
| PAP | Pulmonary arterial pressure |

| | |
|---|---|
| PASMCs | Pulmonary arterial smooth muscle cells |
| PAWP | Pulmonary arterial wedge pressure |
| PASMCs | Pulmonary arterial smooth muscle cells |
| PBS | Phosphate buffered saline |
| PDGF-BB | Platelet-derived growth factor BB |
| PH | Pulmonary hypertension |
| PVDF | Polyvinyllidene disulfide |
| PVR | Pulmonary vascular resistance |
| PVD | Pulmonary vascular disease |
| qPCR | Quantitative polymerase chain reaction |
| RasGAP | Ras GTPase activating protein |
| Rpm | Rotations per minute |
| RV | Right ventricle |
| RVP | Right ventricular pressure |
| RVPsys | Right ventricular systolic pressure |
| SBP | Systemic (arterial) blood pressure |
| SBPsys | Systolic arterial blood pressure |
| SDS | Sodium dodecly sulfate |
| SDS-PAGE | Sodium dodecly sulfate polyacryamide gel electrophoresis |
| SMCs | Smooth muscle cells |
| Stamp2 | Six Trans membrane protein of prostate 2 |
| Stamp2-KO | Stamp2 knock out |
| Su/Hx | Sugen5416/Hypoxia |
| TBS | Tris- buffered saline |
| TBS-T | Tris- buffered saline + Tween 20% |
| TEMED | Tetramethylethylenediamine |
| TWEEN | Polyoxyethylene (20) sorbitan monolaurate (Polysorbat 20) |

| | |
|---|---|
| VEGF | Vascular endothelial growth factor |
| WE | Wood-Einheiten |
| WT | Wild type |
| WU | Wood units |

# 1. Introduction

# 1 Introduction

## 1.1 Pulmonary hypertension

### 1.1.1 Definition

Pulmonary hypertension (PH) can be hemodynamically defined as a condition where the mean pulmonary arterial pressure (mPAP) measured through the right heart catheterization (RHC) is ≥25 mmHg in supine position, which does not exceed 20 mmHg in healthy individuals. It is important to note that an elevated value of mPAP alone is not enough to fully characterize the clinical condition, since increased PAP can be associated with various issues such a pulmonary vascular disease (PVD), increased cardiac output (CO) and elevated pulmonary arterial wedge pressure (PAWP) (Gérald Simonneau et al. 2019).

During the 6$^{th}$ World Symposium on PH (Nice, France 2018), it has been considered to modify the hemodynamic definition of PH. Based on data from normal subjects the normal mPAP is 14±3.3 mmHg, and a definition of the upper limit of normal by the mean plus two standard deviations would lead to a value of >20 mmHg, indicating an abnormal mPAP. In the context of pulmonary vascular disease and pulmonary arterial hypertension (PAH), it has been proposed to add pulmonary vascular resistance (PVR) into the definition of pre-capillary PH (Galiè et al. 2019). The updated ESC/ERS guidelines for the management of pulmonary hypertension have now modified the hemodynamic definitions of PH, considering an mPAP >20 mmHg to define PH, and a PVR >2 Wood units (WU) to define pre-capillary PH (Humbert et al. 2022).

#### 1.1.1.1 Pre-capillary and Post-capillary PH

PH can be either pre-capillary or post-capillary. In pre-capillary PH, increased pulmonary vascular resistance (PVR) is observed owing to pulmonary vascular remodeling. In post-capillary PH an elevated pulmonary venous pressure is observed along with left heart diseases. The two forms of PH can be differentiated by measuring PAWP or the left ventricular end-diastolic pressure (LVEDP). If the measured values are elevated >15 mmHg, it is post-capillary PH or a combined post- and pre-capillary PH condition. Thus, accurate measurement of PAWP and LVEDP is essential to avoid misdiagnosis and misclassification (Naeije and Chin 2019). An elevated PVR >2 WU, an mPAP ≥20mmHg and a normal PAWP ≤15mmHg define pre-capillary PH (Humbert et al. 2022). Thus, the cut-off of the PVR value plays an important role in distinguishing the type of PH. The formula to calculate PVR (PVR=[mPAP-PAWP]/CO) underscores that accurate PAWP measurement is essential to calculate the correct PVR (Gérald Simonneau et al. 2019).

The expanded definition of PH has made it even more crucial to determine accurate hemodynamic evaluation since it is the most critical component that helps assign a proper diagnosis. PAWP is the sole parameter which distinguishes between pre-capillary PH and PH associated with left heart disease. It also helps determine PVR, which can also determine combined post- and pre-capillary PH from isolated post-capillary PH (Viray et al. 2020, Humbert et al. 2022). Right heart catheterization (RHC) is considered the gold standard for PH diagnosis. RHC is used to invasively measure cardiopulmonary hemodynamics including PAWP. Optimum standardization of RHC is crucial owing to its pivotal role in PH identification (Rosenkranz and Preston 2015; Humbert et al. 2022).

### 1.1.2 **PH Classification**

At first, PH was classified into two main sub types known as “primary pulmonary hypertension” and “secondary pulmonary hypertension”. This classification was based on the knowledge of causes and risk factors. If the cause of disease was not known and PH occurred without a detectable condition, it was termed as “Primary pulmonary hypertension”; in case a cause for PH was identified in another organ system, it was termed as “secondary pulmonary hypertension” (Hypertension, Hatano, and Strasser 1975) (Bhatnagar et al. 2018).

An expanded categorization of PH was then created on the basis of similar clinical features and pathogenesis in 1998 at the second World Symposium on PH in Evian, France. This categorization ensured that patients could be classified into homogenous groups with regards to underlying pathophysiology, symptoms and treatment approach (Fishman 2001).

Pulmonary arterial hypertension (PAH) encompasses a subpopulation of PH defined by the presence of pre-capillary PH (Hoeper et al. 2013). PAH is a rare condition affecting the small and medium sized pulmonary arteries resulting in elevated PAP and PVR (Rabinovitch et al. 2014). In patients suffering from PAH the blood pressure in small arteries present in the lungs becomes abnormally high, thus causing hindrance in the passage of blood from heart to the lungs. The thickening of vessel walls and narrowing of vascular lumina causes elevated pressure, and thus the right heart has to work harder to pump blood into the lung to ensure oxygen enrichment and maintenance of the systemic circulation. This chronic pressure overload of right heart can lead to weakening and enlargement of heart muscle, and ultimately right heart failure (Zeller et al. 2012). If left untreated, this condition is associated with high mortality (Rubin 1997), (Gerald Simonneau et al. 2014), (M Humbert et al. 2004). In addition to PAH, other forms of pulmonary hypertension (PH) can

occur secondary to other disorders such as left heart failure or lung disease, which also has substantial impact on patient's life expectancy (Rosenkranz 2015).

During the 6th World Symposium on PH (Nice, France 2018) it was decided that the main scheme of classification of PH which was established and updated during the 4th and 5th World Symposia on PH and subdivides PH into five main groups, will be maintained. Modifications were made by updating which factors are put under which particular group. These are tabulated below as adapted from (Gérald Simonneau et al. 2019).

**Table 1.1: 6th World Symposium on pulmonary hypertension: Clinical classification of PH**

| PH disease groups | Classification of PH groups |
|---|---|
| 1. Pulmonary arterial hypertension (PAH) | 1.1 Idiopathic<br>1.2 Heritable<br>1.3 Caused by drugs and toxins<br>1.4 Associated with:<br>1.4.1 connective tissue disease<br>1.4.2 HIV infection<br>1.4.3 Portal PH<br>1.4.4 Congenital Heart Disease<br>1.4.5 Schistosomiasis<br>1.5 PAH due to long term responders to Calcium channel blockers<br>1.6 PAH with apparent features of venous/capillaries involvement<br>1.7 Persistent pulmonary hypertension of the newborn (PPHN) |
| 2. PH due to left heart disease | 2.1 Systolic dysfunction<br>2.2 Diastolic dysfunction<br>2.3 Valvular disease<br>2.4 Congenital cardiovascular conditions due to post-capillary PH |
| 3. PH due to lung diseases and/or hypoxia | 3.1 Chronic obstructive pulmonary disease<br>3.2 Restrictive lung disease<br>3.3 Other pulmonary diseases<br>3.4 Developmental lung abnormalities<br>3.5 Hypoxia without lung disease |
| 4. PH due to pulmonary artery obstruction | 4.1 Chronic thromboembolic PH<br>4.2 due to other pulmonary artery obstructions |
| 5. PH with unclear and/or multifactor causes | 5.1 Hematological disorders<br>5.2 Complex congenital heart disease<br>5.3 Systemic and metabolic disorders<br>5.4 Others: tumoral obstruction,<br>fibrosing mediastinitis, chronic renal failure |

### 1.1.3 **Epidemiology**

PAH affects 1-2 people per million per year in USA and Europe, thus it is considered to be one of the orphan diseases (McGoon et al. 2013). According to the earliest available PAH registries conducted at national level in USA, 187 patients were identified and followed for 5 years. This study helped characterize the disease and showed a median survival of 2.8 years (D'Alonzo et al. 1991). In the early era, PAH was primarily diagnosed in relatively young adults (particularly women), whereas according to more recent registry data, elderly patients aged between 50±14 – 65±15 are the most frequent patient group diagnosed with PAH (Rosenkranz 2015). A gender difference has also been observed in clinical studies focused on PAH patients where women are more likely to suffer from the disease (Örem 2017). In very early studies and registries, a female to male ratio of 4:1, and more recently of 2:1, has been documented (Örem 2017) (Wagenvoort 1970).

Data acquired from patients with idiopathic (IPAH), hereditary (HPAH) or anorexigen-induced PAH have provided valuable insight into the survival rates. In one study, a total of 354 patients (56 incident and 298 prevalent) were followed for three years and in these cases a better survival rate was observed as compared to earlier reports (Humbert et al. 2010). Data from the REVEAL registry showed an increased survival time of up to five years in almost 60% of IPAH patients (Murali and Benza 2012).

A risk stratification strategy (a process which comprises of assigning a particular risk status to a patient and providing effective care according to this status to ensure better health improvement and cure) was proposed by the 2015 European pulmonary hypertension guidelines (Galiè et al. 2016). The risk groups were termed as low, intermediate or high risk, owing to the estimated annual mortality rate. This risk assessment strategy was subsequently validated in

large registries. Data from COMPERA (Comparative, Prospective Registry of Newly Initiated Therapies for Pulmonary Hypertension), a European-based PH registry, revealed significantly varying mortality rates among the three risk groups, with low risk group having the lowest mortality rate of 2.8%, and the high risk group the highest mortality rate of 21.2% (Hoeper et al. 2017). Another registry study revealed that survival rates remained similar for patients who stayed or improved to the low risk group and was worsened for patients who stayed or had disease propagated to the intermediate or high risk group. A follow-up study also showed reduced mortality among the low risk group patients as compared to the other two risk groups (Kylhammar et al. 2018).

Together, these data show that overall there has been an improvement in techniques and prognostic measures, which help predict survival and improve patient management. Despite these improvements, an advanced understanding of the disease and development of further therapeutic approaches is warranted as mortality remains unacceptably high (Pullamsetti et al. 2014). According to the ASPIRE registry where the disease progression and outcome were studied across the spectrum of the five PH groups, the three year survival rate was observed to be lower for PAH as compared to group 2 and group 4 PH (see table 1.1), further emphasising the need for better diagnosis and treatment of PAH (Hurdman et al. 2012). The convincing data from multiple registry studies implying the risk stratification strategy shows the importance of a comprehensive risk assessment system which would aim at reaching the low risk profile for PH patients (Kylhammar et al. 2018). Nevertheless, the risk stratification strategy still awaits a thorough authorization as a prevalent prognosis tool (Hoeper et al. 2017).

### 1.1.4 **Pathophysiology of PH**

Since its inceptive interpretation, comprehending PH has been met with challenges owing to its multiple and varying causes, along with a poor prognosis. In the last two decades, the understanding of the molecular and genetic basis of PH has substantially improved, describing how cells in the pulmonary vasculature along with multiple secreted factors contribute to onset and development of the disease (de Jesus Perez 2016). PAH is nowadays recognized as a multi-factorial disease, where the pathobiology involves a genetic predisposition combined with external trigger factors (Galiè et al. 2019). The vascular changes are driven by abnormal vasoconstriction, and by remodeling of the vascular wall (thickening of vessel wall and narrowing of vascular lumina), causing elevations of pressure and resistance, and limiting blood flow. Figure 1.1 depicts this, graphically showing narrowed vessel lumen, a leading cause of elevated pressure.

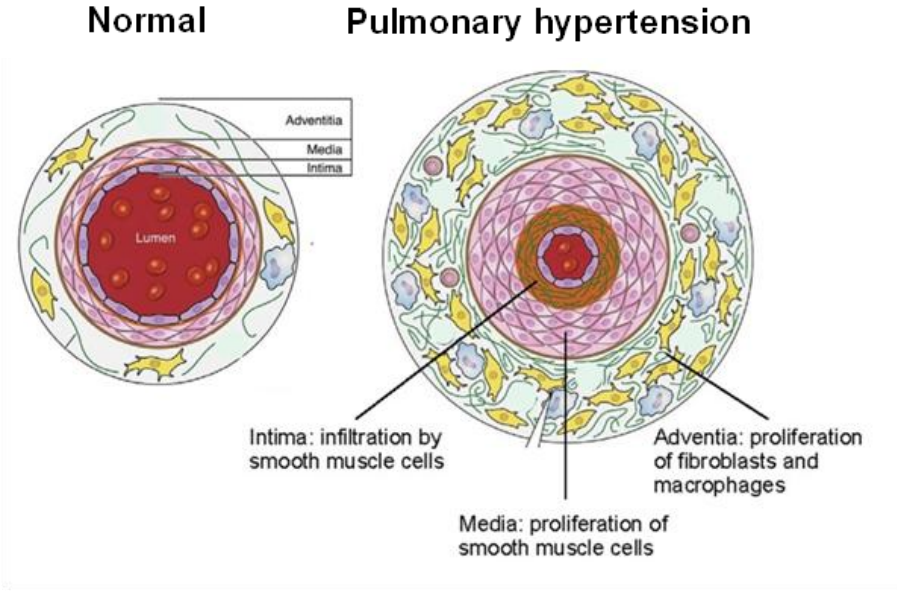


**Figure 1.1: Schematic diagram showing the cross section of normal versus pulmonary hypertension affected arteriole** *(Gordeuk, Castro, and Machado 2016)*

Recent insight into the inflammatory profile of PH has shed light on the function of a number of immune and inflammatory cells in the development of the disease (Huertas et al. 2014). Increased expression of various chemokines and immunomarkers – leading to an overall inflammatory state – contribute to worsening of disease, as they promote proliferation of the cells forming the vascular wall (Rabinovitch et al. 2014); (Huertas et al. 2014). PAH patients show elevated plasma concentrations of inflammatory cytokines including IL-1β, MCP-1, IL-6 (Kherbeck et al. 2013) and TNF-α (Schlosser et al. 2017). Several cytokines affect and control cellular actions like proliferation and migration thus taking active part in disease progression. Among these cytokines, IL-6 acts as a causative agent in PH development in mouse model (Golembeski et al. 2005). Overexpression of IL-6 leads to spontaneous PAH development in mice, whereas absence of IL-6 was found to be protective against disease development (Steiner et al. 2009). Pulmonary smooth muscle cells (SMCs) produce IL-6 when exposed to chronic hypoxia and IL-6 also induces proliferation and migration of these cells thus contributing to advancing PH (Maston et al. 2017). Moreover, patients with PH showed higher expression of lung IL-6 and other cytokines, along with elevated serum levels of cytokines (Steiner et al. 2009). Elevated circulating levels of SDF-1 (stromal derived factor-1) along with MCP-1 and granulocyte-monocyte colony stimulating factor (GM-CSF) have also been observed in IPAH patients (Rabinovitch 2012). Human airway SMC proliferation which is causative of chronic lung diseases has been attributed to TNF-α and cross-talk with ET-1 (Knobloch et al. 2016), showing that elevated inflammation causes cellular actions which are known to cause PH progression. Along with SMCs, endothelial cell (EC) proliferation is also initiated by a number of factors including stress signalling, inflammation, and hypoxic conditions. Together, these factors can lead to accumulation and recruitment of various circulating immune cells into the vasculature,

thus perpetuating disease progression (Montani et al. 2013) Rabinovitch et al. 2014).

In this context, macrophages permeating the pulmonary arterioles appear to play a key role. In experimental PH, a rise in perivascular macrophage cell count is required to advance disease development and progression, and perivascular macrophages are found in lung tissue of IPAH patients (Rabinovitch 2012). The role of macrophages in the immune system to fight off pathogens and their role in regeneration procedures makes these a considerable candidate while looking into vascular inflammation and cardiac dysfunction in PH (Frid et al. 2006). There is evidence pointing towards a vital role of monocytes/CD68+ macrophage recruitment in mouse lungs of hypoxia induced PH, and that macrophages promote SMC proliferation and vascular remodelling (Vergadi et al. 2011). Another inflammatory marker, ET-1 (Endothelin-1), is known to contribute to monocytes stimulation as well, leading to production of cytokines such as IL-1β, IL-6, and TNF-α (McMillen and Sumpio 1995). ET-1 is involved in endothelial dysfunction and vascular remodelling, and elevated ET-1 plasma levels have been observed in human and experimental PH (Schiffrin 1995)(Amiri et al. 2004)

Taken together, dysregulated immunity appears to play a pivotal role in the pathobiology of PAH, but better understanding of the inflammatory profiles and their role in progression of PAH is warranted (Rabinovitch et al. 2014).

## 1.2 Six transmembrane protein of prostate 2 (Stamp2)

### 1.2.1 Structure and function

Stamp2 was cloned after analysis of differentially expressed proteins in early prostate cancer (Korkmaz et al. 2000). It carries a high sequence similarity to Stamp1 (Kemal S Korkmaz et al. 2002). Gene sequencing revealed it consists of five exons and four introns similar to Stamp1. Considering the sequence similarity along with intracellular distribution of Stamp1, it was named Stamp2. The gene size of Stamp2 is almost 26 Kb which is mostly covered by a large introns 1 which is 22516 bp long, while the mRNA transcript amounts to 4Kb. Stamp2 has 495 amino acids and the six transmembrane domains of Stamp2 lie close to the C-terminus, and three conserved motifs are found in the N-terminus (Korkmaz et al. 2005). The structure is shown in Figure 1.2. The first conserved motif is a dinucleotide binding domain, the second is an NADP oxidoreductase motif which is F420 co-enzyme dependent similar to the F420H2:NADP+ oxidoreductase known to be present in archeabacteria (Warkentin et al. 2001) and the third motif resembles pyrroline 5-carboxylate reductase, an enzyme which is known to be involved in amino acid transport and metabolism (Phang 1985). Stamp2 is also referred to as Steap4 (Ohgami et al. 2006).

### 1.2.2 Tissue-specific expression and cellular localization of Stamp2

The tissue-specific expression of Stamp2 has been assessed by northern analysis in various human tissues and its highest expression was found in placenta, lung, heart and prostate with relatively low expression in liver, skeletal muscle, pancreas, testis and small intestine. Almost no expression was detected in brain, kidney, spleen, and colon (Korkmaz et al. 2005). Quantitative real-time PCR evaluation of Stamp2 expression in various human tissues showed

highest expression in bone marrow followed by placenta and fetal liver tissue (Ohgami et al. 2006). In situ expression analysis was used to assess murine Stamp2 expression which showed it is ubiquitously expressed at lower levels, and highest expression was found in adipose tissue (Ohgami et al. 2006).

Evaluation of the intracellular localization of Stamp2 revealed a strong distribution in plasma membrane, vesiculotubular structures and the Golgi complex. The intracellular localization near the nucleus and in the peripheral membrane suggests a role in molecular transportation and trafficking, and involvement in secretory pathways and endocytosis (Korkmaz et al. 2005).

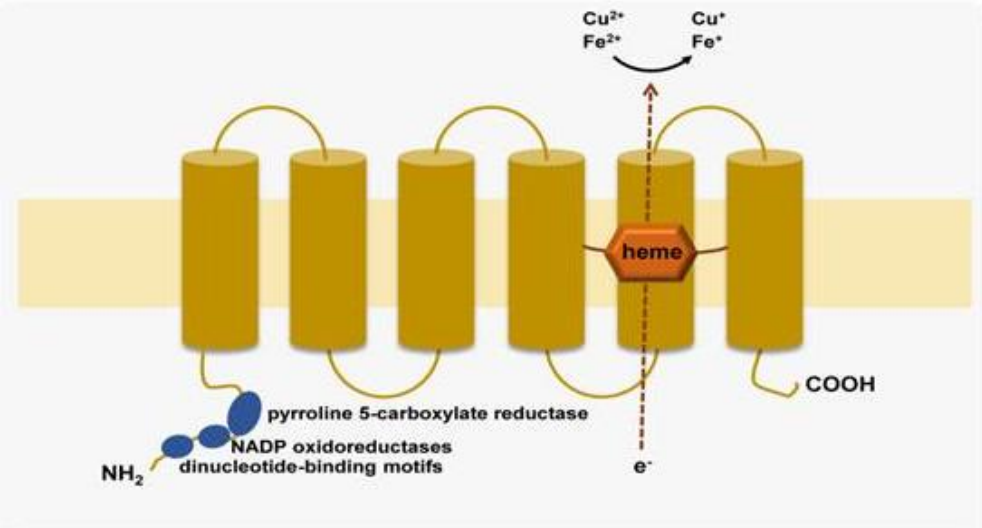


**Figure 1.2: Schematic representation of Stamp2 protein structure**

*Stamp2 is a six transmembrane protein and the N-terminal contains three conserved motifs* (Yoo, Cheong, and Kim 2014).

## 1.3 Stamp2 and related pathophysiolgy

### 1.3.1 Role of Stamp2 in metabolic diseases

Stamp2 has been associated with a regulatory role in insulin sensitivity, obesity, prostate cancer development, inflammation, atherosclerosis and metabolic syndrome (ten Freyhaus et al. 2012), (Hye Y Kim et al. 2015), (Moreno-Navarrete et al. 2011), (Nanfang et al. 2010). Nutrient overload and obesity leads to various metabolic disorders including type2 diabetes, cardiovascular diseases and insulin resistance. Obesity is a known pro-inflammatory disease which leads to production of excessive cytokines, adipokines and expression of the macrophage specific cell surface antigen CD68 in adipose tissue (Wellen et al. 2007), (Catalan et al. 2013).

Visceral white adipose tissue (VWAT) is regarded as the most apposite site for metabolic pathogenesis and thus, is a major player in development of insulin resistance. The presence of an inflammatory profile along with angiogenesis aggravates the development of insulin resistance, which is in turn related to higher risk of cardiovascular diseases and general obesity (Wellen et al. 2007) (Preis et al. 2010). Stamp2 expression was enhanced in fed lean mice as compared to fasted mice, whereas in obese mice this nutrition-based Stamp2 regulation was completely lost. Thus, both inflammatory and nutritional signals impact Stamp2 expression (Wellen et al. 2007).

Lack of differentiation capacity in adipocytes leads to enhanced inflammation and adipose tissue dysfunction along with fat deposition. During adipocyte differentiation, Stamp2 is highly expressed, which further increases dramatically as differentiation proceeds (Patel and Abate 2013). Stamp2 knockdown in 3T3-L1 cells lead to reduced adipogenic differentiation along with reduced

expression of adipogenic markers whereas lack of Stamp2 and impaired adipogenic differentiation lead to increased adipogenic inflammation, suggesting a significant role of Stamp2 in adipogenesis and inflammatory control (Jorgen Sikkeland and Saatcioglu 2013). In humans, Stamp2 expression significantly decreases in visceral adipose tissue during preadipocyte differentiation of obese subjects suffering from type 2 diabetes as compared to lean subjects where a significant increase in Stamp2 expression was observed during differentiation (Moreno-Navarrete et al. 2011).

Marked reduction in hepatic Stamp2 expression has been reported in high fat diet (HFD)-fed mice along with obesity and dyslipidemia, and knockdown of Stamp2 led to heightened hepatic lipid accumulation. Highly reduced hepatic Stamp2 expression was also observed in patients suffering from non-alcoholic fatty liver disease (NAFLD) (Kim et al. 2012). Furthermore, Stamp2 deficiency in mice led to augmented inflammation characterized by higher expression of IL-6, MCP-1 and TNF-α in the adipose tissue along with the development of metabolic syndrome marked by insulin resistance, glucose intolerance, mild hyperglycaemia and fatty liver disease (Wellen et al. 2007). Vice versa, overexpression of Stamp2 in a diabetic mouse model was shown to numerically decrease a number of metabolic indices including body weight, and the levels of insulin, cholesterol, and fasting serum glucose (Wang et al. 2014).

### 1.3.2 **Role of Stamp2 in arthritis**

Stamp2 levels were also highly elevated in joints of mice suffering from arthritis and the expression correlated with the severity of joint swelling (Inoue et al. 2009). Upregulation of Stamp2 was found in 3T3-L1 cells when induced with IL-1β (Kralisch et al. 2009) pointing towards a protective role of Stamp2 against excessive inflammation.

Thus, regulation of Stamp2 in various inflammatory diseases suggests a crucial role in regulating inflammation.

### 1.3.3 **Role of Stamp2 in cardiovascular diseases**

Stamp2 is significantly downregulated in patients suffering from metabolic syndrome as compared to healthy subjects (Wang et al. 2010, Nanfang et al. 2010). It is well established that metabolic diseases such as abdominal obesity, high blood pressure and glucose intolerance (i.e. the metabolic syndrome) affect cardiovascular function and increase the risk of myocardial infarction, heart failure, and stroke (Chinali et al. 2004). Low levels of Stamp2 associated with the metabolic syndrome along with respective augmented inflammation can be causative of impaired heart function since Stamp2 deficiency leads to elevated inflammation which is known to augment cardiovascular risk. CD14+ monocytes were used to study the low expression of Stamp2 in metabolic disease patients as they have the tendency to act like macrophages in atherosclerotic plaque. Monocytes imitating macrophages with downregulated expression of Stamp2 might also cause overt inflammation and worsening of disease (Wang et al. 2010).

In addition to these inflammation-driven diseases, Stamp2 function has been studied in systemic arterial vascular disease, i.e. atherosclerosis. Stamp2 was found in atherosclerotic plaques in mice and humans, and absence of Stamp2 led to accelerated atherogenesis. Stamp2, highly expressed in macrophages, was co-expressed with macrophage markers in atherosclerotic plaques supporting its role in disease development. Moreover, Stamp2 deficiency in atherosclerosis-prone ApoE$^{-/-}$ mice led to larger atherosclerotic lesions and augmented inflammation within the lesions. In line, higher mRNA expression of IL-6, MCP-1, TNF-α and I-1β was observed in primary macrophages from Stamp2-deficient

ApoE$^{-/-}$ mice as compared to WT control leading to the conclusion that Stamp2 absence augments the degree of inflammatory atherosclerosis (ten Freyhaus et al. 2012).

Endogenous expression of Stamp2 is also significantly reduced in atherosclerotic aorta of diabetic mice. Overexpression of Stamp2 led to reduced macrophage apoptosis in brachiocephalic artery of diabetic mice, antagonizing atherogenesis, and stabilizing atherosclerotic plaques thus preventing spontaneous plaque rupture (Wang et al. 2014)

## 1.4 **Stamp2 and inflammation regulation**

Several studies have investigated how Stamp2 may regulate the inflammatory milieu. Stamp2 overexpression was shown to reduce insulin resistance, stabilize atherosclerotic plaques, decrease macrophage infiltration in adipose tissues and lower the expression of pro-inflammatory cytokines by regulating p-Akt protein expression and affecting macrophage polarization (Wang et al. 2014, Han et al. 2013). Other studies showed that Stamp2 overexpression attenuated atherosclerosis in diabetic mice (Chuang et al. 2015), and prevented angiogenesis in adipose tissue along with improving metabolic indices and insulin resistance in diabetic mice (Wang et al. 2017).

The consideration of the multiple inflammatory actions regulated by the presence or absence of Stamp2 and how disease progression is altered by Stamp2 expression leads to defining Stamp2 as an anti-inflammatory protein and supports the hypothesis of a protective role against the development of numerous inflammatory conditions (Yoo et al. 2014, Waki and Tontonoz 2007).

Although many studies have been conducted regarding the role of Stamp2 in metabolic diseases, fewer such studies have focussed on cardiovascular diseases, and no data are available on its role in

pulmonary vascular disease. As PH is nowadays recognized as an inflammation-related proliferative disease of the small pulmonary resistance vessels, more insight and research on a potential role of Stamp2 in the pathobiology of PH is warranted.

## 1.5 Aims of study

The pre-established role of Stamp2 in a number of inflammatory diseases provides a strong rationale to pursue its role, function and involvement in other cardiovascular diseases such as PAH. The prior knowledge regarding the development and progression of PAH shows the disease is accompanied and preceded by inflammation (Kherbeck et al. 2013), and the role of Stamp2 in inflammation regulation has been established, particularly counter-balancing elevated inflammation (Wellen et al. 2007).

In the light of afore mentioned scientific evidence and pre-established role of Stamp2 in a number of inflammatory diseases, the main aim of our study was to investigate the potential role of Stamp2 in the development and progression of pulmonary hypertension.

We hypothesized that lack of Stamp2 in the mouse model of hypoxia-induced PH would augment the degree of pulmonary vascular remodeling and PH. The specific aims pursued during the course of this research work are as follows:

1. To Study the regulation of Stamp2 in experimental and human PH
2. To study the regulation of inflammatory cytokines in the absence of Stamp2
3. To evaluate the inter-cellular crosstalk between cell types related to vascular remodeling

4. To identify the molecular candidate/s regulating the potential cellular and inflammatory alterations in the pulmonary vasculature post Stamp2 deficiency induced PH

# 2. Laboratory Materials

# 2 Laboratory Materials

## 2.1 Animal models for studying PH

### 2.1.1 Stamp2 knock out mouse model

Stamp2 knock-out (KO) mice were originally created at Deltagen Inc. by gene targeting into the embryonic stem cells (ES cells); these ES cells were derived from 129/OlaHsd mice. The ES cells were then injected into C57BL/6 blastocysts. Two heterozygous breeding pairs were acquired by Prof. Gökhan S. Hotamisligil (Sabri Ülker Center, Department of Molecular Metabolism and Broad Institute of Harvard-MIT and Harvard T.H. Chan School of Public Health, Boston, US) and were used to generate the homozygous Stamp2-KO mice after successive breeding. For our project Prof. Gökhan S. Hotamisligil kindly provided us with a Stamp2-KO breeding pair which was then further bred and maintained at the animal facility of the Center for Molecular Medicine Cologne (CMMC), Cologne, Germany. Male Stamp2-KO mice aged 8-14 weeks were used for experiments.

### 2.1.2 Wild type (WT) mouse model

C57BL/6 mice were used as wild type controls. This genotype acted as control against the genetically modified animal model of Stamp2-KO. Male C57BL/6 mice aged 8-14 weeks were used for experiments.

### 2.1.3 Sugen/hypoxia (SuHx) rat model

8 weeks-old male Sprague Dawley rats were injected with SU5416 (20 mg/kg in DMSO) subcutaneously and were exposed to hypoxia (10% oxygen) for 21 days and then kept under normoxia for 14 days. SU5416 is a vascular endothelial growth factor antagonist which along with hypoxia leads to development of PH.

The handling of all animal models was performed in accordance with the German laws for Animal Protection and was strictly according to the guidelines provided by the Directive 2010/63/EU of the European Parliament. These guidelines were ratified by the local animal care and handling committee and district government of Cologne.

## 2.2 Human disease tissue

The lung tissue biopsies were obtained from IPAH patients undergoing lung transplantation and from non-transplanted donor lungs. Human lung tissues were used to investigate human PAH and were used for lung sections preparation, protein extraction and mRNA extraction. The human lung tissues were obtained from the Excellence Cluster Cardio-Pulmonary system (ECCPS), Gießen, Germany. The human tissue donation and experimentation was carried out according to the national law and in accordance with the principles of Helsinki. Consent and permission was acquired prior to obtaining the tissue samples.

## 2.3 Cells, tissues and respective growth media

In order to perform the in vitro studies mouse cells and tissues were obtained from Stamp2-KO and WT mice. All the cells and tissues from the animal model were used in accordance to the German Laws for Animal Protection.

The human cells were bought from Lonza Group Ltd. Following is a list of the cells, tissues and cell culture mediums used.

**Table 2.1: List of cells, tissues and growth media**

| S/N | Name | Origin |
|---|---|---|
| 1. | RPMI 1640 (medium for macrophages) | thermo Fisher scientific |
| 2. | DMEM High glucose (4,5g/l) with L-Glutamine (medium for Endothelial cells) | PAA Laboratories GmbH, Pasching, Austria |
| 3. | Smooth Muscle cell Basal Medium (SmBM) | Lonza Group Ltd., Basel, Switzerland |
| 4. | Smooth Muscle cell Growth Medium (SmGM) | Lonza Group Ltd., Basel, Switzerland |
| 5. | mPASMCs (murine pulmonary arterial smooth muscle cells) | Isolated from murine pulmonary arteries |
| 6. | Peritoneal murine macrophages | Extracted from Stamp2 KO and WT mice |
| 7. | Mouse lung sections from Stamp2-KO and WT mice | The lung tissues were harvested from mice subjected to hypoxia and normoxia conditions |
| 8. | SuHx rat lung sections | The lung tissues were harvested from the rats subjected to sugen hypoxia and normoxia conditions |
| 9. | Human Lung tissue samples (PAH and healthy donors) | Prof. Schermuly, Excellence Cluster Cardio-Pulmonary System (ECCPS), Gießen, Germany |
| 10 | Human PASMCs | Lonza Group Ltd., Basel, Switzerland |
| 11 | HMVECs (Human microvascular endothelial cells) | Lonza Group Ltd., Basel, Switzerland |

## 2.4 Laboratory Equipment and instruments

Following is a list of various instruments and equipment used for conducting experiments.

**Table 2.2: List of laboratory equipments**

| S/N | Name | Description | Origin |
|---|---|---|---|
| 1. | Blotting chamber | TransBlot® SemiDry Transfer Cell | BioRad Laboratries, USA |
| 2. | Centrifuge | Centrifuge 5810, 5415D, Eppendorf | Hamburg, Germany |
| 3. | Thermomixer | Eppendorf Comfort 1,5 ml | Hamburg, Germany |
| 4. | Eppendorf Pipettes | 0,5-10µl, 10-100µl, 100-1000µl | Hamburg, Germany |
| 5. | Curix 60 | AGFA-Gevaert N.V | Mortsel, Belgium |
| 6. | PowerLab 4/35 | Data acquisition hardware | ADinstruments, Australia |
| 7. | ELISA-Reader | PowerWave340 Bio-TEK Instruments | Winooski, USA |
| 8. | Fastblot B 44 | Biometra GmbH | Göttingen, Germany |
| 9. | Minigel Twin Gel | Electrophoresis Apparatus | Göttingen, Germany |
| 10. | iCycler Thermocycler | BioRad Laboratories | USA |
| 11. | Incubator | CO2 Incubator MCO-20AIC | Sanyo, Japan |
| 12. | Isoflurane Evaporator | Vapor 19.3 Dräger Medizintechnik | Lübeck, Germany |
| 13. | Laminar flow | Biowizard Golden Line GL 103 Class II | Vilppula, Finland |
| 14. | Light Cycler 480 II | Roche Applied Science | Mannheim, Germany |

| | | | |
|---|---|---|---|
| 15. | Magnetic stir bar | Digital Hotplate Stirrer HTS 2013 | Brigachtal, Germany |
| 16. | Hemostats | Fine Science Tools | Heidelberg, Germany |
| 17. | Microscope | Mikroskop CKX41 Olympus | Japan |
| 18. | Mice heating plate | Föhr Medical Instruments GmbH | Seeheim, Germany |
| 19. | Millar Pressure Catheter | 1,0 F SPR-1000 Föhr Medical Inst. | Seeheim, Germany |
| 20. | Millar Pressure Catheter | 2,0 F SPR-320NR Föhr Medical Inst. | Seeheim, Germany |
| 21. | Millar Pressure Catheter | Amplifier Patient Isolation PCU-2000 | Seeheim, Germany |
| 22. | Temperature control | Module for heating plate | Seeheim, Germany |
| 23. | Spectrophotometer | NanoDrop TM ND 1000 | ThermoFisher, USA |
| 24. | PCR system | Step one plus Real-time | California, USA |
| 25. | Tissue-homogeniser | PotterS Biotech International | USA |
| 26. | Tissue Processor | ASP300S Leica Microsystems | Wetzlar, Germany |
| 27. | Vortex mixer | VTX 3000 L LMS Consult | Tokyo, Japan |
| 28. | Water bath | Memmert GmbH & Co. KG | Schwabach, Germany |
| 29. | Transfer device | Western blot Trans-Blot SD Semi Dry | Germany |
| 30. | Accuracy weighing scale | R200D Sartorius AG | Göttingen, Germany |
| 31. | BioDoc | Analyze Darkho Analytik Jena AG | Jena, Germany |

## 2.5 Laboratory Chemicals and solutions

A number of chemicals and reagents were used to perform the various experiments. These included general chemicals, enzymes, antibodies and buffers along with chemical kits. These are tabulated below in separate tables.

### 2.5.1 General chemicals

**Table 2.1: List of laboratory chemicals**

| S/N | Name | Origin Description |
|---|---|---|
| 1. | Acetic acid | Merck-Schuchardt, Hohenbrunn, Germany |
| 2. | Sodium fluoride | Merck KGaA, Darmstadt, Germany |
| 3. | Hydrogen Peroxide | Merck, Darmstadt, Germany |
| 4. | Magnesium chloride | Merck, Darmstadt, Germany |
| 5. | Bradford-Reagent | Bio-Rad Laboratories GmbH |
| 6. | Oxgen ($O_2$) | Linde AG, Munich, Germany |
| 7. | Nitrogen ($N_2$) | Linde AG, Munich, Germany |
| 8. | Methyl green (H-3402) Vector | Linaris Biologische Produkte, Wertheim, Germany |
| 9. | Acrylamide | Carl Roth GmbH & Co. Karlsruhe, Germany |
| 10. | Hydrochloric Acid (HCl) | Merck, Darmstadt, Germany |
| 11. | Rotiphorese® Gel 30 (37.5/1) (Acrylamide/Bis-acrylamid 30%) | Carl Roth GmbH + Co. KG, Karlsruhe, Germany |

| | | |
|---|---|---|
| 12. | Ethanol | Carl Roth GmbH + Co. KG, Karlsruhe, Germany |
| 13. | Isopropanol | Carl Roth GmbH + Co. KG, Karlsruhe, Germany |
| 14. | Methanol 99% | Carl Roth GmbH + Co. KG, Karlsruhe, Germany |
| 15. | Xylole | Carl Roth GmbH + Co. KG, Karlsruhe, Germany |
| 16. | 6-aminohexanoic acid | Sigma-Aldrich Chemie GmbH, Steinheim, Germany |
| 17. | Aprotinine | Sigma-Aldrich Chemie GmbH, Steinheim, Germany |
| 18. | β-mercaptoethanol | Sigma-Aldrich Chemie GmbH, Steinheim, Germany |
| 19. | BSA > 96 % (Bovine serum albumin) | Sigma-Aldrich Chemie GmbH, Steinheim, Germany |
| 20. | Chloroform | Sigma-Aldrich Chemie GmbH, Steinheim, Germany |
| 21. | DMSO (Dimethyl sulfoxid) | Sigma-Aldrich Chemie GmbH, Steinheim, Germany |
| 22. | Ethidiumbromide | Sigma-Aldrich Chemie GmbH, Steinheim, Germany |
| 23. | HEPES | Sigma-Aldrich Chemie GmbH, Steinheim, Germany |
| 24. | Insulin solution, human | Sigma-Aldrich Chemie GmbH, Steinheim, Germany |
| 25. | (Phenylmethylsulphonylfluoride) | Sigma-Aldrich Chemie GmbH, Steinheim, Germany |
| 26. | Collagenase | Sigma-Aldrich Chemie GmbH, Steinheim, Germany |
| 27. | Penicillin/streptomycin,Invitrogen | Sigma-Aldrich Chemie GmbH, Steinheim, Germany |
| 28. | Potassium Chloride | Sigma-Aldrich Chemie GmbH, Steinheim, Germany |

| | | |
|---|---|---|
| 29. | Sodium Orthovanadate ($Na_3VO_4$) | Sigma-Aldrich Chemie GmbH, Steinheim, Germany |
| 30. | TWEEN 20® | Fermentas GmbH, St. Leon-Rot, Germany |
| 31. | Tripsin Inhibitor | Santa Cruz Biotechnologies, Dallas, USA |
| 32. | Weigert`s Iron Hematoxylin A &B | Life Technologies GmbH, Darmstadt, Germany |
| 33. | TEMED (N,N,N',N'-Tetra-methylethylenediamine) | BiozymScientific GmbH, Oldendorf, Germany |
| 34. | Weigert`s Iron Hematoxylin A & B | AppliChem GmbH, Darmstadt, Germany |
| 35. | Sodium orthovanadate ($Na_3VO_4$) | AppliChem GmbH, Darmstadt, Germany |
| 36. | dNTPs (Desoxy-Ribonucleotid-Triphosphate) | AppliChem GmbH, Darmstadt, Germany |
| 37. | Formalin 4% in PBS | AppliChem GmbH, Darmstadt, Germany |
| 38. | Fetal calf serum Gibco | AppliChem GmbH, Darmstadt, Germany |
| 39. | Agarose Biozym LE | AppliChem GmbH, Darmstadt, Germany |
| 40. | APS (Ammonium-persulfate) | AppliChem GmbH, Darmstadt, Germany |
| 41. | Bromophenol blue | AppliChem GmbH, Darmstadt, Germany |
| 42. | DTT (Dithiothreitol) | AppliChem GmbH, Darmstadt, Germany |
| 43. | EDTA (Ethylenediaminetetraacetic acid) | AppliChem GmbH, Darmstadt, Germany |
| 44. | Sodium chloride | AppliChem GmbH, Darmstadt, Germany |
| 45. | Glycine | AppliChem GmbH, Darmstadt, Germany |

| | | |
|---|---|---|
| 46. | Glycerol | AppliChem GmbH, Darmstadt, Germany |
| 47. | Tris | AppliChem GmbH, Darmstadt, Germany |
| 48. | Triton X-100 | AppliChem GmbH, Darmstadt, Germany |
| 49. | Sodium chloride | AppliChem GmbH, Darmstadt, Germany |
| 50. | SDS (Sodium dodecylsulfat) | Roche Diagnostics GmbH, Mannheim, Germany |
| 51. | Dnase | Roche Diagnostics GmbH, Mannheim, Germany |
| 52. | Protease inhibitor Cocktail | Roche Diagnostics GmbH, Mannheim, Germany |
| 53. | Random Primer | Roche Diagnostics GmbH, Mannheim, Germany |
| 54. | Ethly Green Counterstain | Linaris Biologische Produkte, Wertheim, Germany |
| 55. | Paraformaldehyd solution (4% in PBS) | Santa Cruz Biotechnology, Inc., USA |
| 56. | Pertex | Medite GmbH, Burgdorf, Germany |
| 57. | Resorcinol/Fucsine | Chroma, Munster, Germany |
| 58. | Trypsin Digest All2 | Zytomed Systems, Berlin, Germany |
| 59. | Oligonucleotides | Eurofins Genomics GmbH, Ebersberg, Germany |

### 2.5.2 Enzymes

**Table 2.4: List of enzymes**

| S/N | Name | Origin |
|---|---|---|
| 1. | Collagenase | Sigma-Aldrich Chemie GmbH, Steinheim, Germany |
| 2. | Dnase | Invitrogen Corporation, CarlsbadCA, USA |
| 3. | Elastase | Serva Electrophoresis GmbH, Heidelberg, Germany |
| 4. | GoTaq Polymerase | Promega Corporation, Madison, USA |
| 5. | Proteinase K | Roche Diagnostics GmbH, Mannheim, Germany |
| 6. | Trypsin | PAA Laboratories GmbH, Pasching, Austria |

### 2.5.3 Cytokines and neutralizing antibodies

The cells were stimulated with cytokines to observe different cell activities such as proliferation and migration. In another set of experiments, neutralizing antibodies for these cytokines were also used individually and collectively to evaluate how these activities are affected. Following is a list of all the cytokines and neutralizing antibodies used.

**Table 2.5: List of cytokines**

| S/N | Name | Origin |
|---|---|---|
| 1. | Recombinant human SDF-1 (CXCL12) | #250-20A, PeproTech, Rocky Hill, USA |
| 2. | Recombinant human IL-6 | #AF-200-06, PeproTech, Rocky Hill, USA |
| 3. | Recombinant Murine MCP-1 | #250-10, PeproTech, Rocky Hill, USA |

**Table 2.6: Cytokine neutralizing antibodies**

| S/N | **Name** | **Origin** |
|---|---|---|
| 1. | Anti-SDF-1 (CXCL12) antibody) | ab9797, Abcam, Cambridge, UK |
| 2. | Anti-hIL-6-IgG antibody | mabg-hil6-3, InvitroGen, Carlsbad, USA |
| 3. | Anti-MCP-1 antibody | ab25124, Abcam, Cambridge, UK |

### 2.5.4 Antibodies

A number of antibodies were used to perform protein detection in immunohostochemistry (IHC) and Western blotting (WB) experiments.

**Table 2.7: Antibodies used for western blot and immunohistochemical staining**

| **S/N** | **Name** | **Dilution** | **Use** | **Origin** |
|---|---|---|---|---|
| 1. | Anti-mouse (A5278) | 1:1000 | WB | Sigma-Aldrich Chemie GmbH, Steinheim, Germany |
| 2. | Anti-rabbit (A6154) | 1:2000 | WB | |
| 3. | Alpha smooth muscle actin (A2547) | 1:900 | IHC | |
| 4. | RasGAP | 1:1000 | WB | A. Kazlauskas, Harvard Medical School, Boston, MA |
| 5. | Von Willebrand factor (A0082) | 1:1200 | IHC | Dako GmbH, Hamburg, Germany |
| 6. | Anti-rabbit (A6154) | 1:1000 | WB | Sigma-Aldrich Chemie GmbH, Steinheim, Germany |
| 7. | Anti-STEAP4 antibody (ab63967) | 1:1000 | WB | Abcam, Oregon, USA |

### 2.5.5 Buffers and solutions

**Table 2.8: Buffers and solutions used in experimental procedures**

| S/N | Name | Origin |
|---|---|---|
| 1. | Amersham ECLTM Western | GE Healthcare UK Ltd; England |
| 2. | Blotting Detection Reagents | GE Healthcare UK Ltd; England |
| 3. | Anode solution I | 0.3M TRIS 20% methanol |
| 4. | Anode solution II | 25mM TRIS 20% methanol |
| 5. | Cathode solution | 40mM 6-aminohexanacid 0.01% SDS 20% methanol |
| 6. | Enzyme solution | 24mg collagenase type I, 8mg elastase, 8mg trypsin inhibitor, 24 ml DMEM (high glucose + 1% penicillin/streptomycin) |
| 7. | PBS | NaCl 8g, KCl 0.2g, Na2HPO4 1.44g, K2HPO4 0.24g<br>at pH 7.4 with HCl 6M, ad 1l with ddH2O |
| 8. | Resolving gel pH 8.8 | TRIS 90.75g ad 500ml with dd$H_2O$ with HCl conc. at pH 8.8 |
| 9. | SDS 4x buffer | 250mM TRIS-HCl (pH 6.8)<br>8% SDS<br>40% glycerol<br>200mM DTT(Dithiothreitol)<br>0.04% bromphenol blue |
| 10. | Stacking gel pH 6.8 | TRIS 12.0g<br>with HCl conc. at pH 6.8<br>ad 200ml with ddH2O |
| 11. | TAE 50x | 2M TRIS<br>0.05M EDTA<br>1M acetic acid<br>with NaOH at pH 8 |

| | | |
|---|---|---|
| 12. | Tail-lysis buffer | 3M TRIS pH 8.5<br>250mM EDTA<br>20% SDS<br>5M NaCl |
| 13. | TBS | TRIS 2.42g<br>NaCl 8.0g<br>ad 1l with ddH2O |
| 14. | FBS (Fetal bovine serum) | Gibco, Invitrogen, Corporation, CarlsbadCA, USA |
| 15. | Pen/Strep (Penicillin Streptomycin) | Gibco, Invitrogen, Corporation, CarlsbadCA, USA |
| 16. | Protein Standard Page Ruler Perstained Protein Ladder | Fermentas GmbH, St. Leon-Rot, Germany |

### 2.5.6 Biological kits

**Table 2.9: List of biological kits**

| S/N | Name | Origin |
|---|---|---|
| 1. | Cell Proliferation ELISA, BrdU | Roche Diagnostics GmbH, Mannheim, Germany |
| 2. | Vector<br>Vip. Substrate Kit | Linaris Biologische Produkte, Wertheim, Germany |
| 3. | DAB Substrate Kit | Linaris Biologische Produkte, Wertheim, Germany |
| 4. | Power SYBR® Green PCR master mix | Applied biosystems by thermo Fisher scientific |
| 5. | MM HRP Polymer Kit | Zytomed Systems, Berlin, Germany |
| 6. | RNeasy MiniKit | Qiagen GmbH, Hilden, Germany |
| 7. | High capacity RNA-to-cDNA kit | Applied biosystems by thermo Fisher scientific |
| 8. | Cell death detection ELIZA | Roche Diagnostics GmbH, Mannheim, Germany |

| | | |
|---|---|---|
| 9. | MTT assay kit | Sigma-Aldrich, St. Lousis, USA |
| 10. | IL-6 ELISA Kit | Abcam, Massachusetts, USA |
| 11. | Mouse Cytokine array panel A | R&D systems, Minneapolis, USA |

## 2.6 Primers

### 2.6.1 Primers for Quantitative PCR (qPCR)

The qPCR amplified the cDNA which was obtained by using the extracted mRNA. The mRNA was converted into cDNA using High capacity RNA-to-cDNA kit. Following is a list of primers used for qPCR experiments. All the qPCR primers were ordered from Eurofins Genomics GmbH, Ebersberg, Germany.

**Table 2.10: Primers used for quantitative PCR**

| Sequence (5'-3') | Characteristic |
|---|---|
| Forward AGTCCCTGCCCTTTGTAC<br>Reverse CGATCCAGGGCCTCACTA | 18S |
| Forward CCACCACGCTCTTCTGTCTAC<br>Reverse TCCGAGGTCCTGACTCTGTC | TNF-α |
| Forward CCACTCACCTGCTGCTACTAC<br>Reverse TGGTGATCCTCTTGTAGCTCTCC | MCP-1 |
| Forward ATCTTTTGGGGTCCGTCAACT<br>Reverse CACGATTTCCCAGAGAACATGTG | IL-1β |
| Forward ACAACCACGGCCTTCCCTACT<br>Reverse CACGATTTCCCAGAGAAC | IL-6 |

| | |
|---|---|
| Forward TCAAATGCGGAATACCTTGCT<br>Reverse GCATCTAGTGTTCCTGACTGGA | Stamp2 |
| Forward CCAGCTATGAACTCCTTCTC<br>Reverse GCTTGTTCCTCACATCTCTC | Human IL-6 |
| Forward CAGAGTACCTTGCTCATTTGGT<br>Reverse TGTCATTTCCACACACAAACAC | Human Stamp2 |

### 2.6.2 Genotyping primers

The genotyping primers were used to confirm the genotypes of the mice used for experiments (Stamp2-KO or WT). The protein bands observed thus indicated the presence or absence of the particular genotype.

**Table 2.11: PCR primers for WT and Stamp2 KO genotyping**

| Sequence (5'-3') | Characteristic |
|---|---|
| GGTCTTTCAAAGTGAGGCAACACTTC | TE (Common) |
| GGGCCAGCTCATTCCTCCCACTCAT | T (KO) |
| GGTGCTGAAGTGCATCCTCATCATG | E (WT) |

All genotyping primers were purchased from Eurofins Genomics GmbH, Ebersberg, Germany.

### 2.6.3 siRNA transfection

In order to perform Stamp2 gene downregulation in PASMCs and HMVECs, siRNA transfection was performed. Cells were transfected using Stamp2 siRNA along with transfection reagent (INTERFERin® Polyplus, New York City, USA). Scrambled siRNA was used as control. Following is the list of siRNAs used for transfection along

with the target Stamp2 sequence. The siRNAs were purchased from Qiagen, Hilden, Germany.

**Table 2.12: siRNA sequences for Stamp2 downregulation**

| Sequence (5'-3') | Characteristic |
|---|---|
| CACAATGGTGACCACTGATAA | Target sequence |
| CAAUGGUGACCACUGAUAATT | Antisense strand |
| UUAUCAGUGGUCAUUGTG | Sense strand |

## 2.7 Consumable articles

**Table 2.13: List of consumable articles**

| S/N | Name | Description | Origin |
|---|---|---|---|
| 1. | Blotting membrane | ImmunBlotTM PVDF Membrane for Protein Blotting | BioRad Laboratories, USA |
| 2. | Blotting paper Whatman | Gel Blotting Paper | Schleicher & Schuell, Germany |
| 3. | Butterfly needle | 21G 25G Braun Melsungen AG | Melsungen, Germany |
| 4. | Hypodermic needls | 26G x ½ 20G x 1 ½ Braun Melsungen AG | Melsungen, Germany |
| 5. | IV line | Intratix Air-matic | Melsungen, Germany |
| 6. | Three-way-stopcock | Discofix C-3 Braun Melsungen AG | Melsungen, Germany |
| 7. | Cell culture dishes | ∅ 10cm dish ∅ 6cm dish 6-well-, 24-well- & 96-well-dish | Trasadingen, Switzerland |
| 8. | Serological Pipettes | 5ml pipette, 10ml pipette, Trasadingen, Switzerland 25ml pipette | Trasadingen, Switzerland |

| | | | |
|---|---|---|---|
| 9. | Serological Pipettes | 5ml pipette, 10ml pipette, Trasadingen, Switzerland<br>25ml pipette | Trasadingen, Switzerland |
| 10. | Photopaper Amersham | HyperfilmTM ECL GE Healthcare | England |
| 11. | Reaction tubes | 0,5 ml tube, 1,5 ml tube, 2 ml tube<br>Eppendorf AG | Hamburg, Germany |

## 2.8 Computational Software Programs

**Table 2.14: Computer software programs for quantification**

| S/N | Name | Description | Origin |
|---|---|---|---|
| 1. | AIDA (Version 4.00.027) | Raytest | Straubenhardt, Germany |
| 2. | GraphPad Prism 5.03 | GraphPad Software, Inc | California, USA |
| 3. | LabChart7 | AD Instruments | Sydney, Australia |
| 4. | Leica Q Win | Leica Microsystems GmbH | Wetzlar, Germany |
| 5. | Microsoft office 2003 | Microsoft Corporation | Redmond, USA |
| 6. | Keyence BZ II analyzer software | Keyence corporation | USA |
| 7. | ImageJ | National Institute of Health (NIH) | USA |

# 3. Laboratory Techniques and Methods

# 3 Laboratory Techniques and Methods

## 3.1 Cell culture

### 3.1.1 Isolation and cultivation of murine PASMCs

Murine PASMCs were isolated from Stamp2-KO and WT mice aged between 9-12 weeks. Post sacrifice the mouse thoracic cavity was cut open and the heart-lung complex was removed. Ice cold PBS buffer containing penicillin/streptomycin was filled in a Petri dish and the lung heart complex was placed in it to perform isolation of PASMCs. The pulmonary artery was removed from the complex and was placed in an Eppendorf tube filled with enzyme solution (collagenase, elastase, trypsin-inhibitor). The tube was then incubated at 37°C for 30 minutes. This incubation helped remove the adventitious layer of the pulmonary artery. The remaining arterial structure was then cut into smaller pieces and was incubated again in the enzyme solution at 37°C for 90 minutes to disintegrate the tissue. The tube was centrifuged for 2 minutes at 5000 rpm after incubation and the supernatant was removed. The remaining cell pellet was suspended in 2 ml of DMEM containing 20% FCS and antibiotics (penicillin/Streptomycin). The suspended cell pellet was seeded in a 24-well plate and was expanded upon reaching 80% confluence into 12-well plate. Once the 12-well plate reached 80% confluence it was further expanded into a 6-well plate. When the cells in the 6-well plate showed 70-80% confluence, cells were seeded on a 10 cm plate which was passaged subsequently for cellular expansion and use in experiments.

### 3.1.2 Cultivation of human PASMCs

Human PASMCs were bought from Lonza (Basel, Switzerland). The cell vials received were from lots 00003639143 and 13981. According to the provider's information these cell lots belonged to a 43 years old male and a 2.5 months old male donors, respectively, both were Caucasian. Upon arrival the vial was thawed in a warm water bath at 37°C. The cells were than plated in a 24-well plate using SmGm (Smooth Muscle cell Growth Medium, Clonetics). Upon reaching 80% confluence the cells were transferred to 12-well plates followed by 6-well plates and then finally seeded onto the 10 cm Petri dishes. Once the cells were stably growing in the Petri dishes, these were passaged further and used for experiments. Cells were also frozen and saved for future use. The frozen cells were kept at -80°C.

### 3.1.3 Cultivation of human MVECs

HMVECs were bought from LONZA (Basel, Switzerland). The lots used were 0000489936 belonging to a 2 years old, Black female donor, 0000580578 belonging to a 57 years old, Hispanic male and 0000582655 belonging to a 17 years old Hispanic male. Upon receiving, the vials were plated using EBM (Endothelial cell Basal medium, clonetics) in a 10 cm Petri dish. The cells were expanded according to the protocol provided in the data sheet upon reaching 70-85% confluence. In order to expand into multiple passages, the plated cells were rinsed with 5 ml HEPES-BSS and 2 ml trypsin was added. The Petri dish was placed in the incubator at 37°C for 3-5 minutes and was examined periodically. Once around 90% confluence was reached, 5 ml of trypsin neutralizing solution was added to the Petri dish to enable cell detachment and the cells were transferred to a 15 ml sterile falcon tube and centrifuged for 5 minutes at 200g. The supernatant was aspirated and the cells were re-suspended in EBM and seeded onto new Petri dishes. These cells

were then used for experiments. Cells were also frozen and saved for future use. The frozen cells were kept at -80°C.

### 3.1.4 Isolation and cultivation of murine peritoneal macrophages

Mice were injected with thioglycollate three to four days prior to isolation of macrophages. On the day of macrophage harvesting, mice were killed via cervical dislocation after administering deep anaesthesia using isoflurane. Mice were then pinned on to the operating plate and thoroughly sprayed with 70% ethanol to ensure a clean exterior. The skin was carefully cut open making sure the peritoneal cavity was not punctured. Gently the underlying connective tissue was removed to ensure easy spreading and pinning of the skin flaps to the sides. 10 ml of ice cold PBS taken in a syringe was injected into the peritoneal cavity. Using the same syringe the PBS was sucked back collecting the macrophages from the peritoneal cavity, around 8 ml was sucked back and exported to a falcon tube kept on ice. The procedure was repeated twice to ensure maximum retrieval of cells. The collected PBS-macrophage solution was then centrifuged at 1200 rpm for ten minutes. Afterwards the PBS was discarded and the pellet was resuspended in 10 ml of DMEM culture medium and transferred onto the culture plate. The harvested macrophages were kept at 37°C for 4-5 hours to allow attachment of viable cells. After 5 hours the culture medium was aspirated using a suction pump and the cells were washed using PBS to remove loose and unattached cells. Fresh medium was poured onto the cells and plates were again kept at 37°C in the incubator and used according to experimental plan.

## 3.2 Tissue harvesting and preparation

### 3.2.1 Mouse lung tissue

Lung tissues were harvested from Stamp2-KO and WT mice kept under hypoxia (10% oxygen) and normoxia conditions for 21 days. The lungs were perfused thoroughly using PBS for 8-10 minutes to ensure complete removal of blood. The right lung tissue was snap frozen and kept at -80 degrees for protein and RNA extraction.

The left lung tissue was fixed in 4% phosphate-buffered paraformaldehyde solution. Mouse lungs were embedded in paraffin blocks and stored at room temperature until sections had to be prepared. The blocks were put at -20°C overnight prior to cutting sections. The sections were cut using a microtome and the paraffin blocks were kept on the cooling plate in-between to prevent softening of block and to avoid breaking of sections. 3 µm thick sections were cut and were transferred to water heated up to 40°C to unfold them. The flattened sections were then transferred onto slides and dried overnight in a 37°C heating chamber. The sections were then stored at room temperature until immunohistochemical staining was performed.

### 3.2.2 Rat lung tissue

Lungs were harvested from rats which developed Sugen/hypoxia induced PH and rats kept in normoxia. The procedures for lung tissue harvest, paraffin sections preparation and for freezing the tissue were performed in a similar manner as explained for mouse lung tissue above. Once prepared, the sections were labelled and stored at room temperature. These sections were then used for different immunohistochemistry staining protocols.

### 3.2.3 Human lung tissue

The donated human lung tissues from IPAH patients and healthy donors were used for this project. The donation and experimental procedures were approved by the Ethics committee of the University of Giessen, Germany. The experiments were performed according to the national law. A part of individual lung tissues was snap frozen and kept at -80 degrees for protein and RNA extraction. Another part was first fixed in 4% phosphate-buffered paraformaldehyde solution and was used for 3 µm section preparation. The sections were prepared following the same method described for mouse lung sections preparation.

## 3.3 Animal models of pulmonary hypertension

### 3.3.1 Sugen/Hypoxia induced pulmonary hypertension

Male Sprague Dawley rats were used as PH model. PH was induced by injecting the rats with SU5416 (20mg/kg dissolved in DMSO) and keeping them in hypoxia for 21 days followed by two weeks of normoxia. Rats kept under normoxia acted as controls. The rats were used primarily for harvesting lung tissue and using those for immunohistochemical staining and performing protein and RNA extraction for further experiments.

### 3.3.2 Hypoxia-induced pulmonary hypertension mouse model and hemodynamic assessment

Hypoxia conditions were used to induce PH in WT and Stamp2-KO mice. Male mice aged between 8-14 weeks were used for the experiments. The hypoxia conditions (10% oxygen) were maintained for a period of three weeks. Mouse cages were cleaned and changed on alternate days along with fresh water and food replacement and

the hypoxia conditions were restored immediately. WT and Stamp2-KO Mice were kept in similar manner at normoxia receiving 20% oxygen, served as controls. After three weeks mice were subjected to hemodynamic measurements.

Mice were kept under deep anaesthesia using constant flow of isoflurane during surgical procedure of hemodynamic measurements. Post measurement recording, mice were sacrificed. Lung and heart tissues were harvested from sacrificed mice for experimental use. Measurements of the following parameters were recorded:

- Right ventricular systolic pressure (RVSP)
- Systolic blood pressure (SBP)
- Right heart hypertrophy (RV/LV+S)
- Heart rate

Following is a graphical description of how hypoxia was administered in the mouse model to develop PH, showing the time point of hypoxia exposure and completion of experiment.

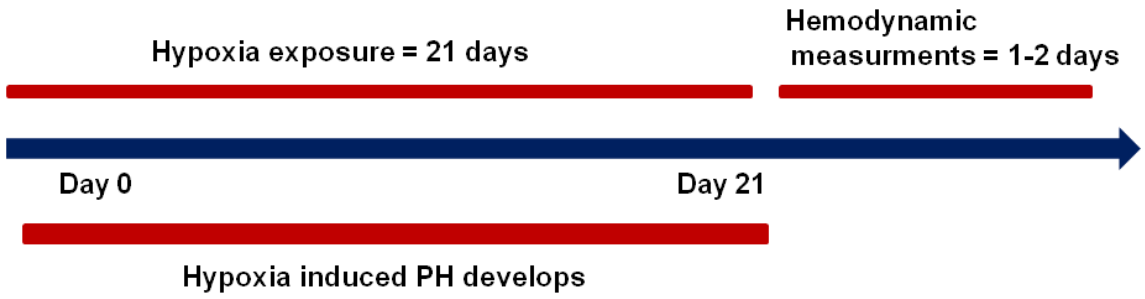


**Figure 3.1: Timeline of hypoxia-induced PH development in WT and Stamp2-KO mice**

## 3.4 Measurement of hemodynamic parameters

### 3.4.1 Right ventricular systolic pressure

Mice were given initial anaesthesia by putting them in an isoflurane containing chamber for 20-30 seconds. The anaesthetized mice were then placed on a heating plate to maintain the body temperature, and kept under constant anaesthesia by a supply of anaesthesia gas through a gas mask placed over the nose and mouth. The anaesthetic gas consisted of 1-1.2 l/min oxygen, 0.6 l/min compressed air and 2% isoflurane. Foot reflexes were checked to ensure deep anaesthesia administration. The jugular vein was dissected using a 30G1/2 needle, and a millar® catheter was inserted. The catheter was moved forward until it reached the right ventricle of the heart. Once the catheter was in the right position, the right ventricular pressure was recorded. The pressure curves were displayed using LabChart® software (AD instruments). PowerLab amplifier® was used to obtain amplified pressure curves. Heart rate (HR) was calculated via the same software along with the pressure curve recording. The pressure curve was recorded for 2-4 minutes constantly.

### 3.4.2 Systemic blood pressure

To measure systemic blood pressure the carotid artery was dissected. The proximal end of the artery was ligated to prevent blood flow, the artery was opened using a 26G1/ needle, and a millar® catheter was inserted. Once the catheter was inside the ligation was untied to help the catheter move forward. After obtaining a stable pressure curve, the ligation was tightened again to stabilize the catheter position inside the artery. The systemic blood pressure

was then recorded in the similar fashion as explained above for RVSP recording.

### 3.4.3 Perfusion of organs and tissue fixation

Once measurement of hemodynamic parameters was complete, the mice were sacrificed by cervical dislocation. The chest cavity was cut open and thorax was fully exposed. A butterfly needle connected to PBS supply was inserted into the left ventricle and the right atrium was opened and the heart was perfused for 3-4 minutes. Afterwards the butterfly was inserted into the trachea and the lungs were perfused for 5-7 minutes. The right lung was cut and shock frozen in liquid nitrogen. The left lungs were kept in 4% formalin in PBS solution overnight at 4°C and were transferred to PBS the next day. After 24 hours the lungs were kept in 70% ethanol until ready for tissue infiltration and paraffin embedding.

### 3.4.4 Right heart hypertrophy

The heart was removed and kept in chilled PBS. The left and right atria were separated, and the left ventricle along with septum was dissected away from the right ventricle. The dissected pieces were weighed, and ratio of right ventricle to left ventricle and septum (RV/LV+septum) was drawn. The calculated value (so-called Fulton index) showed the development of right heart hypertrophy. The left and right ventricles were also shock frozen and stored at -80°C.

## 3.5 Immunohistochemical staining (IHC)

The paraffin lung sections were stained using immunohistochemical methods to look for various factors and markers. The lung sections were stained to detect the expression of Stamp2, von willebrandt

factor (endothelial cell marker), smooth muscle actin and CD68 positive cells. The staining experiments were performed according to optimized protocols as tabulated below.

### 3.5.1 Staining protocol for Stamp2

Paraffin lung sections were obtained from WT and Stamp2-KO mice kept in hypoxia and normoxia, from rats subjected to sugen/hypoxia and control rats and from healthy and PH patients. Stamp2 protein was stained in brown colour. The staining was performed according to the following protocol.

**Table 3.1: IHC protocol for Stamp2 staining**

| Time(min) | Reagent/instrument | procedure |
|---|---|---|
| 60 | 58°C incubator | Place the slides in a slide rack and let them heat for an hour |
| 3x10 | NeoClear® | Wash to remove the paraffin and reveal sections |
| 2x5 | Ethanol (99.8%) | Serial hydration |
| 5 | Ethanol (96%) | Serial hydration |
| 5 | Ethanol 70% | Serial hydration |
| 15 | $H_2O$-Methanol (3%) | Serial hydration |
| 2x5 | Distilled $H_2O$ | hydration |
| 2x5 | PBS | Washing |
| | Dako pen | Draw a hydrophobic circle around the section |
| 15 | Trypsin solution (Life technologies) | Put the soln. on the sections and incubate at 37°C in a humidified box |
| 3x5 | PBS | washing |
| 20 | Serumblock I (ImmPRESS Kit Anti-rabbit Ig) normal horse serum 2.5% | blocking |
| Overnight | Steap4 antibody (ProteintechR)<br>Diluted in Antibody diluent (Zytomed systems) | The section were incubated overnight at 4°C dilution: 1:20 |
| 4x5 | PBS | washing |

| | | |
|---|---|---|
| 30 | ImmPRESS kit Anti-Rabit ig Peroxidase | |
| 4x5 | PBS | washing |
| | DAB substrate kit | Visualize the development of colour |

### 3.5.2 CD68 + smooth muscle actin (SMA) co-staining

Paraffin lung sections from WT and Stamp2-KO mice kept under hypoxia and normoxia were subjected to SMA-CD68 double staining. At first the sections were stained for SMA followed by CD68 staining. The SMA staining appeared in brown colour while CD68 staining appeared in fuchsia-red colour.

**Table 3.2: IHC double staining protocol for CD68+ cells and Smooth muscle actin (SMA)**

| Time(min) | Reagent/instrument | procedure |
|---|---|---|
| 60 | 58°C incubator | Place the slides in a slide rack and let them heat for an hour |
| 3x10 | xylene | Dewaxing of sections |
| 20 | Citrate buffer pH:6 ((Spring PMB-1-250 Antigen Retrival Buffer) | Boil section in buffer |
| 15 | $H_2O$-Methanol (3%) | Serial hydration |
| 2x5 | TBS (TRis Buffered Saline Tween 20 TA-999-TT Thermo) | Washing |
| 10 | Avidin (avidin biotin block DAKO X0590) | blocking |
| 2x5 | TBS | Washing |
| 10 | Biotin (avidin biotin block DAKO X0590) | Blocking |
| 30 | Smooth muscle actin antibody 1:200 | Incubate at room temperature |
| 3x5 | TBS | Washing |
| 10 | DAB development | |
| 2x5 | TBS | Washing |
| 30 | CD68 antibody 1:100 | Incubate at room temperature |
| 3x5 | TBS | Washing |
| 30 | Poly AP (POLAP 100 zytomed systems) | |
| 2x5 | TBS | Washing |

| | | |
|---|---|---|
| 20 | Fast red (RED 055 Zytomed systems) | |
| 10-15 sec. | Haematoxylin | Counterstain |
| | Cover with water (glycerin gelatin Merck 1.085620050) | |
| | Neo mount® 1 drop | Mount the slides using glass cover slips and leave to dry overnight |

### 3.5.3 Staining protocol for smooth muscle actin (SMA) and von willebrand factor (vWF)

Double staining was performed to stain endothelial and smooth muscle cells. VWF is expressed in the endothelial cells and is stained in brown colour while smooth muscle actin in the smooth muscle cells was stained in violet-purple colour. The nuclei were stained green. The protocol for staining is as follows:

**Table 3.3: IHC protocol for Smooth muscle actin and endothelial cell marker (vWF )**

| Time (min) | Reagent/instrument | procedure |
|---|---|---|
| 60 | Incubator 58°C | Place the slides in a slide rack and let them heat for an hour |
| 3x10 | NeoClear® | Wash to remove the paraffin and reveal sections |
| 2x5 | Ethanol 99,8% | Serial hydration |
| 5 | Ethanol 96% | Serial hydration |
| 5 | Ethanol 70% | Serial hydration |
| 15 | $H_2O_2$ Methanol 3% | Serial hydration |
| 2x5 | Aqua dest. | hydration |
| 2x5 | PBS | Washing |
| | Orbit tissue with Dako Penn | Draw a hydrophobic circle around the section |

| | | |
|---|---|---|
| 15 | Trypsin solution (life technologies) 37°C incubator | Put the soln. on the sections and incubate at 37°C in a humidified box |
| 3x5 | PBS | Washing |
| 20 | 10% BSA in PBS | Blocking |
| 3x5 | PBS | Washing |
| 30 | Rodent Block M (Zytomed Systems) | Put 2-3 drops on each section and incubate |
| 3x5 | PBS | Washing |
| 30 | Alpha-smooth muscle actin antibody 1:900 in 10%BSA PBS | The section were incubated at room temperature |
| 4x5 | PBS | Washing |
| 20 | MM HRP Polymer (Zytomed Systems) | |
| 3x5 | PBS | Washing |
| 3 to 4 | Vector VIP Substrate | Visualize the development of color under microscope |
| 5 | $H_2O$ | |
| 2x5 | PBS | Blocking |
| 20 | 10%BSA in PBS | Blocking |
| 3x5 | PBS | Washing |
| 20 | Serumblock I Impress Kit Normal Horse Serum 2.5% | |
| 30 | Von Willebrandt factor antibody 1:1200 in 10% BSA PBS at 37°C | Incubate at 37°C |
| 4x5 | PBS | Washing |
| 30 | ImmPRESS Reagent anti rabbit ig Peroxidase | |
| 4x5 | PBS | Washing |
| 0.5 | DAB substrate | Visualize the development of colour under microscope |
| 5 | $H_2O$ | Put slides at 60°C for counter stain |

| | | |
|---|---|---|
| 3 | Methylgreen on a heating plate 60°C | |
| 1 | Aqua dest. | |
| 2x2 | Ethanol 96% | |
| 2x5 | Isopropanol | |
| 3x5 | NeoClear ® | Mount the slides using glass cover slips and leave to dry overnight |
| | Cover slide with NeoMount® | |

## 3.6 **Measurement of vascular muscularization**

The paraffin lung sections were subjected to double staining for vWF (von willebrandt factor) staining the endothelium and SMA (smooth muscle actin) for staining smooth muscle cells. The stained vessels in the lung sections were located and photographed using 40X magnification of the microscope (KEYENCE). 100-80 vessels (diameter <100 µm) were chosen from each lung. The individual vessel photos were then analyzed for the muscularized area using the Keyence BZ II analyser software. Measurement of vessel diameter, area and lumen area were used to draw the percentage of muscularized area. The SMA stained area showed violet colour whereas the vWF stained area showed brown colour. The violet region was measured in proportion to the measured vessel area to generate values indicating the level of muscularization. Vessels with <5% muscularized region were titled as non- muscularized, 5-70% as partially muscularized and >70% as fully muscularized.

## 3.7 **Endothelin-1 Immunoassay**

Elisa measurement for ET-1 in mouse serum was performed using QuantiGlo® ELISA kit (R&D systems). The immunoassay was

performed in accordance with the manufacturer's protocol. Serum samples from WT and Stamp2-KO mice kept under hypoxia and normoxia were used. All the samples and working standards were prepared according to the protocol and were added to the microplate wells along with the assay diluent called RD1-19. The samples were then incubated at room temperature for 90 minutes. All the wells were then washed and Endothelin-1 conjugate was added to each well and the plate was again incubated at room temperature for 3 hours. 100 µL of working Glo Reagent was added to each well and relative light units (RLU) were calculated using a luminometer. The wells were read using Tecan Safire 2 multimode reader. The RLU values obtained were than analysed using regression analysis to obtain the ET-1 concentration values.

## 3.8 **IL-6 ELISA**

IL-6 concentration in mouse serum samples was measured using Mouse IL-6 ELISA Kit (Interleukin-6) (ab100712 Abcam). Mouse serum samples from WT and Stamp2-KO mice kept under hypoxia and normoxia were used to detect IL-6 levels. The ELISA was performed according to the manufacturer's protocol. All the samples, standards and reagents were prepared according to the protocol instructions. The samples and standards were added to the wells pre-coated with IL-6 antibody and were incubated at room temperature. The wells were then washed and biotin antibody was added to the wells followed by incubation at room temperature. Streptavidin solution was added to the wells and incubated. The wells were then incubated with TMB one step development solution. The samples were read after adding stop solution at 450 nm using the Power Wave 340 Elisa reader.

## 3.9 **BrdU Incorporation: proliferation assay**

Cell proliferation was measured via BrdU incorporation assay. Cell Proliferation ELISA (Roche Diagnostics, Rotkreuz, Switzerland) was used to perform the assay. On day 1 the cells (PASMCs or MVECs) from mouse and/or human source were cultured in a 96-well plate. Cell density of 7500 cells per well for human cells and $1X10^4$ cells per well for mouse cells was used. On day 2 the cells were serum starved to bring all cells into the G1 phase of the cell cycle. On day 3 after 24 hours of serum starvation the cells were incubated with different proliferating agents whose effect had to be studied (growth medium, IL-6, ET-1, PDGF etc.). After 24 hours BrdU was added to the cells. BrdU is a synthetic analogue of the nucleoside thymidine so it intercalates with the replicating DNA and acts as a marker of proliferating cells. After 24 hours of BrdU labelling, the medium was removed and cells were fixed using FixDenat® fixing solution. Anti-BrdU antibody was then added to the cells. After incubation the cells were washed to remove unbound antibody and reaction substrate solution (TMB) was added to the cells. The absorbance was measured by reading the 96-well plate on an Elisa reader at wavelengths of 370 nm and 492 nm. The Power Wave 340 ELISA reader was used (Bio-TEK Instruments, Winooski, USA).

## 3.10 **Chemotaxis assay**

Modified Boyden chamber was used to perform the assay. Cells are made to migrate towards a chemoattractant through pores (8 µm) of a polycarbonate PVPF membrane. The stained cells passing through pores of the membrane are then counted to measure cell migration.

10 cm plates with confluent cells were starved 24 hours prior to performing the assay. Alongside the PVPF membrane was incubated

for 30 minutes each side in an extracellular mimicking solution comprising of 0.01M acetic acid (2ml) and 3.41mg/ml collagen type1 (36.2 µL) and is air dried overnight.

Next day the cells were trypsinized and re-suspended in starvation medium at a density of 50,000-70,000 cells per 50 µL. The wells of the lower plate of chamber were filled with the desired chemoattractant and starvation medium as negative control. The wells were covered with PVPF membrane ensuring no air bubbles were trapped underneath the membrane. The wells in the upper chamber were filled with 50 µl of cell suspension and placed on top of the membrane such as the membrane was sandwiched between the two plates. Both upper and lower plates were screwed together. The chamber was then placed in a humidified plastic box cleaned with 70% ethanol and kept in 5% $CO_2$-37°C incubator for 5 hours to allow cell migration. After incubation the chamber was disassembled and the membrane was allowed to air dry for 30 minutes.

### 3.10.1 **Staining of membranes:**

The fixation and staining of membranes was performed using the Diff-Quick® kit. A multi compartment container was taken and the fixing solution, reagent I and reagent II were put in separate compartments. Two separate compartments were filled with distilled water, used for washing the membrane after staining. Holding with tweezers the membrane was put in each solution for a minute and then transferred to next. After final water wash the membrane was covered with a glass slide and observed under the microscope. The stained pores were counted for migrated cells using a 20X raster ocular magnification.

## 3.11 **Cell death detection: Apoptosis assay**

Cell death was measured using the cell death detection Elisa kit (Roche Diagnostics, Rotkreuz, Switzerland). On day 1 the cells (PASMCs or MVECs) from mouse and/or human were cultured in a 96-well plate. Cell density of 7500 cells per well for human cells and $1X10^4$ cells per well for mouse cells was used. On day 2 the cells were serum starved to bring all cells into the G1 phase of the cell cycle. On day 3 after 24 hours of serum starvation the cells were incubated with different concentrations of 3% hydrogen peroxide 10M solution to have 100,200 or 500 µM concentration in the well along with growth medium and starvation medium conditions as controls. After 24 hours the cells were assayed. The 96-well plate was centrifuged for 10 minutes at 1000 rpm. The wells were studied under the microscope and wells that had to be assayed were chosen. 200 µl of lysis buffer was added to the chosen wells and the plate was incubated for 30 minutes with mild shaking. After incubation the plate was again centrifuged for 10 minutes at 1000 rpm. Afterwards the antibody solution was prepared using anti-histone, anti-DNA solutions and incubation buffer. 20 µl of supernatant were taken from selected wells, put in a separate strip of wells and incubated with the antibody solution for 2 hours at room temperature with mild shaking. After incubation, the contents of the wells were removed and washed using incubation buffer three times (five minute incubation per wash), after washing 100 µl of substrate buffer was added. The absorbance was measured by reading the 96-well plate in the Power Wave 340 ELISA reader at wavelengths of 405 nm and 490 nm.

## 3.12 **siRNA administration**

PASMCs and HMVEC were cultured in desired wells according to the experiment plan. After 24 hours medium was changed and siRNA mix

was added to the wells. The siRNA was administered by preparing a siRNA and INTERFERin® (transfection agent) solution which was then added to the well along with the cell culture medium. The medium was changed after 48 hours with fresh culture medium and let sit for another 24 hours. Next day the cells were starved using starvation medium. After 24 hours the transfected cells were used for desired experiments. The gene downregulation was confirmed by performing western blot analysis of protein lysates of the cells. The silencing at the mRNA level was checked by performing qPCR.

## 3.13 **Viability Assay**

Following Stamp2 silencing the cells were checked for their survival efficiency. A colorimetric MTT assay ((Sigma-Aldrich, St. Lousis, USA) was used to assess the cell viability. Cells were seeded in 96-well plates at a density of $1x10^4$ cells per well. Depending on the cell type seeded, respective medium was used on the cells (Clonetics EBM, Lonza, Basel, Switzerland). After 24 hours the MTT reagent was added to the wells and the cells were incubated for 4 hours. After 4 hours the absorbance was measured by reading the 96-well plate in the Power Wave 340 ELISA at the wavelength of 600 nm.

## 3.14 **Preparation of protein-lysate samples**

### 3.14.1 **Protein extraction from cells**

Cells plated on 10 cm or 6-12 well plates were used for protein extraction. The cells were washed with PBS buffer and the plates were immediately transferred onto ice to prevent protein degradation. 2X SDS buffer was added to the cells and with the help of a cell scraper the cells were scraped off the plates ensuring SDS buffer completely homogenizes the cells. SDS buffer helps break the

secondary and tertiary protein structures. The samples were then cooked at 95°C for 3-5 minutes which ensured complete protein denaturation. The samples were stored at -20°C.

### 3.14.2 Protein extraction from Lung tissue

The lung tissue was homogenized in ripa buffer while keeping the samples on ice. The tissue was completely homogenized for complete protein retrieval. The samples were then put on a gentle shaker for two hours at 4°C and were centrifuged on full speed for ten minutes; the lysate was separated from the pellet and discarded. The protein concentration of the lysate was measured on Nanodrop. The protein-in-buffer samples were added to 2X SDS buffer and were cooked at 95°C for 3-5 minutes. After cooling down, the samples were stored at -20°C. The ripa buffer protein samples were stored at -80°C for future usage.

## 3.15 Western blot

### 3.15.1 SDS polyacrylamide gel electrophoresis (SDS-PAGE)

SDS (Sodium dodecylsulfate) gel electrophoresis allows molecular weight based protein separation by applying an electric current field to pull down negatively charged proteins. Protein samples along with protein markers are loaded into the wells of a polyacrylamide gel cassette which is placed inside an electrophoresis buffer filled chamber. The polyacrylamide gel consists of a stacking gel and a separating gel. The stacking gel has a pH of 6.8 and holds the protein samples in wells; the separating gel has a pH of 8.8 and separates the proteins. A 10% gel is used for the set of experiments documented here containing 10% acrylamide. The electric current

facilitates the movement of protein toward the anode, thus moving the protein samples while separating different protein units depending on their molecular weight. The lighter proteins separate earlier and travel faster towards the anode whereas the heavier proteins migrate slower. The protein molecular weight marker running alongside the samples helps mark the weight of the desired protein and guides depending on the separation when to stop the electrophoresis and blot the gel.

### 3.15.2 **Protein blotting on membrane**

Once the protein bands were separated the polyacrylamide gel was blotted onto a PVDF membrane. The blotting chamber applies electric current that helps the negatively charged protein bands to transfer from the gel on to the membrane as they travel towards the anode. The lower platform of the blotting chamber acts as the anode while the upper lid acts as the cathode. The membrane and gel are sandwiched between buffer soaked filter papers which facilitate the transfer of current through the gel and the membrane. Before preparing the sandwich the PVDF membrane was activated by one minute incubation in Methanol. The order of this sandwich is as follows, starting from layering the first set of filter papers at the base and building the sandwich up.

- Lid of blotting chamber (Cathode)
- Four filter papers soaked in cathode buffer
- Polyacrylamide gel
- PVDF membrane
- Two filter papers soaked in anode buffer II
- Three filter paper soaked in anode buffer I
- Lower platform of blotting chamber (Anode)

Once the gel-membrane-filter papers sandwich was ready the blotting chamber was closed and 100 mA current was passed through it for one hour. After one hour the protein bands were transferred onto the membrane. The blotted membrane was then transferred to a plastic box containing 5% BSA solution in TBS and incubated at room temperature for one hour with gentle shaking. This step helps prevent the unspecific antibody binding. After incubation the membrane was cut into strips at the exact molecular weight points for the desired target protein and control protein. The strips were then placed in respective primary antibodies diluted in 5% BSA in TBS solution and were incubated overnight at 4°C. Next day the membranes were washed with TBS-T buffer three times for 15 minutes per wash to remove unbound antibody residues. The membranes were then incubated for one hour with secondary antibody diluted in 5% BSA in TBS solution and were again washed four times with TBS-T buffer.

### 3.15.3 Enhanced chemiluminescence Protein Detection

The protein detection was carried out by using the Pierce® ECL Western Blotting Substrate (prod #: 32106) kit. 1 ml each of Reagent 1 and 2 were mixed and the membrane was incubated in it for one minute. The detection reagent was HRP conjugated to the secondary antibody and resulted in oxidation of ECL substrate; this reaction caused emission of light which was detected using light sensitive films. In a dark room the photosensitive x-ray films (AmershamTM Hyperfil ECL) were exposed to the membranes and the signal appearing as protein bands was viewed after developing the films in Curix 60 developer (AGFA). The exposure time was 10 seconds to 10 minutes.

### 3.15.4 **Densitometric analysis**

The protein bands on developed photosensitive films were scanned and the image was then analyzed using adobe Photoshop software. Intensity of individual bands for each sample was calculated and background noise was subtracted, all values were normalized to their respective control bands. The numerical values obtained from the software were then analyzed using student's *t*-test.

## 3.16 **Genotyping of mice**

### 3.16.1 **Isolation of DNA from tail biopsies**

Tail biopsies were obtained from 3 weeks old mice and were lysed using tail lysis buffer. In an Eppendorf tube 500 µL of lysis buffer and 5 µL of proteinase K were added along with the tail cuts and were shaken on a thermo mixer overnight at 58°C. The samples were then centrifuged for 1 minute at 7000 rpm. The supernatant was transferred to fresh tubes and the pellet was discarded. 500 µL of isopropanol was added to the supernatant and the tubes were shaken vigorously to ensure maximum DNA precipitation. The samples were then centrifuged at 13,000 rpm for 15 minutes and isopropanol was carefully removed while keeping the DNA pellet. 150 µL of 70% ethanol was added to wash the DNA and samples were centrifuged for another 15 minutes at 13,000 rpm. Ethanol was dried and the DNA pellet was left to dry for 5-10 minutes at 60°C. The dried DNA pellet was suspended in 50 µL of DNAse free water and samples were stored at -20°C.

### 3.16.2 **Genotyping PCR**

The DNA from tail biopsies was then genotyped by PCR (polymerase chain reaction) amplification to reveal the genotype of mice (WT or Stamp2-KO). The Stamp2 KO mice were created by gene targeting into embryonic stem cells by insertion of a cassette to disrupt the gene. Genotyping primers included one primer specific for the cassette and a primer specific for WT gene and a common primer, shown in the table below. The inserted cassette in KO mice DNA is not detectable by the wild type specific primer. The PCR mixture with a total volume of 20 µL was prepared. The PCR mix comprised of the components shown in the table below.

**Table 3.4: List of genotyping PCR mix components**

| Components | Volume (µL) |
|---|---|
| Distilled water | 12 |
| 10X PCR-$MgCl_2$ | 2.0 |
| 59mM $MgCl_2$ | 1.0 |
| 10nM dNTPs | 0.5 |
| 10nM KO primer | 0.3 |
| 10nM WT primer | 0.3 |
| 10nM common (TE) primer | 0.6 |
| Platinum® Taq DNA Polymerase | 0.6 |
| DNA sample | 3.0 |

### 3.16.3 **PCR protocol for Genotyping**

The Genotyping protocol was optimized and was regularly used with the settings shown in table 3.5, to confirm the genotype of mice.

These confirmed results were recorded in the online animal data input software along with information regarding the age, sex and generation history. This information was used when selecting animals for experiments.

**Table 3.5: PCR conditions for genotyping PCR**

| Steps | Temperature | Time |
|---|---|---|
| Denaturation (1 cycle) | 95°C | 7:00 minutes |
| Denaturation<br>Annealing<br>Extension (35cycles) | 96°C<br>58°C<br>68°C | 10.00 seconds<br>30.00 seconds<br>1:30 minutes |
| Final extension (1 cycle) | 68°C | 7:00 minutes |
| Hold | 4°C | 0:00 |

The amplified DNA product was then separated using gel electrophoresis. A 2% agarose gel containing EtBr (Ethidium Bromide) was prepared. The gel was placed in an electrophoresis chamber filled with TAE buffer and DNA samples were filled in the gel wells along with DNA loading dye for better viewing of the samples while pipetting. 10 µL of each sample was loaded per well. The wells on both ends of the gel were filled with DNA band size marker. The gel was run at 120 volts for 30 minutes, this allowed adequate separation of the amplified DNA bands. The gel was viewed in the UV light chamber. The Stamp2-KO mice showed a band against 509 bp, while wild type showed a band measuring up to 265 bp.

## 3.17 **RNA isolation**

RNA isolation from cells and lung tissues was performed using RNeasy® mini kit (Qiagen) in accordance with the protocol provided by the manufacturer.

### 3.17.1 **Lung homogenate preparation**

The lung tissue weighing up to 30 mg was homogenized with RLT buffer using Potter S tissue homogenizer; the tissues were kept on ice all along. The homogenate was then centrifuged at maximum speed for 3 minutes and the supernatant was saved and used to isolate the RNA.

### 3.17.2 **Cell lysates preparation**

Cells plated on 10 cm plates or 6 well plates were used for RNA isolation. The cells were washed with PBS and placed on ice. RLT buffer was added to the plates to perform cell lysis. The cells were effectively scraped off the plate surface using cell scraper to ensure effective cell lysis. The cell lysates were then transferred to storage tube and later used for experiments.

### 3.17.3 **RNA Isolation method**

The prepared lung/cell lysates were then transferred to Eppendorf tubes and homogenized. 70% ethanol was added to the lysate samples and these were transferred to the RNeasy silica membrane mini columns. Once the RNA was bound to the membrane, the contaminants were removed by washing. Pure RNA was finally eluted using 10-30 µl of RNAse free water and the RNA concentration was measured using Nanodrop®. The samples were stored at -80°C.

These RNA sample were then used to prepare cDNA for use in qPCR experiments.

## 3.18 cDNA synthesis

The cDNA from RNA was prepared using the Applied Biosystems® High Capacity RNA-to-cDNA kit using the manufacturer's protocol. RNA samples are very fragile and can disintegrate very quickly thus, the entire procedure was carried out keeping all ingredients on ice. This ensured stability of samples along with good yield of final product.

**Table 3.6: List of RNA to cDNA PCR synthesis components**

| Components | Volume (µL) |
|---|---|
| 2X RT buffer | 10.0 |
| 20X Enzyme Mix | 1.0 |
| RNA sample | Up to 9 µL |
| Nuclease free water | Quantity sufficient to 20 µL |
| Total reaction volume | 20.0 |

The reaction mix was aliquotted in PCR tubes and was briefly centrifuged to remove any air bubbles. The reaction was incubated at 37°C for one hour and the reaction was held at 95°C for five minutes followed by 4°C hold. The cDNA was then ready to be used for further applications and was stored at -20°C.

## 3.19 Quantitative PCR (qPCR)

Quantitative PCR allowed measurement of relative expression of different genes relative to a house keeping. Quantitative or real-time PCR follows the amount of amplification of DNA while the reaction

takes place and can report the amplification in a linear manner. The amount of end product is dependent on the fluorescence produced by the reporter dye, which was SYBER®Green (Thermo Fisher Scientific) in this case. It is a DNA binding dye which emits light upon binding to the DNA which is then calculated by the system to give a measure of end product produced. This measurement is done for all the genes of interest along with a house keeping gene. Comparison of individual gene expression to the house keeping gene provides the relative expression of different genes.

### 3.19.1 **Preparation of master mix**

The master mix was prepared by mixing the forward and reverse primers along with water and SYBER®Green. The prepared samples were kept at ice during the entire length of time. The plate was also kept at ice while samples were pipette into the wells. This is important to avoid disintegration of any component and ensure smooth amplification. The reaction mix is prepared as follows:

**Table 3.7: Primer mix for quantitative PCR**

| Reaction components | Amount per well (µL) |
|---|---|
| Reverse primer (10 pmol) | 0.5 |
| Forward primer (10 pmol) | 0.5 |
| $H_2O$ | 2.5 |
| SYBER®Green | 7.5 |

### 3.19.2 **Preparation of standards and samples**

The prepared cDNA was diluted 1:1. Amount of water for each standard solution was calculated by multiplying the number of wells required for each standard with 4.5. The calculated amount of water divided by 4 gave the amount of cDNA required for each standard

dilution. Sum of the calculated water and cDNA amount equalled as the standard 1, which was used for preparing subsequently diluted standards. Standard1 had a concentration of 100% with no water added. It was prepared by mixing equal amounts of cDNA from all individual samples. Standard 2 was prepared by taking calculated amount of cDNA mix from Standard 1 and adding the calculated amount of $H_2O$, it had a concentration of 20% relative to standard 1. In similar manner standard 3 was prepared from standard 2 and standard 4 was prepared using standard 3. Standard 3 and 4 had a concentration of 4% and 0.8%, respectively.

The individual samples were prepared by making 1:10 diluted samples using water. The final volume was calculated and prepared so that 4 µl of sample could be added to each well where the master mix was already pipetted.

### 3.19.3 **Preparing the qPCR plate**

Once the samples, standards and master mix were prepared they were pipetted in the LightCycler® 480 multi-well plate, 96 (Roche). The columns on the qPCR plate were different genes of interest. The master mix containing the particular gene primers was pipetted into the wells designated for that gene. Once the master mix for all genes was pipetted 4 µL of the standard solutions and samples were pipetted in each well. Each time the sample was pipetted a fresh tip was used to ensure the sample solution was not contaminated by the master mix already present in the wells.

Following is the qPCR sample loading plate layout. Each sample was loaded in triplicate to avoid error. Rows were assigned to particular genes and samples were labelled properly.

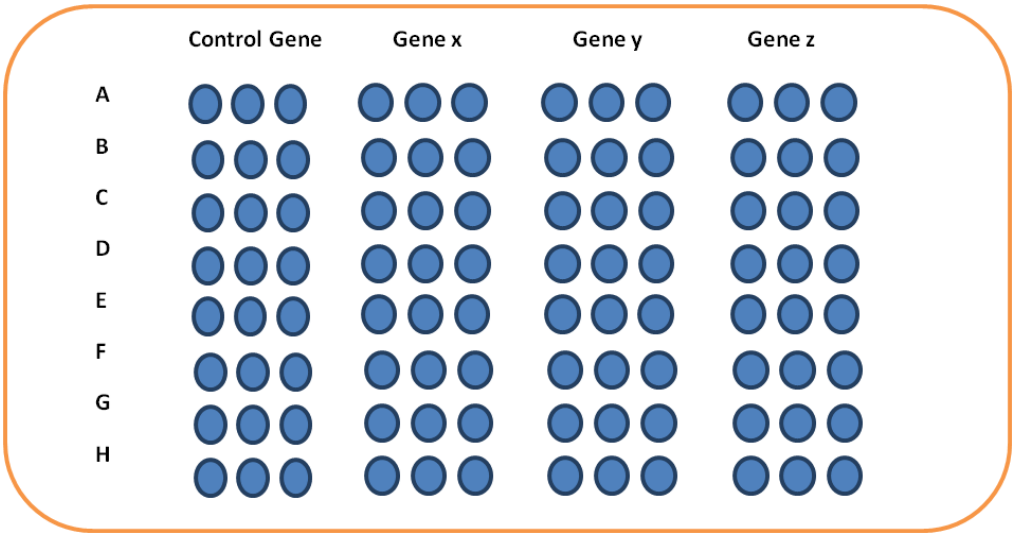


**Figure 3.2: Schematic diagram of sample plating arrangement for qPCR**

Once the pipetting was complete the plate was covered with a sticky plastic flap provided with the qPCR plates. The plates were then rotated in a centrifuge machine at 1000 rpm for 1 minute to settle down all the components. The plate was then loaded into the thermal cycler. The PCR conditions applied are as follows:

**Table 3.8: Conditions for Quantitative PCR**

| Steps | Temperature | Time |
|---|---|---|
| Denaturation (1 cycle) | 95°C | 7:00 minutes |
| Denaturation<br>Annealing (35 cycles)<br>Extension | 96°C<br><br>58°C<br><br>68°C | 10.00 seconds<br>30.00 seconds<br>1:30 minutes |
| Final extension (1 cycle) | 68°C | 7:00 minutes |
| Hold | 4°C | 0:00 |

## 3.20 Mouse cytokine array

Cytokine and chemokine expression in macrophage supernatant from WT and Stamp2-KO mice was analysed using Mouse Cytokine array panel A (R&D systems®). Selected capture antibodies on nitrocellulose membranes were incubated with the sample and detection antibody mix. All the reagents were brought to room temperature and working solutions were prepared according to the provided instructions. 2 ml of array buffer 6 was pipetted into each well of the 4 well multi-dish. The membranes were placed in the wells containing buffer 6 and incubated for one hour. This buffer acts as a block buffer. While the membranes were blocking the samples were prepared. 700 µL of macrophage supernatant was added to 500 µL of array buffer 4. The final volume was adjusted to 1.5 ml using array buffer 6. 15 µL of detection antibody cocktail were added to each sample and incubated at room temperature for one hour. Buffer was aspirated from the multi-well dish, samples placed in the wells along with membranes and incubated overnight at 2-8°C with gentle rocking. The following day, membranes were removed from the sample-detection antibody mix and placed in a separate plastic container; 20 ml of 1X wash buffer were added and put on a shaking platform for 10 minutes. Membranes were then washed three times. Subsequently, the diluted Streptavidin-HRP was added to each well and membranes transferred into it. The samples were then incubated at room temperature for 30 minutes, and washing of membranes repeated as explained earlier. 1 ml of chemi-reagent mix was then added onto each membrane and incubated for 1 minute. The membranes were then transferred onto an autoradiography cassette and covered with clear plastic sheet. In a dark room, the photosensitive x-ray films (AmershamTM Hyperfil ECL) were exposed to the membranes and the signals appeared as dots representing various cytokines and chemokines were viewed after developing the

films in Curix 60 developer (AGFA). The exposure time was kept at 10 seconds to 10 minutes.

### 3.20.1 Cytokine array data analysis

The membrane images along with the dots representing various cytokines and chemokines on developed photosensitive films were scanned and the image was then analyzed using adobe Photoshop software. Intensity of individual dot for each sample was calculated and background noise was subtracted. The numerical values obtained from the software were then added onto a separate excel sheet along with the corresponding panel codes representing each dot and what it refers to.

## 3.21 PASMCs and HMVECs in hypoxia

Human and mouse PASMCs and HMVECs were cultured on 10 cm Petri plates and grown until plates were almost confluent. The cells were then prepared to be put in the hypoxia chamber, washed with PBS and fresh medium added. At first the 72 hour time point plates of cells were put in the hypoxia chamber, next day the 48 hour and the finally the 24 hour time point plates were added. Growth medium was changed on alternate days for all the plates which was done rather quickly to ensure the hypoxia effect was continued. Cells kept at normoxia were added as 0 hour control. Upon completion of defined time points the plates were removed and the cells were subjected to protein and RNA extraction. These samples were then used for western blot and qPCR to determine required gene expression.

## 3.22 **Wound healing/Scratch assay:**

PASMCs were cultured in 24-well-plates at a density of $1x10^5$ cells per well. After 24 hours the medium was aspirated and the wells were washed with PBS. The cells were then starved with starvation medium for 24 hours. On the following day using a 1000 µl tip a straight scratch was made vertically in the centre of each well. The wells were then filled with the conditioned medium according to the experiment, hunger medium (HM), normal medium (NM) and supernatant from WT and Stamp2-KO macrophages, various cytokines and/or neutralizing antibodies. At two time points of 0 and 24 hours the region of the well where scratch was made was photographed. The level of scratch cover defined the level of cell migration; the cells covering the scratch could be clearly seen. The area of the scratch before and after treatment at defined time points was measured using ImageJ software and analysis was performed. The covered area relative to the initial clear scratch determined the extent of wound healing.

# 4. Results

# 4 Results

## 4.1 Regulation of Stamp2 in disease

### 4.1.1 Stamp2 is downregulated in human and experimental PAH lung vessels

Detailed immunohistological analysis of lung sections revealed that the induction of PAH by hypoxia and Sugen/hypoxia as well as human disease were associated with reduced Stamp2 expression in the pulmonary vessels (Figure 4.1). The lung sections obtained from experimental PH models of mouse (21 days hypoxia) or rat (Sugen/ hypoxia) as well as human idiopathic PAH (IPAH) patients showed decreased staining for Stamp2.

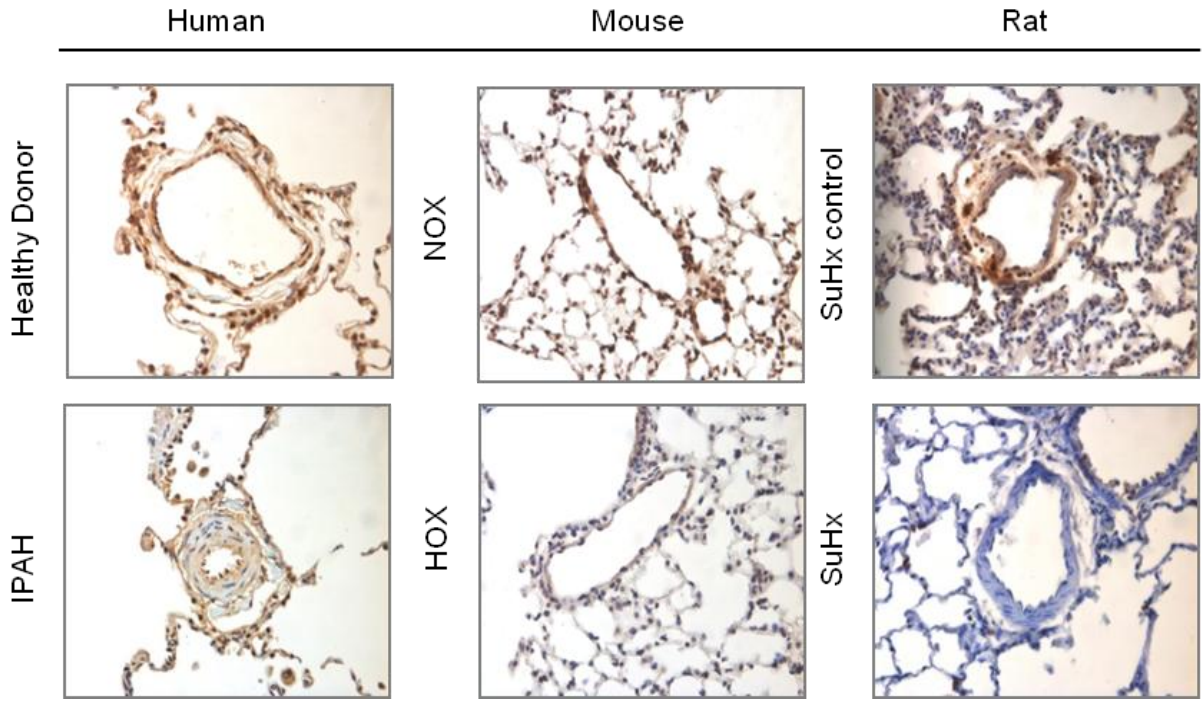


**Figure 4.1: Stamp2 is downregulated in human and experimental PH**

*Stamp2 expression in lung sections of mouse or rat model of PH and PAH patients studied using immunohistochemistry. The brown colour represents Stamp2 around the pulmonary vessels viewed at 400x magnification.*

### 4.1.2 Downregulation of Stamp2 expression in human PAH, mouse lung from hypoxia induced PH, rat lungs from Sugen/hypoxia induced PH

Protein lysates and cDNA were used to perform Western blotting and qPCR to evaluate Stamp2 expression. The human tissue from PAH patients showed a downregulation in Stamp2 expression at the protein level when compared to human lung lysates from healthy subjects (Figure 4.2A). Densitometry analysis was performed on the Western blot images to obtain quantitative values (Figure 4.2B).

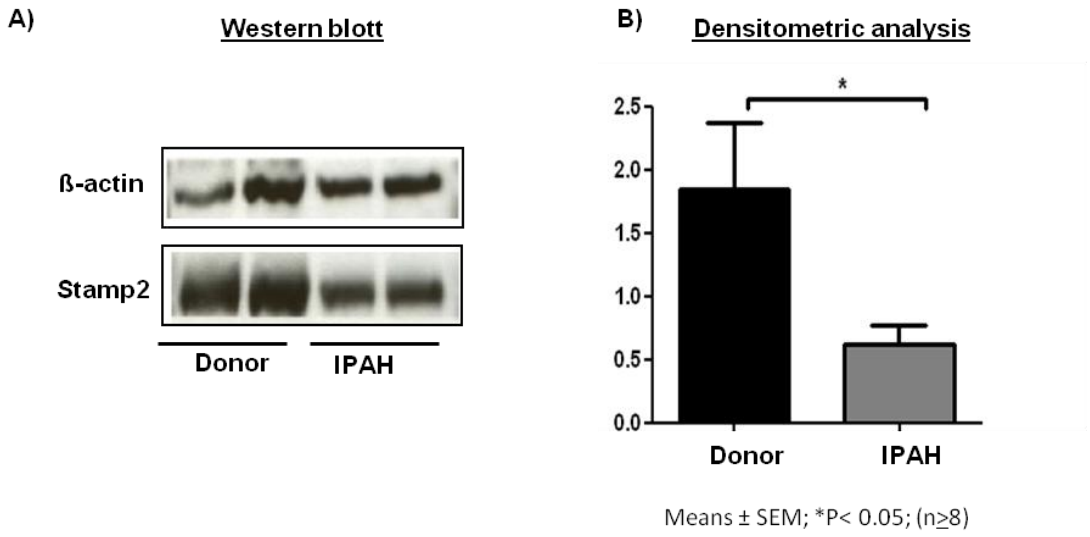


**Figure 4.2: Downregulation of Stamp2 expression in human lungs from IPAH patients and healthy donors**

*(A-B) Western blot protein bands and respective densitometry analysis shows Stamp2 downregulation in human PAH lung lysates as compared to healthy donor lungs. β-actin was used as loading control for western blot, and 18s was used as the housekeeping gene to normalize the Stamp2 expression in qPCR.*

In order to monitor the regulation of Stamp2 expression upon development of PH in mice, we looked at the STAMP2 protein and mRNA expression in lung lysates. Protein and mRNA samples from lungs of mice kept in normoxia and hypoxia were used. Stamp2 expression was significantly downregulated at both the protein and

mRNA levels in lungs of WT mice kept under hypoxia as compared to the normoxia control.

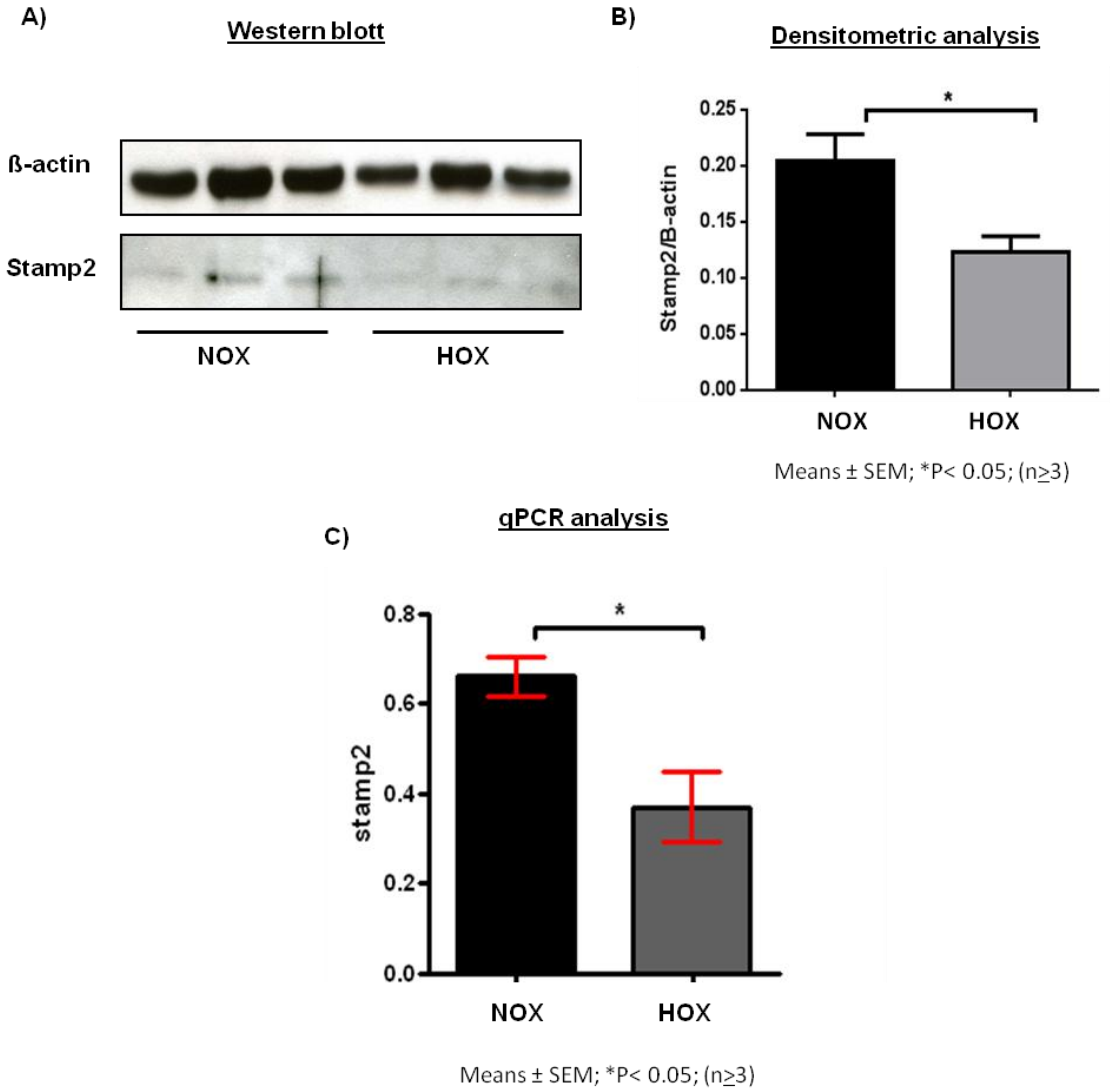


**Figure 4.3: Downregulation of Stamp2 expression in mouse lungs from hypoxia induced PH and normoxia controls**

*(A-B) Western blot protein bands and respective densitometry analysis shows Stamp2 downregulation in hypoxia mouse lung lysates as compared to normoxia mouse lungs. β-actin was used as loading control.*

*(C) qPCR demonstrating Stamp2 downregulation at mRNA level in hypoxia mouse lungs in comparison to normoxia mouse lungs. 18s was used as housekeeping gene to normalize the Stamp2 expression in qPCR.*

Stamp2 expression was also significantly downregulated in lungs of rats with experimental PH, who were subjected to Sugen/hypoxia as compared to control rats. Stamp2 downregulation was observed at both protein and mRNA levels (Fig 4.4). Densitometry analysis was performed on the Western blot images to obtain quantitative values.

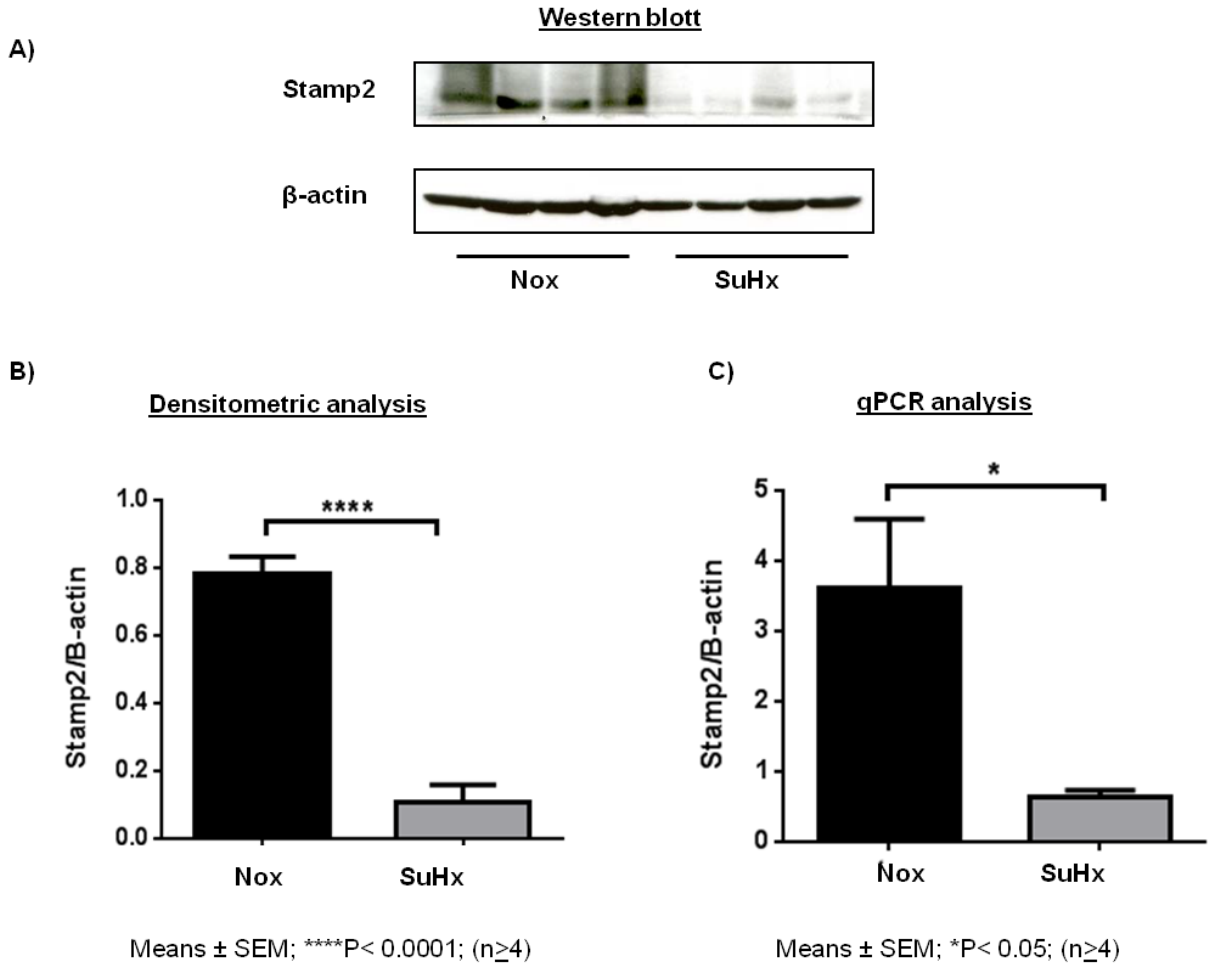


**Figure 4.4: Downregulation of Stamp2 expression in rat lungs from Sugen/ hypoxia induced pulmonary hypertension**

*(A) Western blots showing Stamp2 downregulation in Sugen/hypoxia rat lung lysates as compared to normoxia control. β-actin was used as loading control.*

*(B) Densitometry analysis of the western blots shows a significant downregulation of Stamp2 in Sugen hypoxia rat lungs*

*(C) Significant Stamp2 downregulation at mRNA level measured by qPCR, 18s was used as housekeeping gene to normalize the Stamp2 expression in qPCR.*

### 4.1.3 Stamp2 is downregulated in left and right mouse ventricles upon exposure to hypoxia

When looking at myocardial tissue in the hypoxia mouse model, the left ventricle (LV) and right ventricle (RV) lysates from mice kept under three weeks of hypoxia showed significantly lower Stamp2 expression in comparison to the normoxia controls (Fig 4.5) indicating that Stamp2 regulation by hypoxia is not limited to vascular tissue but also involves heart.

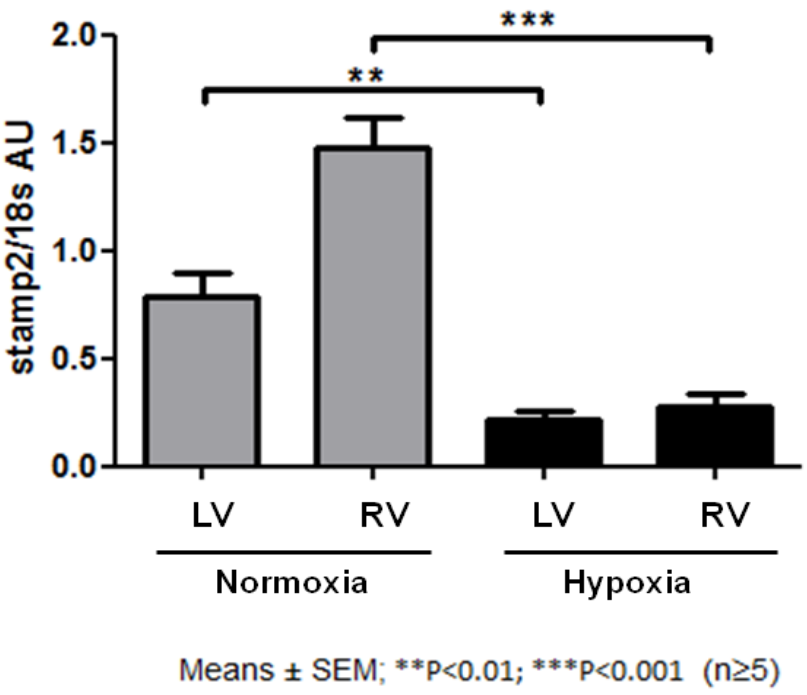


**Figure 4.5: Stamp2 is downregulated in the left and right mouse ventricles upon exposure to hypoxia**

*qPCR analysis showing significantly lower Stamp2 mRNA expression in left ventricle (LV) and right ventricle (RV) lysates as compared to the normoxia controls. 18s was used as housekeeping gene to normalize the Stamp2 expression.*

## 4.2 Stamp2 deficiency leads to development of hypoxia-induced pulmonary hypertension in mice

### 4.2.1 Development of higher right ventricular pressure in Stamp2 KO mice

In order to determine if and how Stamp2 deficiency in mice leads to development of pulmonary hypertension, a hypoxia (10%O2) versus normoxia experiment was performed. Mice were kept in hypoxia conditions for three weeks and control mice were kept in normoxia. After the described time point, the RVSP was measured. The WT and Stamp2-KO mice kept under normoxia showed no significant difference in the RVSP. In contrast, WT mice kept under hypoxia showed a significantly higher RVSP (30.36 ± 1.1 mmHg) as compared to their respective control normoxia WT mice (23.96 ± 0.7 mmHg) (Figure 4.6 A). This confirmed the validity of the experiment and also ensured hypoxia as the right tool to develop PH in mice. The same was observed for the Stamp2-KO mice under hypoxia.

However, a significantly more pronounced increase in RVSP (33.24 ± 0.5 mmHg) was observed in the Stamp2-KO mice kept under hypoxia in comparison to the WT counterparts (30.36 ± 1.1 mmHg) (Figure 4.6 A). This indicated that absence of Stamp2 leads to enhanced PH development in mice.

During the measurement of RVSP, other hemodynamic parameters were also recorded alongside, including the heart rate (HR) and systemic arterial blood pressure (SAP). These parameters served as control for the RVSP measurements since the measured values for HR and SAP remained minutely different among different groups and conditions (Figure 4.6 B and C).

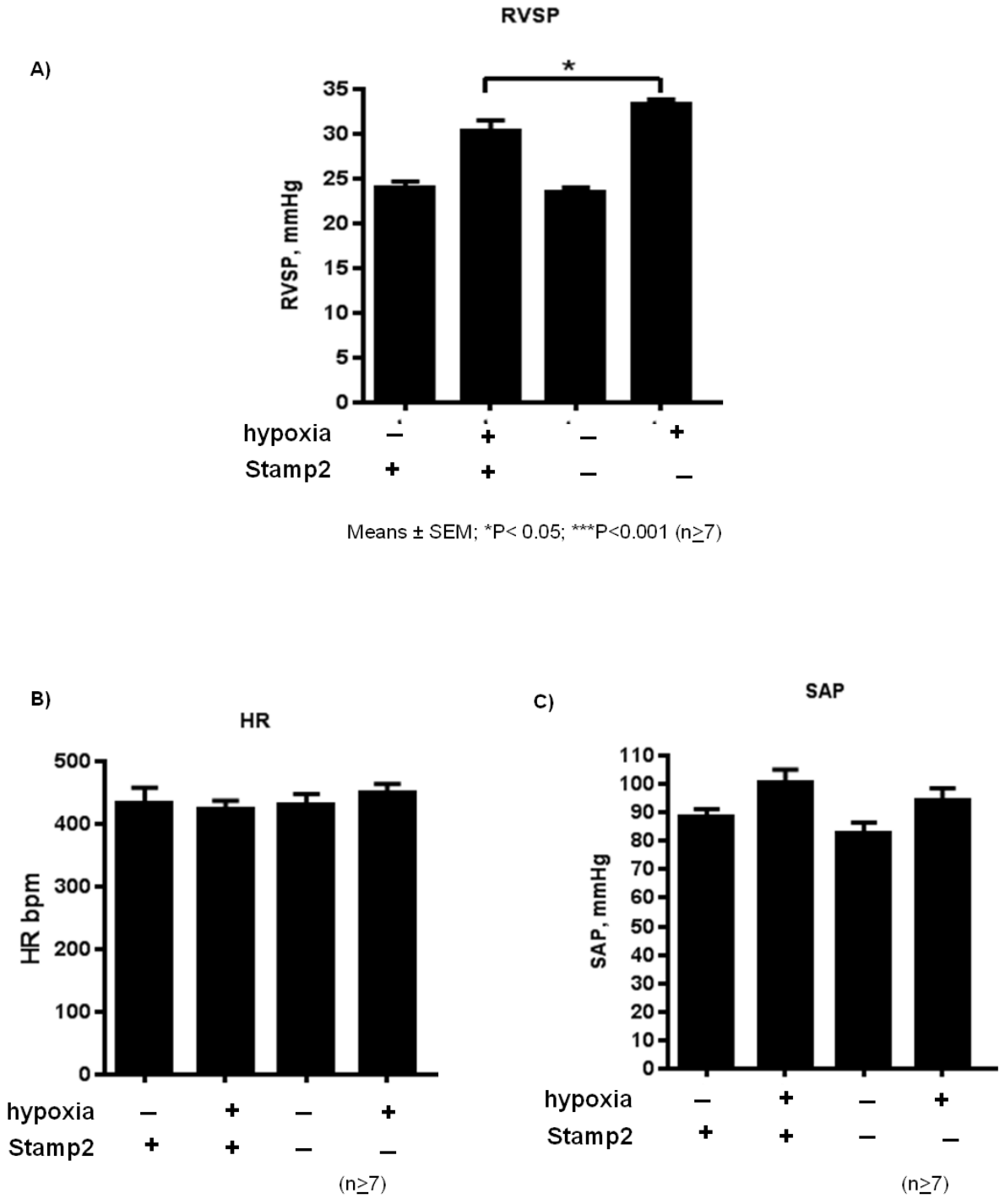


**Figure 4.6: Stamp2 deficiency leads to development of hypoxia induced pulmonary hypertension in mice**

*(A) Stamp2-KO mice show significantly higher RVSP as compared to WT*

*(B) –(C) WT and Stamp2-KO mice kept under hypoxia and normoxia showed no significant difference in the systemic arterial pressure (SAP) and the heart rate (HR).*

### 4.2.2 Right ventricular hypertrophy in normoxia versus hypoxia exposed mice

Right ventricular (RV) hypertrophy was determined by calculating the weight ratio of the dissected right ventricle and left ventricle along with septum (RV/LV+S). Although a significantly higher RVSP was recorded for the Stamp2-KO mice under hypoxia in comparison to WT, such increase in RV hypertrophy was not observed. While a significant increase in RV hypertrophy in both WT and Stamp2-KO mice under hypoxia was observed in comparison to normoxia, the difference between WT and Stamp2-KO under hypoxia was not statistically different (Figure 4.7).

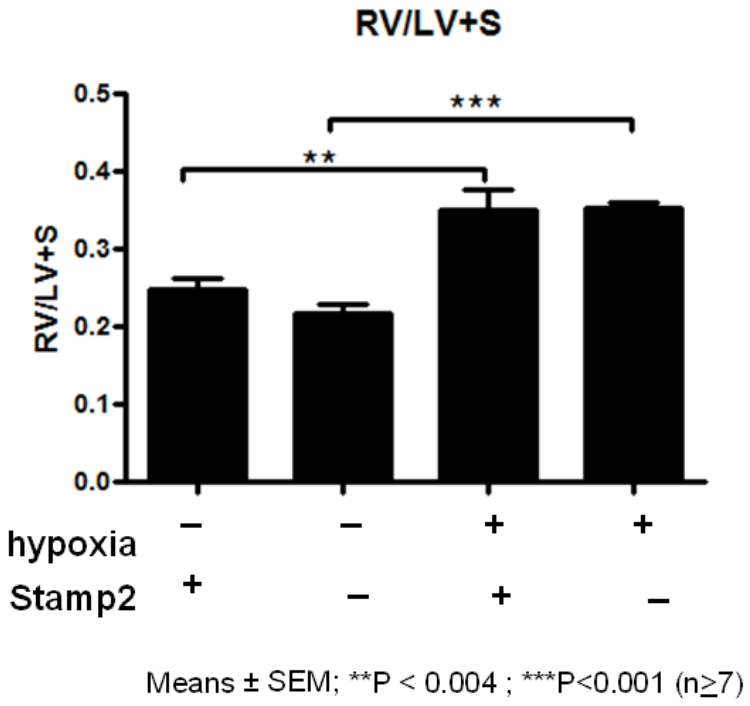


**Figure 4.7: Right ventricular hypertrophy in normoxia and hypoxia exposed mice**

*Both WT and Stamp2-KO right ventricle showed development of significantly higher degree of hypertrophy under hypoxia as compared to normoxia controls*

### 4.2.3 Stamp2 deficiency leads to higher muscularization in the pulmonary arteries

Hypoxia-induced PH was associated with higher muscularization of the pulmonary arteries. The lung vessels from WT and Stamp2-KO mice kept in normoxia and hypoxia were profoundly analysed. Vessels showing more than 70% muscularization were considered fully muscularized (m), compared to partially muscularized (p) (less than 70% muscularization) or non-muscularized (n) vessels (less than 5% muscularization). Hypoxia-exposed lung vessels were visibly more muscularized as compared to the normoxia in both WT and Stamp2-KO mice (Figure 4.8 A). Quantitative analysis revealed that the hypoxia-induced muscularization of pulmonary vessels was significantly more pronounced in the Stamp2-KO mice as compared to the vessels from WT mice. 90-100 vessels per lung per animal were analysed and each group had a minimum 4 mice. Each group on the graph represents 400-500 vessels (Figure 4.8 B).

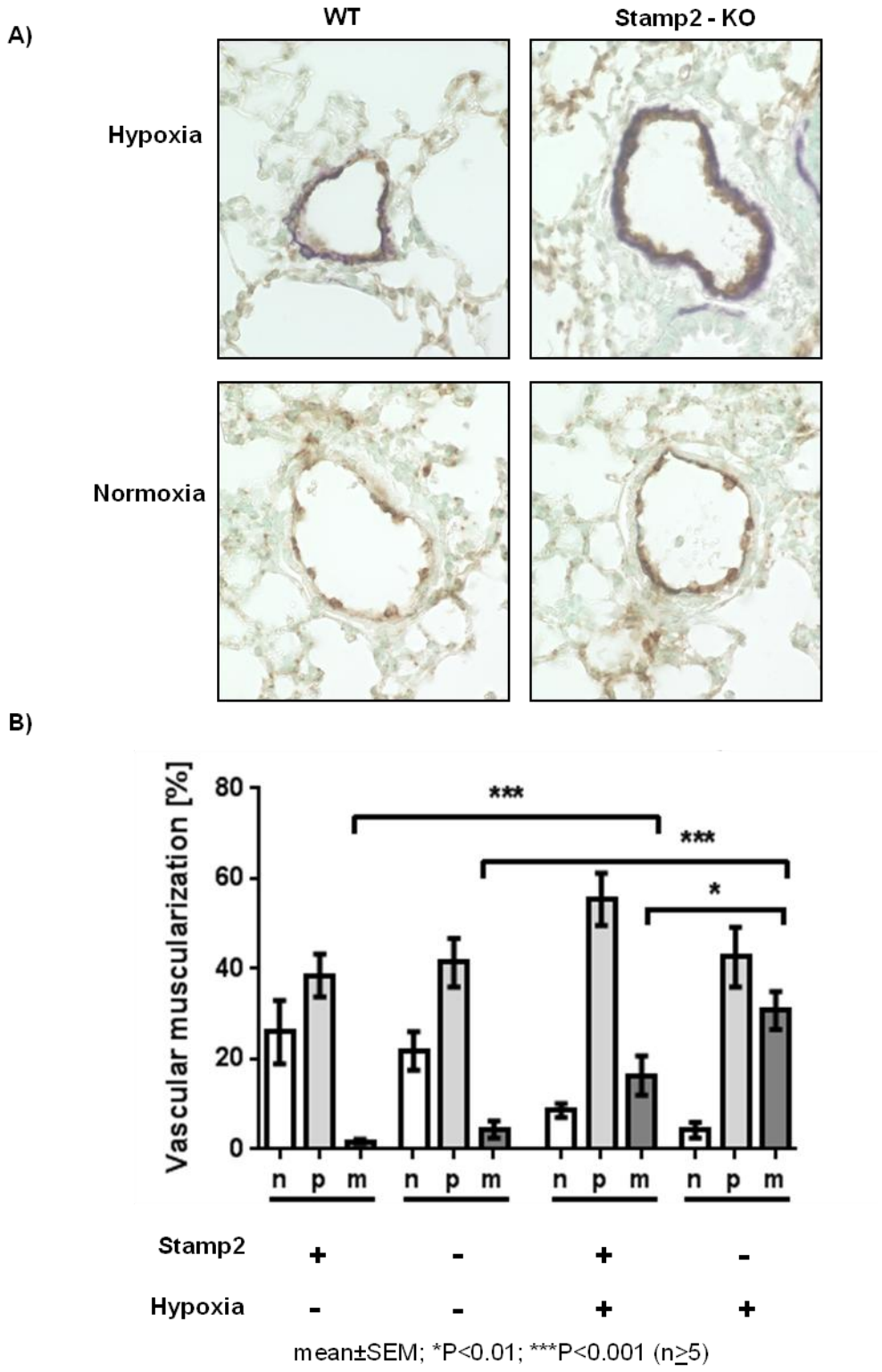


**Figure 4.8: Muscularization of pulmonary vessels in WT vs. Stamp2-KO mouse lungs exposed to normoxia or hypoxia**

*(A) Lung tissues from normoxia and hypoxia treated mice were double stained for endothelial cells and smooth muscle cells, staining shown in brown and violet colour respectively. Vessels were viewed at 400x magnification*

*(B) The smooth muscle cells stained vessels analyzed to generate quantitative values, n=non muscularized vessels), p= partially muscularized vessels and m= fully muscularized vessels*

## 4.3 Expression of Stamp2 in different cell types

In order to study how absence of Stamp2 enhances the development of PH and how the inflammation profile in the lungs is affected upon exposure to hypoxia and in absence of Stamp2, it appeared important to analyze the expression of Stamp2 in the distinct cells forming the vasculature. These cell types are responsible of secreting immunomarkers or for drawing immune reactions which may contribute to disease development. Thus, it is imperative to first assess how Stamp2 expression is regulated in these cell types, and how presence or absence of Stamp2 regulates different cellular actions in these cell types. Once we established how various cells exhibit Stamp2 expression and regulate it under diseased conditions we were able to follow the inflammatory action around these cell types.

### 4.3.1 Stamp2 expression in various human cells

Various cell types that are part of the vasculature were assessed for the Stamp2 expression. In order to confirm whether Stamp2 is expressed in these cells, the expression was assessed at both protein and mRNA levels (Figure 4.9). Stamp2 expression was found in all investigated cell types, which included monocytes, macrophages, fibroblasts, PASMCs, hCAECs, and hMVECs. The hCAECs and hMVECs showed significantly higher expression as compared to the other cell types at the mRNA level. The protein expression of Stamp2 was also observed in all cell types except for monocytes. The expression in monocytes appeared too minimal to be detected on western blot although mRNA expression was clearly seen. The other cell types showed similar expression levels.

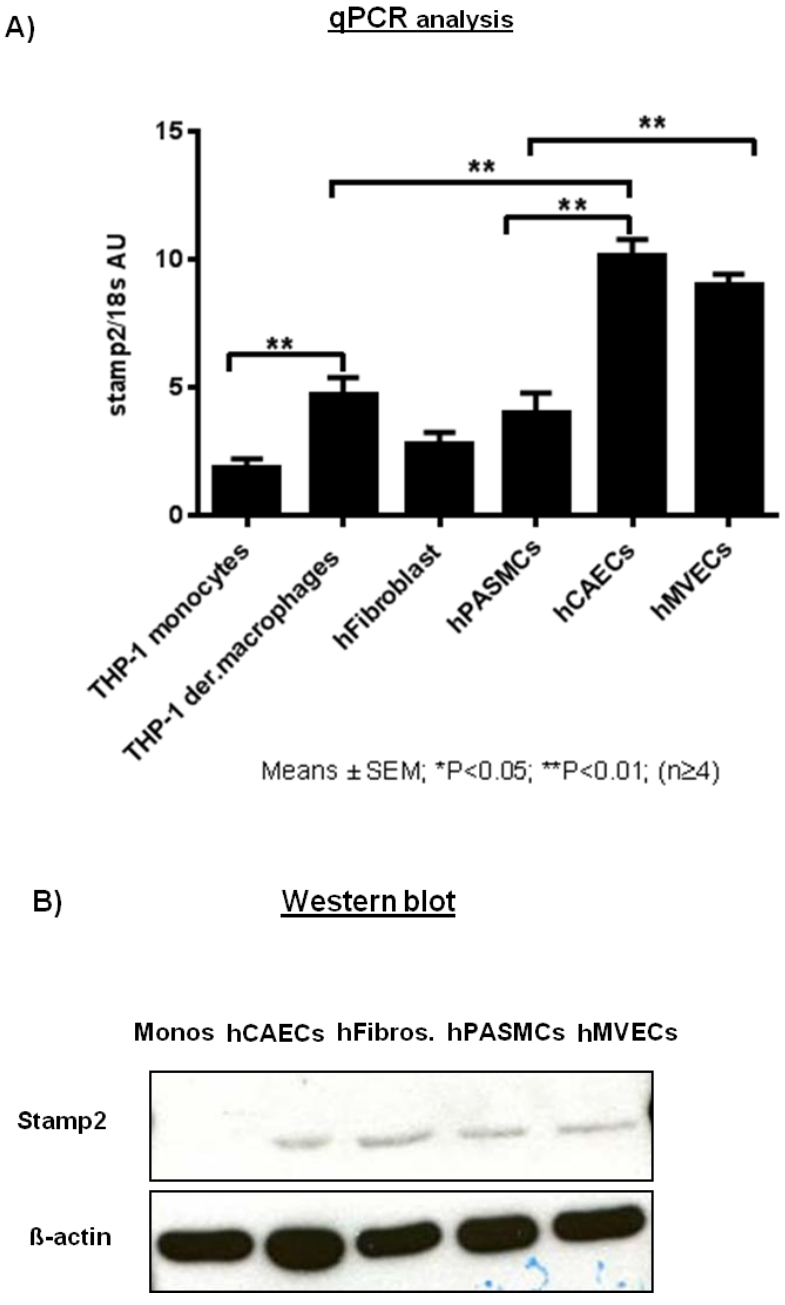


**Figure 4.9: Expression of Stamp2 in different human cell types**

*(A) mRNA expression of Stamp2 in RNA from different cell types was assessed using qPCR, all cell types. Monos = THP-1 monocytes, hCAECs = human coronary arterial endothelial cells, hFibros = human fibroblasts, hPASMCs = human pulmonary arterial smooth muscle cells, hMVECs = human microvascular endothelial cells.*

*(B) The protein expression of Stamp2 was similar in all cell types except for monocytes which showed minimal expression.*

### 4.3.2 Differentiation of human monocytes into macrophages

**As evident in the Figure 4.9**

Figure 4.9: Expression of Stamp2 in different human cell types and 4.10, the THP-1 monocytes showed no Stamp2 expression at protein level in comparison to other cells of the vasculature but the expression was clearly visible at the mRNA level (Figure 4.9 A). The monocytes were then differentiated into macrophages using PMA. The differentiated monocytes showed significantly higher Stamp2 expression at the mRNA level, and now expressed higher and detectable protein levels in comparison to monocytes as shown in Figure 4.10.

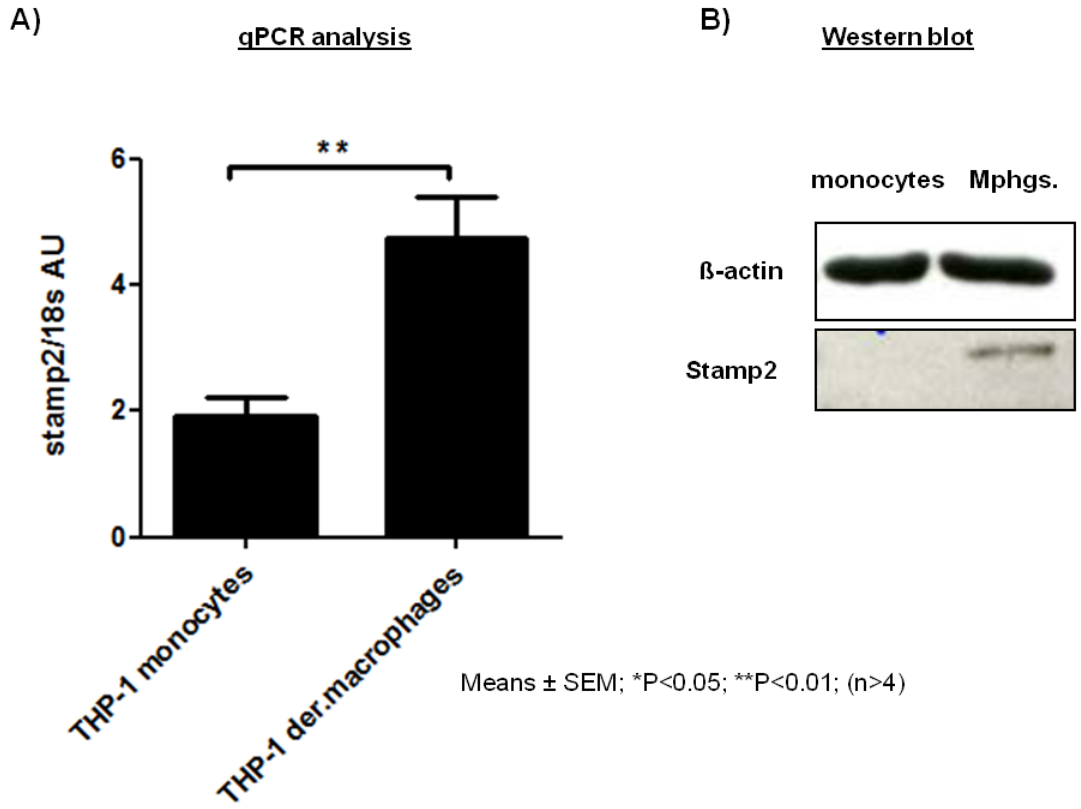


**Figure 4.10: Expression of Stamp2 in the THP-1 monocytes and THP-1 monocyte-differentiated macrophages**

*(A) mRNA expression of Stamp2 is low in THP-1 monocytes as compared to THP-1 monocytes derived macrophages.*

*(B) Western blot showing higher Stamp2 expression in THP-1 monocytes derived macrophages as compared to the THP-1 monocytes.*

### 4.3.3 Stamp2 expression in various mouse cells

In addition to human cells, various mouse cell types were also analyzed for Stamp2 expression at mRNA and protein levels. Here, Stamp2 was detected in PASMCs, macrophages, and fibroblasts (Figure 4.11). These cell types were selected considering the fact that most experiments used these cells and it ensured that the cells in question do express Stamp2. Notably, PASMCs and macrophages showed relatively higher Stamp2 expression as compared to fibroblasts.

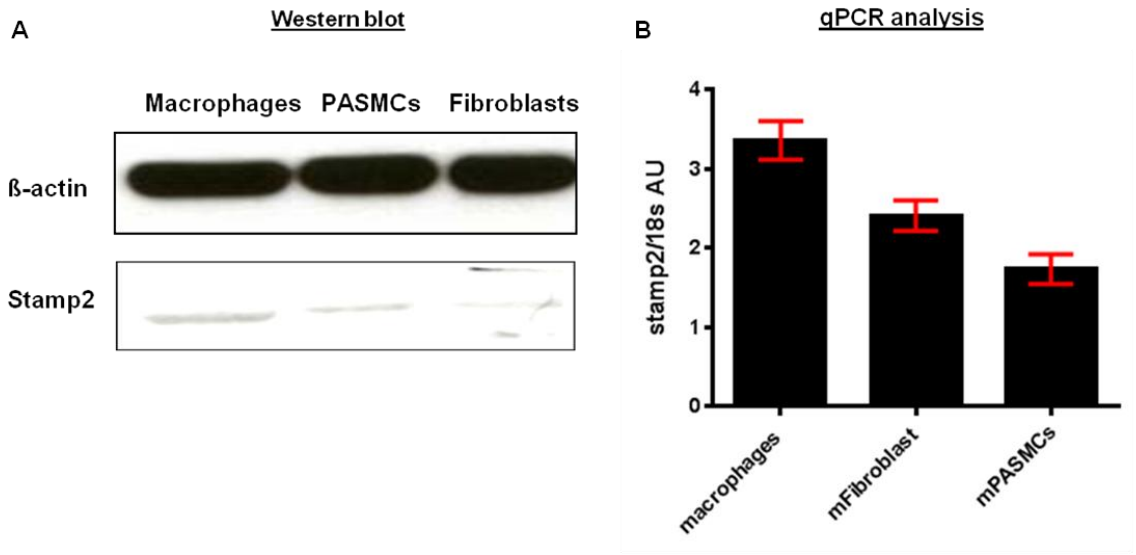


**Figure 4.11: Stamp2 expression in different mouse cells**

*Selected cells including macrophages, PASMCs and fibroblasts showed Stamp2 expression. The Stamp2 protein showed expression both at protein level as shown by western blot (A) and mRNA level measured by qPCR (B)*

## 4.4 Stamp2 regulation in vascular cells under hypoxia

### 4.4.1 Stamp2 is downregulated in hMVECs after exposure to hypoxia

Human microvascular endothelial cells were subjected to 24, 48, and 72 hours of hypoxia. The 0 hour time point represented the control condition of normoxia. Exposure to hypoxia resulted in downregulation of Stamp2 expression, and the expression level was minimal after 72 hours of hypoxia at both protein and mRNA levels (Figure 4.12). This confirms that exposure to hypoxia affects Stamp2 expression in this crucial cell type formulating the vasculature in humans. Our earlier results have established that lack of Stamp2 along with hypoxia leads to a higher degree of muscularization. This experiment showed that lack of proper oxygenation correlates with diminished expression of Stamp2.

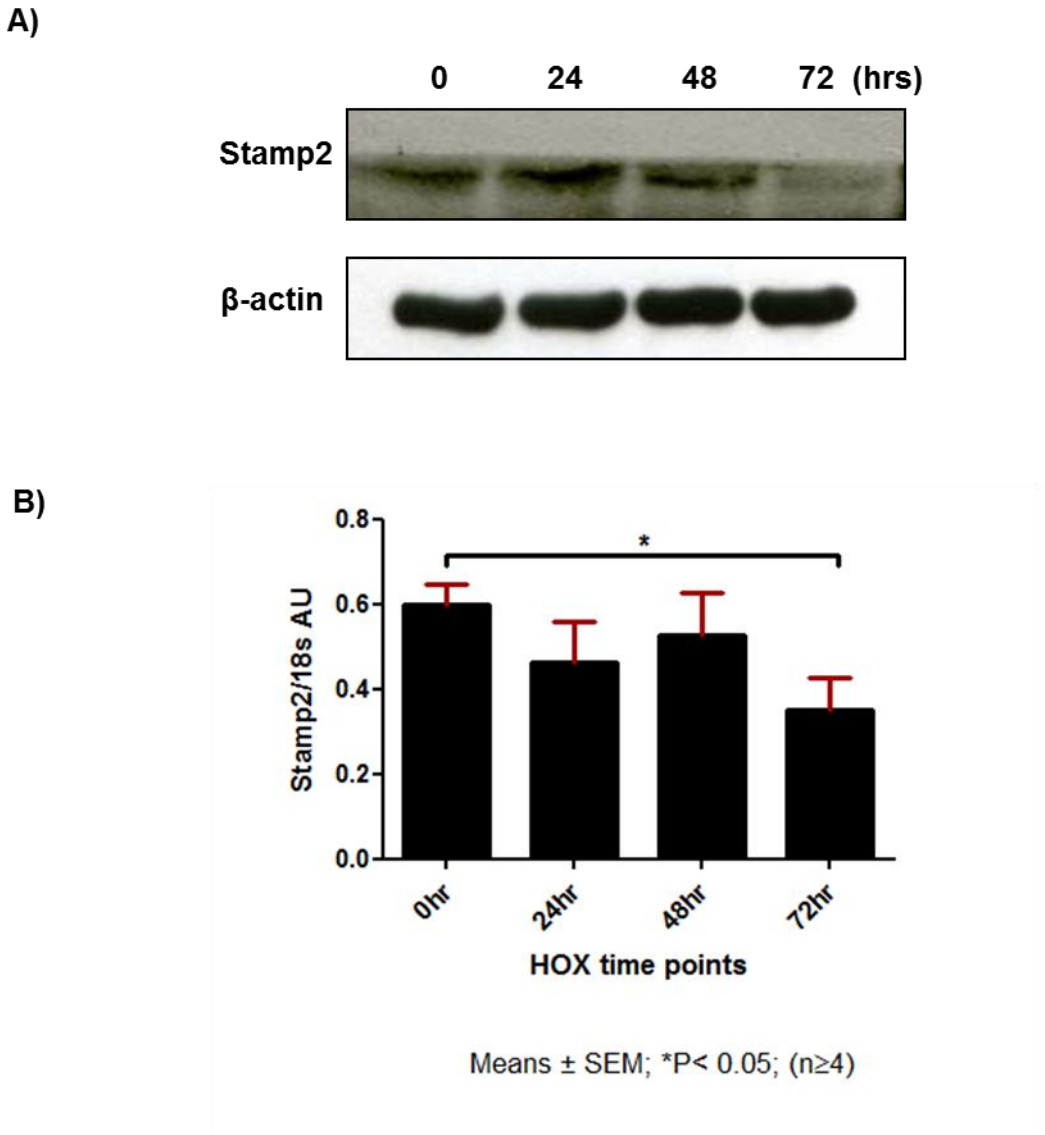


**Figure 4.12: Stamp2 is downregulated in human microvascular endothelial cells (hMVECs) after exposure to hypoxia**

*A) Western blot showing Stamp2 downregulation in hMVECs after 72 hours of hypoxia as compared to the 0 hour hypoxia control, β-actin was used as the loading control.*

*B) qPCR analysis showing significantly lower Stamp2 mRNA expression in (hMVECs) after 72 hours of hypoxia as compared to the 0 hour hypoxia control.18s was used as the housekeeping gene to normalize the Stamp2 expression.*

### 4.4.2 Stamp2 is downregulated after exposure to hypoxia in human and mouse PASMCs

Human and mouse PASMCs subjected to 24, 48, 72 versus 0 hours of hypoxia were utilized to analyse the regulation of Stamp2 expression. Hypoxia in a time-dependent manner led to decrease in Stamp2 expression at the protein and mRNA levels in both human and mouse cells (Figure 4.13). PASMCs are one of the most important cells involved in the development of increased pulmonary vascular resistance by actions of proliferation and apoptosis resistance, and the results shown here demonstrate that these cells regulate Stamp2 expression upon hypoxia exposure.

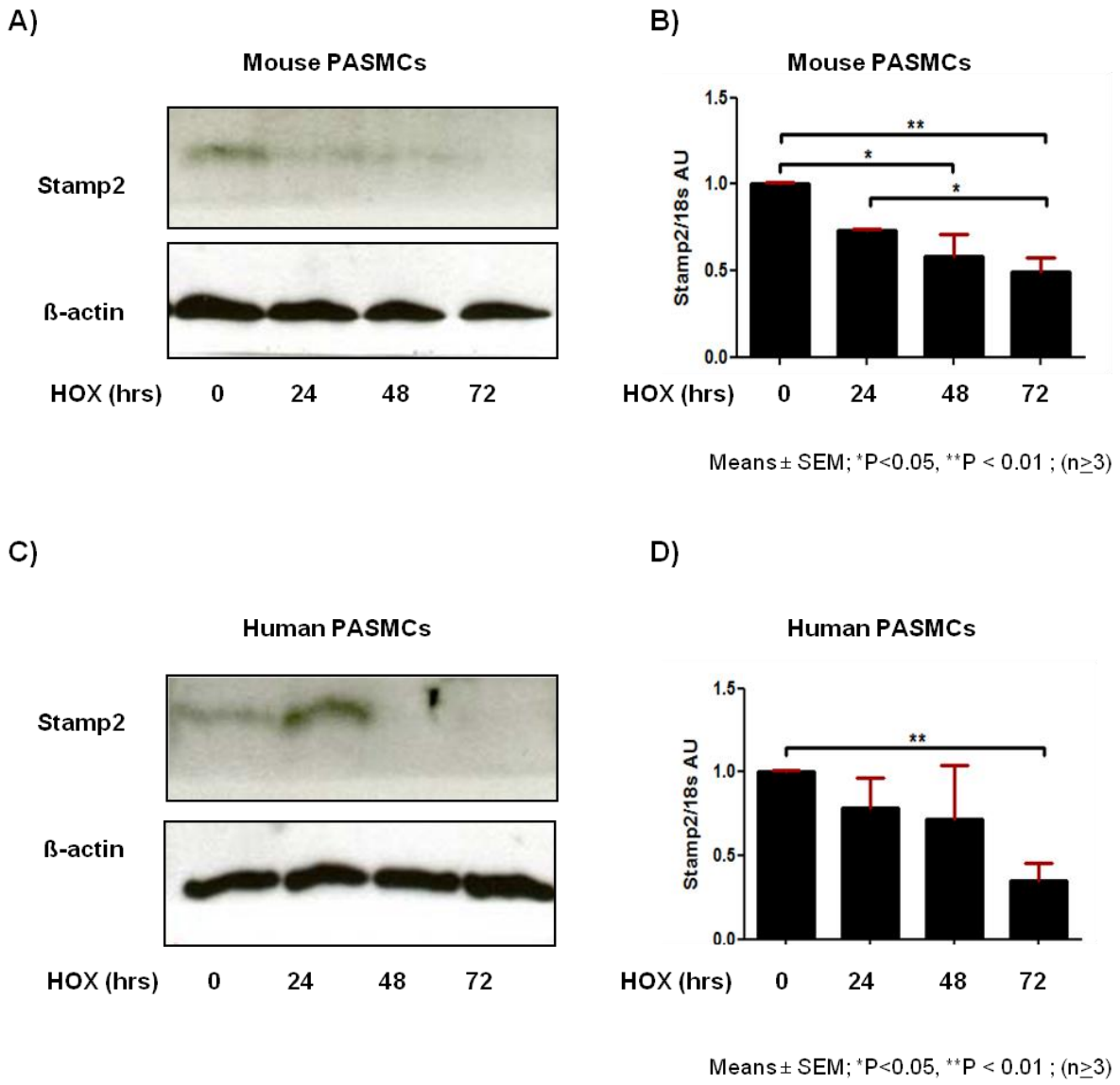


**Figure 4.13: Stamp2 is downregulated in human and mouse PASMCs after exposure to hypoxia**

*(A-B) Western blot showing Stamp2 downregulation in mouse PASMCs after 72 hours of hypoxia, qPCR analysis showing significantly lower Stamp2 mRNA expression in mouse PASMCs after 72 hours of hypoxia*

*(C-D) Western blot showing Stamp2 downregulation in human PASMCs after 48 hours of hypoxia, qPCR analysis showing significantly lower Stamp2 mRNA expression in mouse PASMCs after 72 hours of hypoxia*

### 4.4.3 Stamp2 is downregulated in mouse macrophages after exposure to hypoxia

Peritoneal macrophages from WT mice were subjected to 0, 24, 48 and 72 hours of hypoxia. Stamp2 expression under hypoxia was measured at the mRNA and protein levels by qPCR and western blot analysis. After 48 and 72 hours, a significant downregulation in Stamp2 expression was observed at both mRNA and protein levels (Figure 4.14).

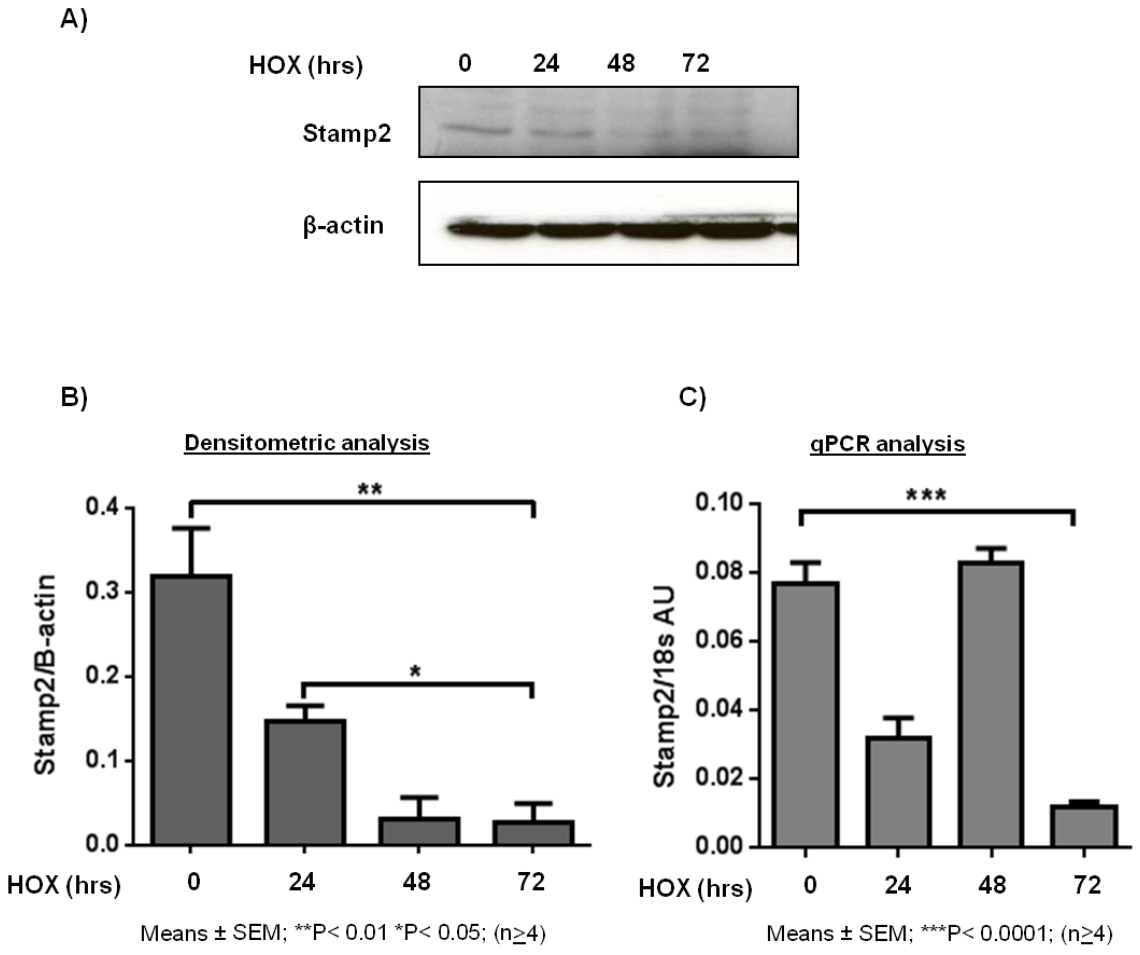


**Figure 4.14: Downregulation of Stamp2 in mouse macrophages under hypoxia**

*(A) Western blot showing Stamp2 downregulation in mouse macrophages after 48 and 72 hours of hypoxia. β-actin was used as the loading control*

*(B) Densitometry analysis for the western blot bands sown in (A)*

*(C) qPCR analysis showing significantly lower Stamp2 mRNA expression in mouse macrophages after 72 hours of hypoxia as compared to the 0 hour hypoxia control. 18s was used as the housekeeping gene to normalize the Stamp2 expression*

## 4.5 Stamp2 deficiency leads to elevated pulmonary inflammation

### 4.5.1 Stamp2 absence leads to accumulation of CD68 positive cells in the vessels

CD68+ staining was performed on lung sections from mouse lungs kept for three weeks in hypoxia or normoxia. The hypoxic Stamp2-KO mouse lung sections showed much stronger staining as compared to hypoxic WT lungs. The WT and Stamp2-KO normoxia control lung sections showed relatively less staining (Figure 4.15).

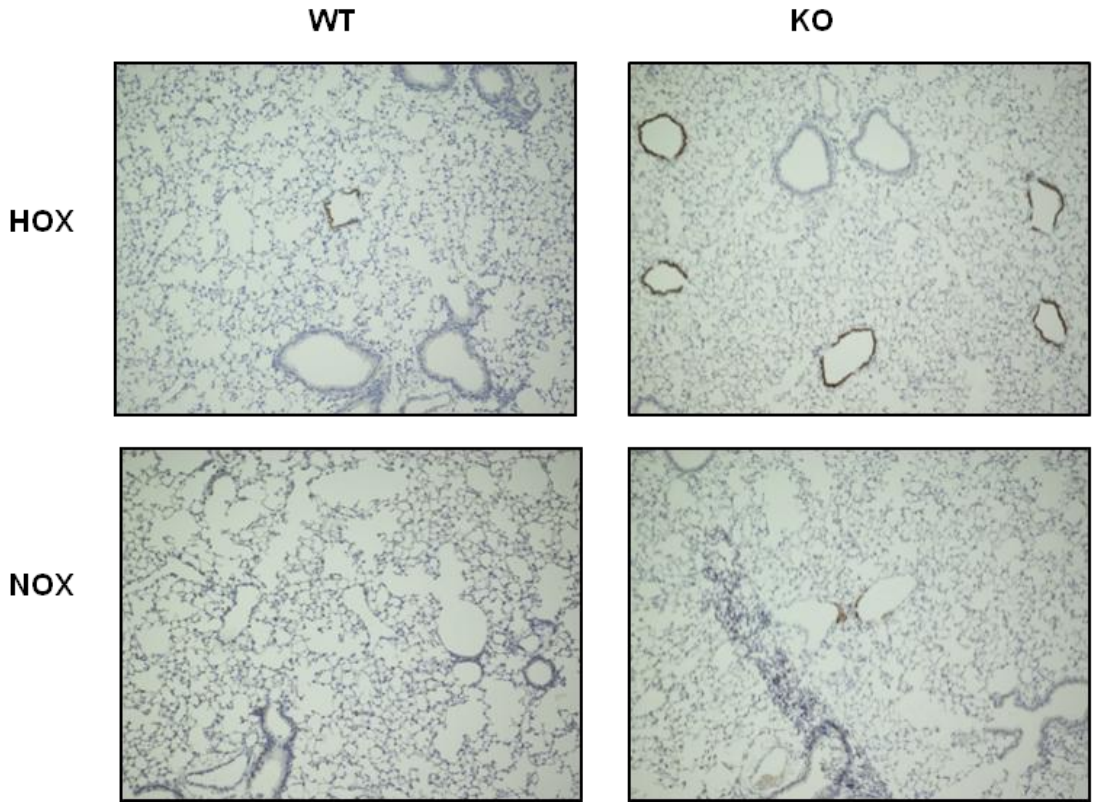


**Figure 4.15: Immunohistochemical staining for CD68+ cells in WT and Stamp2-KO mouse lungs**

*Immunostaining of WT and Stamp2-KO mouse lung sections was performed to observe CD68+ staining. Stamp2-KO mouse lung sections showed stronger staining in higher number of vessels as compared and normoxia control.*

In order to obtain quantitative data, equal numbers of positively stained vessels were counted from each lung and the stained area was measured for each vessel. Quantitative analysis revealed a hypoxia-induced increase of CD68+ cells in both genotypes, and a significantly higher number of positively stained vessels for CD68+ for hypoxia Stamp2-KO lung sections as compared to the hypoxia WT lung sections (Figure 4.16).

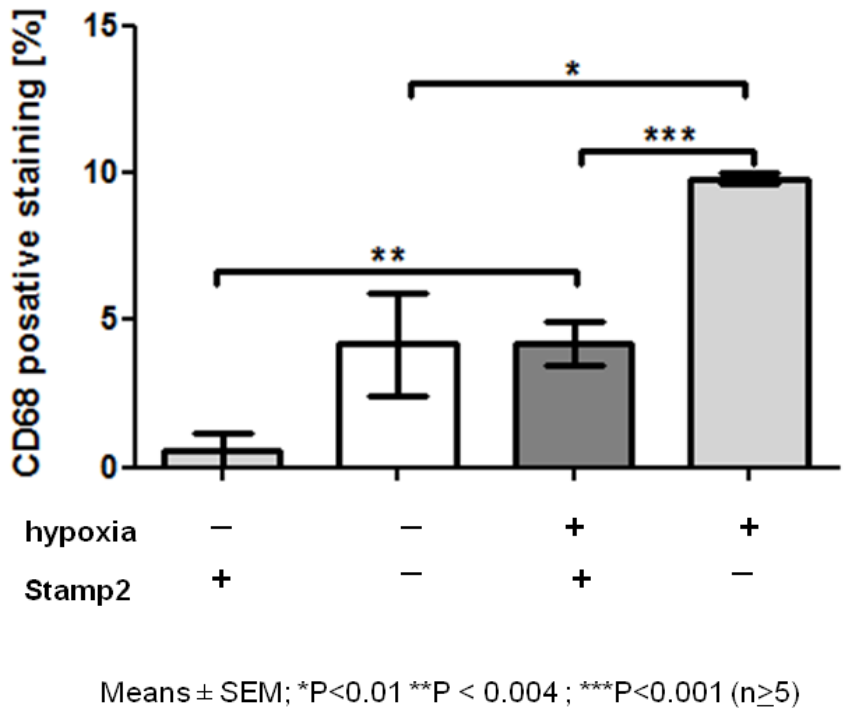


**Figure 4.16: schematic graph showing CD68+ staining in WT and Stamp2 KO mouse lungs**

*Stamp2-KO mouse lungs show significantly higher number of positively stained vessels for normoxia and hypoxia as compared to WT*

### 4.5.2 Double staining of mouse lungs to identify CD68+ stained cell type

In order to identify which cell type is exactly being stained for CD68 and to separate smooth muscle cells from the rest, double staining was performed for CD68+ cells and smooth muscle actin (SMA). Brown colour represents SMA, and violet/red colour represents CD68+ staining. As shown in Figure 4.17, the hypoxia Stamp2-KO lung sections showed stronger CD68+ staining then WT. The double staining showed another layer of CD68+ cells on top of smooth muscle cells stained which is different from the smooth muscle cells which are stained brown.

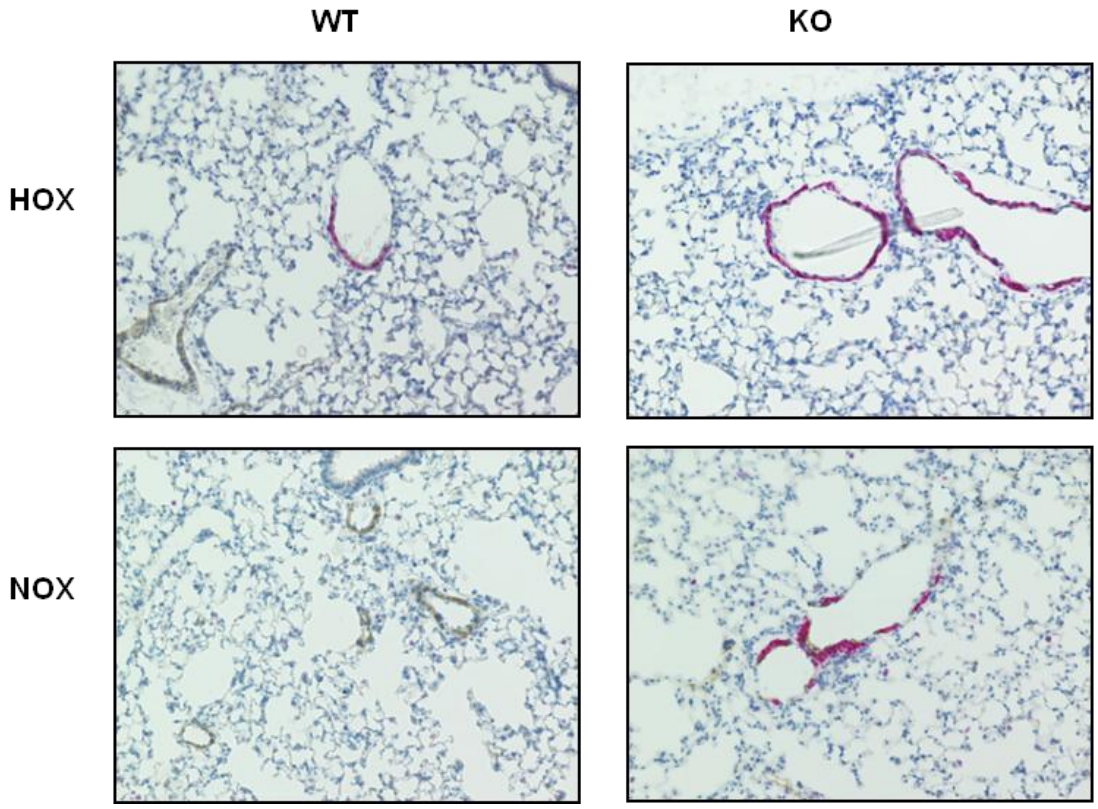


**Figure 4.17: Double staining of WT and Stamp2-KO mouse lungs to observe CD68+ cells and smooth muscle cells**

*Stamp2-KO mouse lung showed higher staining as compared and normoxia and the CD68+ cells (violet colour) appears to be present on top of smooth muscle cells (brown colour), vessels were viewed at 400x magnification.*

### 4.5.3 Cytokine expression in Stamp2-KO mouse lung is increased

Development of PH is known to be associated with an increase in inflammation; this was further observed in the lungs of mice which developed PH in comparison to control healthy mice. Once higher CD68+ staining in Stamp2-KO mouse lungs was observed it made sense to look into the inflammation profile of these mouse lungs.

To this end, mouse lung lysates were prepared form lungs of mice which were kept for three days and three weeks under hypoxia. The mRNA expression of the cytokines was measured using quantitative PCR. Lysates isolated from normoxia and hypoxia-exposed Stamp2-KO mouse lungs showed higher expression of inflammatory cytokines as compared to the control WT lung lysates. The differences were much more pronounced after three weeks of hypoxia as compared to the three day hypoxia exposure. Significantly higher expression was particularly observed for the cytokines IL-1β, IL-6, MCP-1, and TNFα (Figure 4.18).

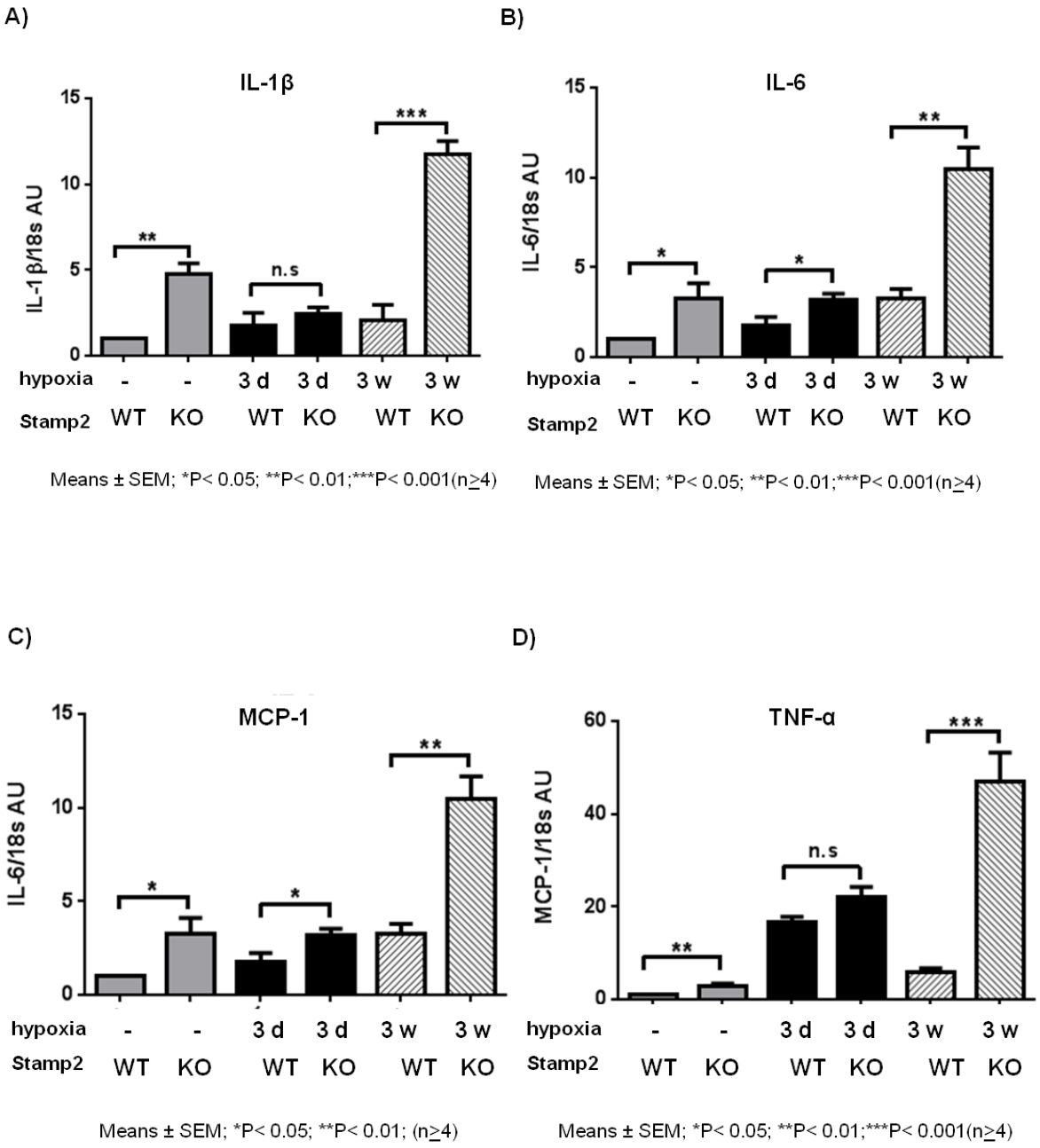


**Figure 4.18: Stamp2 deficiency leads to elevated pulmonary inflammation**

*RNA from Stamp2-KO and WT mouse lungs from hypoxia and normoxia exposed mice was used for qPCR; the Stamp2-KO mouse lungs showed significantly higher mRNA expression of IL-1β (A),IL-6 (B),MCP-1 (C) and TNF-α (D). Two different hypoxia exposure time points of three days (3d) and three weeks (3w) were used and 0 hours of hypoxia was used as the control.*

### 4.5.4 Stamp2 deficiency leads to higher Endothelin-1 (ET-1) expression

Stamp2-KO mouse lung lysates from mice subjected to three weeks of hypoxia showed significantly higher ET-1 expression as compared to hypoxic WT mouse lungs (Figure 4.19). Interestingly, this marked difference was only observed under hypoxic conditions. ET-1 is a known contributing factor to the development of PH and is also known to contribute to vascularisation and vessel wall thickening, suggesting that regulation of ET-1 is relevant in this context.

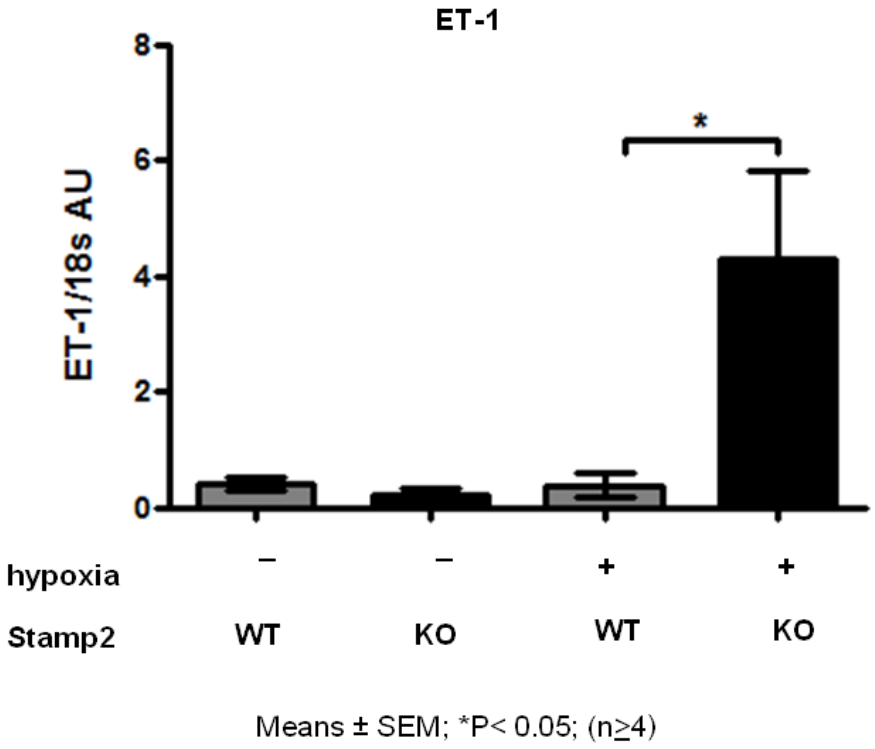


**Figure 4.19: Endothelin-1 (ET-1) expression in WT vs Stamp2-KO mouse lungs**

*mRNA from WT and Stamp2-KO mouse lungs kept in hypoxia and normoxia was used for qPCR, It shows higher mRNA expression of Endothelin-1 (ET-1) in Stamp2-KO as compared to the WT control.*

## 4.6 Stamp2 deficiency leads to increased general inflammation

### 4.6.1 Effect of hypoxia and Stamp2 deficiency on the concentration of ET-1 in mouse serum

Serum was isolated from Stamp2-KO and WT mice kept for three weeks under hypoxia and normoxia. Serum taken from hypoxia-exposed Stamp2-KO mice showed slightly but significantly higher ET-1 concentration as compared to hypoxia-exposed WT mice (Figure 4.20), whereas no significant differences were found among normoxia exposed WT and Stamp2-KO animals.

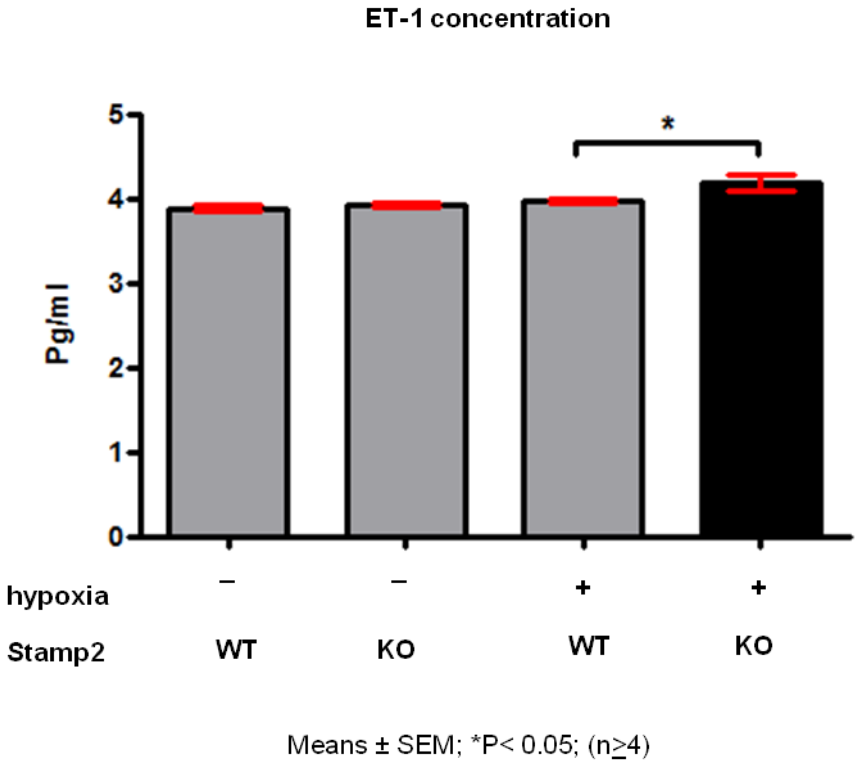


**Figure 4.20: Stamp2 deficiency leads to slightly higher Endothelin-1 (ET-1) concentration in serum**

*The expression of ET-1 was significantly higher in the serum of Hypoxia treated Stamp2-KO mice as compared to the WT mice. Hypoxia time point of three weeks was used and 0 hours of hypoxia served as the control.*

### 4.6.2 Stamp2 deficiency does not affect IL-6 levels in mouse serum

Serum isolated from mice was used to assess IL-6 concentrations. The serum from hypoxic Stamp2-KO mice showed slightly higher IL-6 concentration as compared to that from hypoxic WT mice but this difference was not statistically significant (Figure 4.21). Likewise, no significant difference in IL-6 concentrations was observed among the WT and Stamp2-KO normoxia controls.

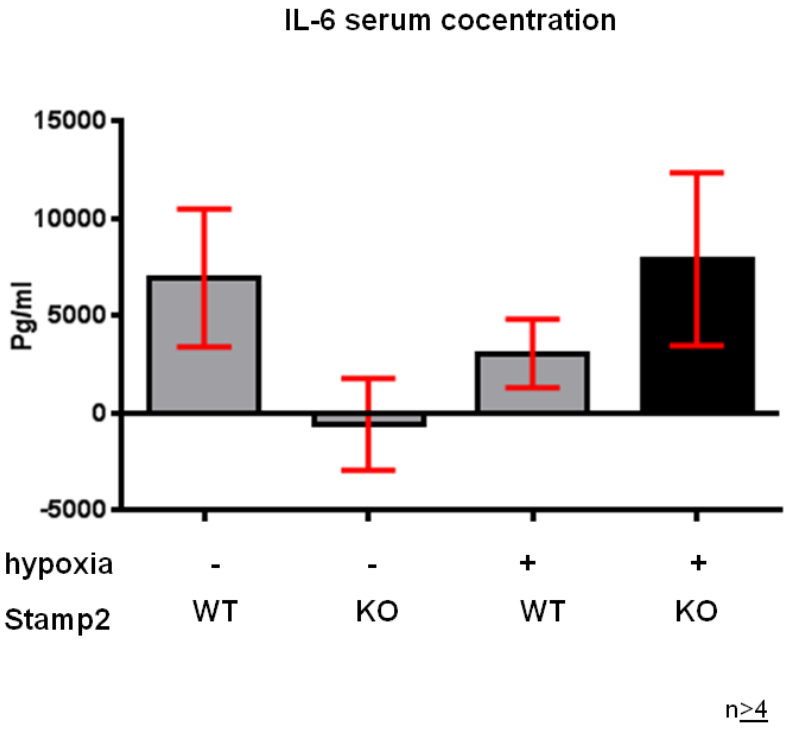


**Figure 4.21: Stamp2 deficiency does not affect IL-6 levels in mouse serum under hypoxia**

*The protein expression of IL-6 was measured using ELISA, slightly higher but not significantly different IL-6 expression was observed in serum from Stamp2-KO mice serum kept under hypoxia.*

## 4.7 Effect of Stamp2 deficiency on cellular actions

In order to evaluate how Stamp2 deficiency may contribute to the development of PH, we explored its effect on various cellular actions such as proliferation, migration and apoptosis/viability in relevant cell types (SMCs, ECs).

### 4.7.1 Effect of Stamp2 deficiency on PASMC proliferation

PASMCs were isolated from WT and Stamp2-KO mice and were used for further experiments after multiple healthy passages. PASMCs from both genotypes were incubated with starvation medium and normal growth medium to study proliferation using a BrdU incorporation kit. Upon stimulation with FCS, Stamp2-KO PASMCs showed no significantly different proliferation in comparison to WT PASMCs (Figure 4.22).

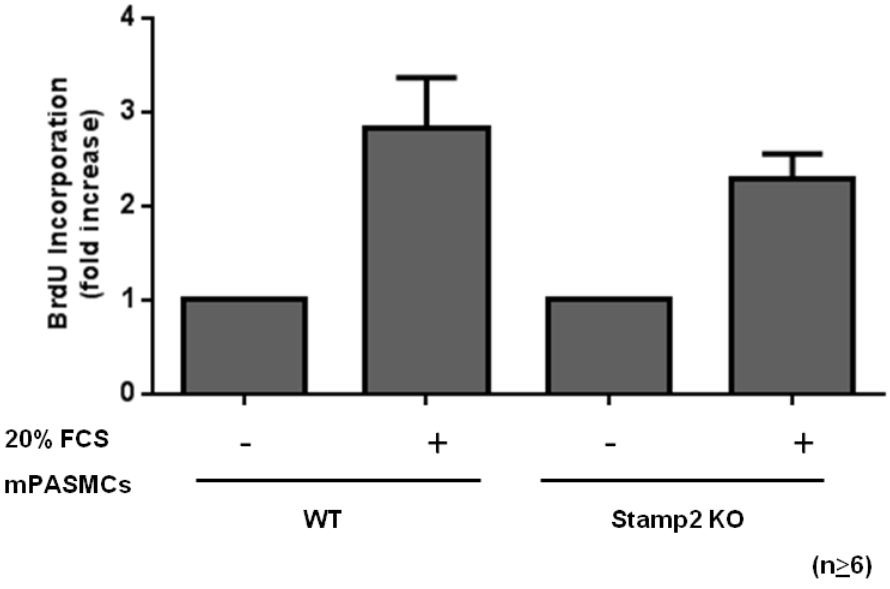


**Figure 4.22: Effect of Stamp2 deficiency on PASMCs proliferation**

*FCS-dependent proliferation (as assessed by BrdU incorporation) of WT and Stamp2-KO PASMCs showed no significant difference in the absence and presence of normal growth medium*

### 4.7.2 Effect of IL-6 and hypoxia on WT and Stamp2-KO PASMCs proliferation

As Stamp2 deficiency had no significant effect on FCS-dependent PASMCs proliferation under basal conditions, we next explored the potential impact of IL-6 and hypoxia. Stamp2 deficiency had no significant effect on FCS and IL-6 dependent PASMCs proliferation under basal conditions of normoxia (Figure 4.23 A). However, under hypoxic conditions both FCS and IL-6 induced PASMC proliferation in both genotypes, and the effect of FCS was significantly more pronounced in Stamp2-KO PASMCs as compared to WT cells, whereas no significant difference was observed in case of IL-6 (Figure 4.23 B).

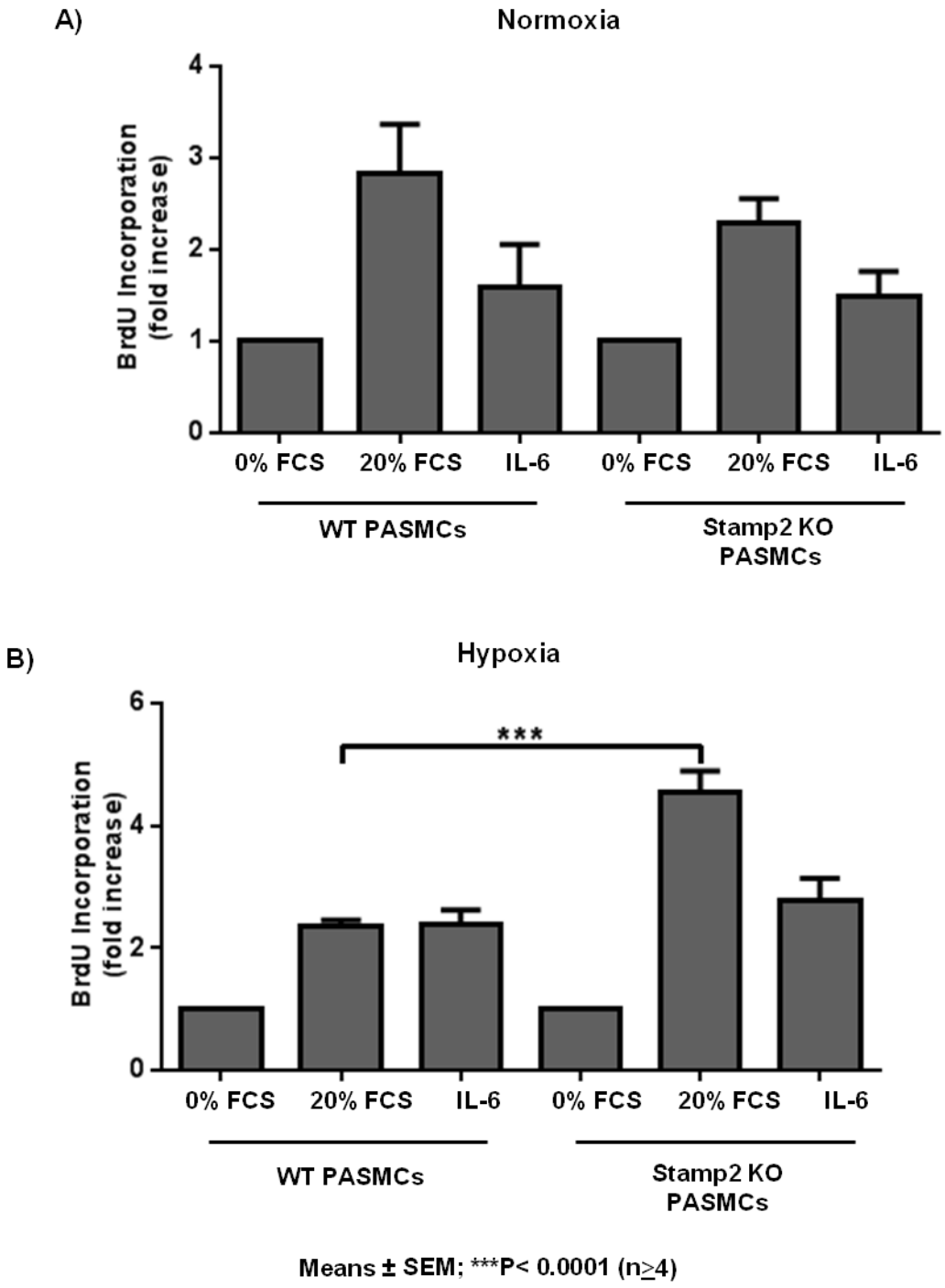


**Figure 4.23: Effect of FCS20% and IL-6 on WT and Stamp2-KO PASMCs proliferation under hypoxic conditions**

*(A) WT and Stamp2-KO PASMCs did not show significant difference in FCS and IL-6 mediated proliferation under normoxia conditions.*

*(B) Stamp2-KO PASMCs show significantly higher proliferation rate in response to FCS as compared to WT PASMCs under hypoxia, whereas similar responses were not observed for IL-6.*

### 4.7.3 Stamp2 gene silencing in human microvascular endothelial cells (hMVECs) using siRNA

In hMVECs, gene silencing by siRNA was used in order to induce Stamp2 deficiency. Sufficient Stamp2 silencing was observed after 72 hours of incubation with siRNA, which was confirmed by qPCR and Western blotting (Figure 4.24).

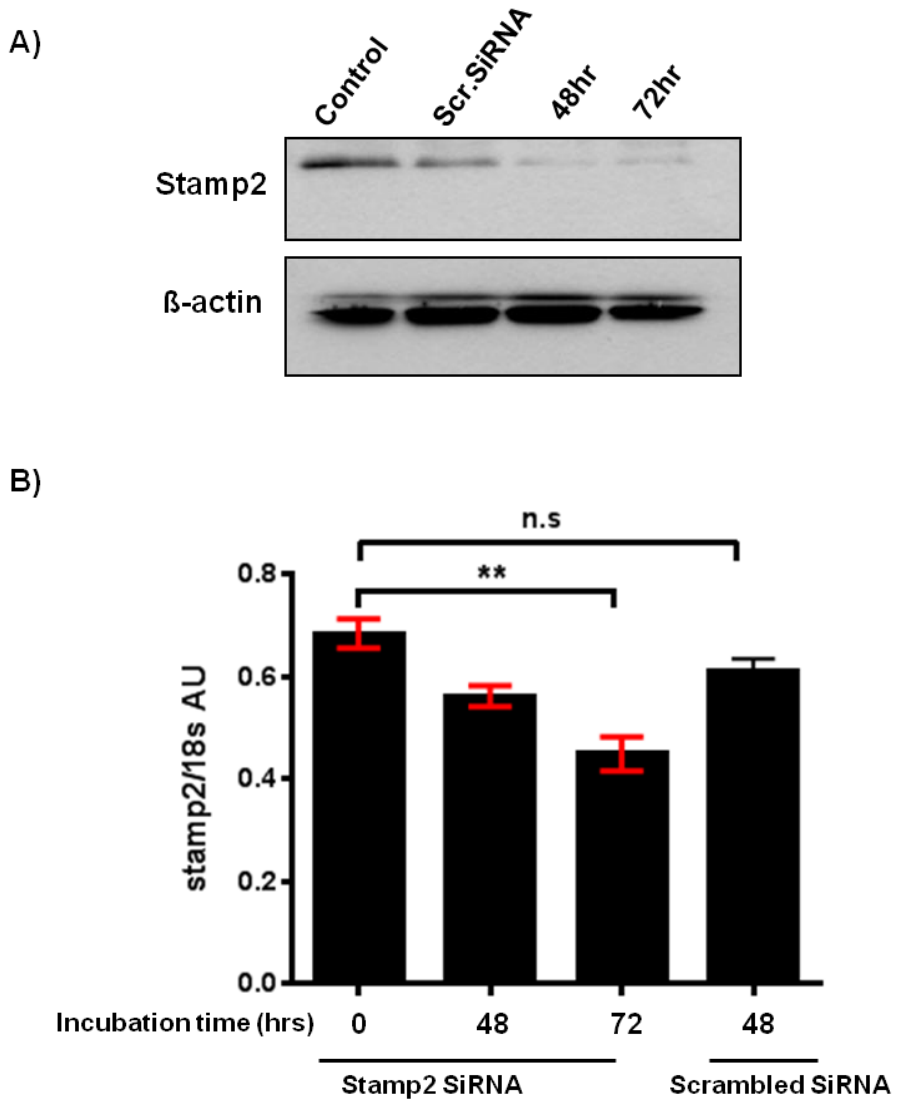


**Figure 4.24: Stamp2 siRNA sufficiently induced gene silencing in hMVECs**

*The hMVECs showed significant downregulation of Stamp2 expression after 72 hours of incubation with the 10 nm siRNA. Scrambled siRNA was used as control to ensure zero error.(A) Gene silencing at protein levels was confirmed via Western blot, (B) Effective downregulation was observed at mRNA level using qPCR*

### 4.7.4 Cell death detection of human microvascular endothelial cells (hMVECs)

Once the successful gene silencing of Stamp2 was achieved by using siRNA, these cells were used as Stamp2-deficient hMVECs. The untreated hMVECs acted as WT control. All experiments included a scrambled siRNA control as well. The hMVECs showed no significant difference in cell death rate upon silencing of the Stamp2 gene. Stamp2 siRNA treated hMVECs showed a trend towards higher apoptosis rate which was however not statistically significant as compared to the scrambled siRNA control (Figure 4.25). Hence, gene silencing of Stamp2 did not show any significant effect on the apoptotic activity of these cells.

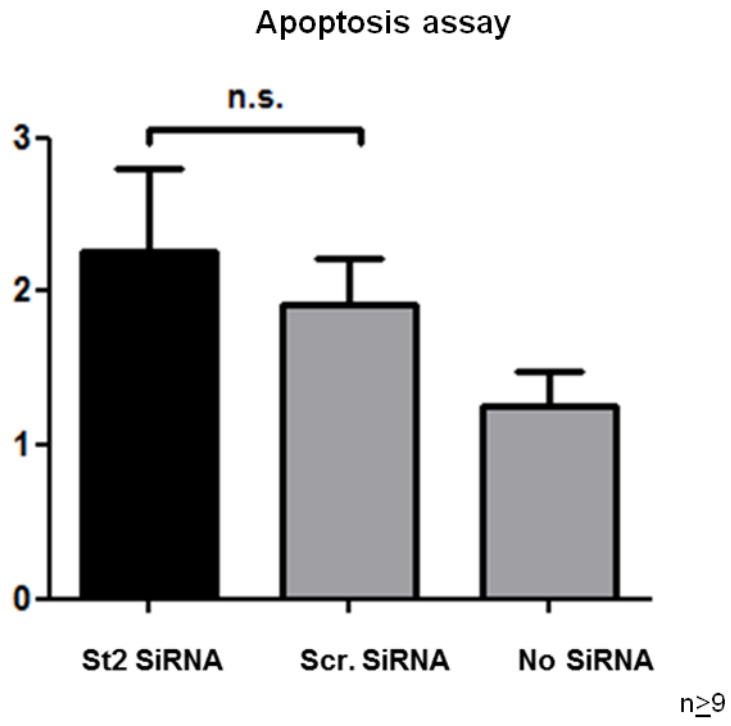


**Figure 4.25: Apoptosis assay (cell death detection ELIZA) showing hMVECs cell death in the presence or absence of Stamp2**

*Upon Stamp2 siRNA mediated Gene silencing hMVECs showed a trend towards higher apoptosis (statistically insignificant); scrambled siRNA was used as control.*

### 4.7.5 Cell viability detection of human microvascular endothelial cells (hMVECs)

Similar to the above experiments, hMVECs were also subjected to cell viability assays under the influence of siRNA downregulated Stamp2. Stamp2 siRNA-treated cells did not show a significantly lower viability as compared to the scrambled siRNA control (Figure 4.26). Although a trend towards lower viability was observed in Stamp2 siRNA-treated hMVECs, there was no statistically significant difference. These findings indicate that downregulation of Stamp2 does not impact cellular death/viability of hMVECs, thus the impact of Stamp2 on PH is achieved by action of other cells.

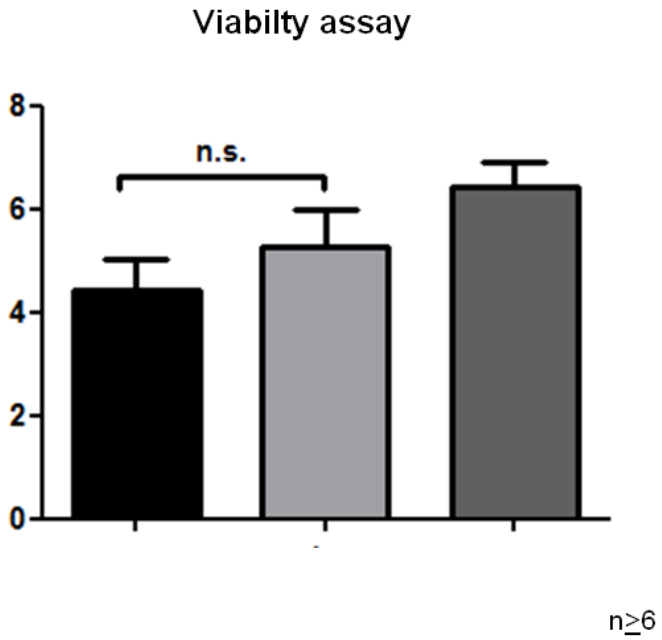


**Figure 4.26: Viability assay showing hMVECs viability upon Stamp2 gene silencing**

*Gene silencing was performed by using Stamp2 siRNA, whereas scrambled SiRNA served as control. hMVECs showed a trend towards higher viability upon Stamp2 silencing.*

## 4.8 Effect of WT and Stamp2-KO macrophage supernatant on PASMCs migration

In order to explore potential paracrine effects and cellular cross-talk involving inflammatory and vascular cells, we next evaluated the effect of macrophage supernatant form WT or Stamp2-deficient mice on PASMC cellular responses.

When supernatant from WT and Stamp2-KO macrophages was used for induction of PASMC migration using a scratch assay, we observed an almost complete cover of the scratch after 24 hours in the presence Stamp2-KO macrophage supernatant. The scratch cover could be visually observed very clearly and was later quantified indicating higher migration of PASMCs in presence of Stamp2-KO macrophage supernatant (Figure 4.27A).

The quantitative analysis after measuring the scratch area shows significantly higher migration of mouse PASMCs induced by Stamp2-KO macrophage supernatant as compared to WT (Figure 4.27B). Positive and negative controls with and without cell growth media were included in all scratch assay experiments.

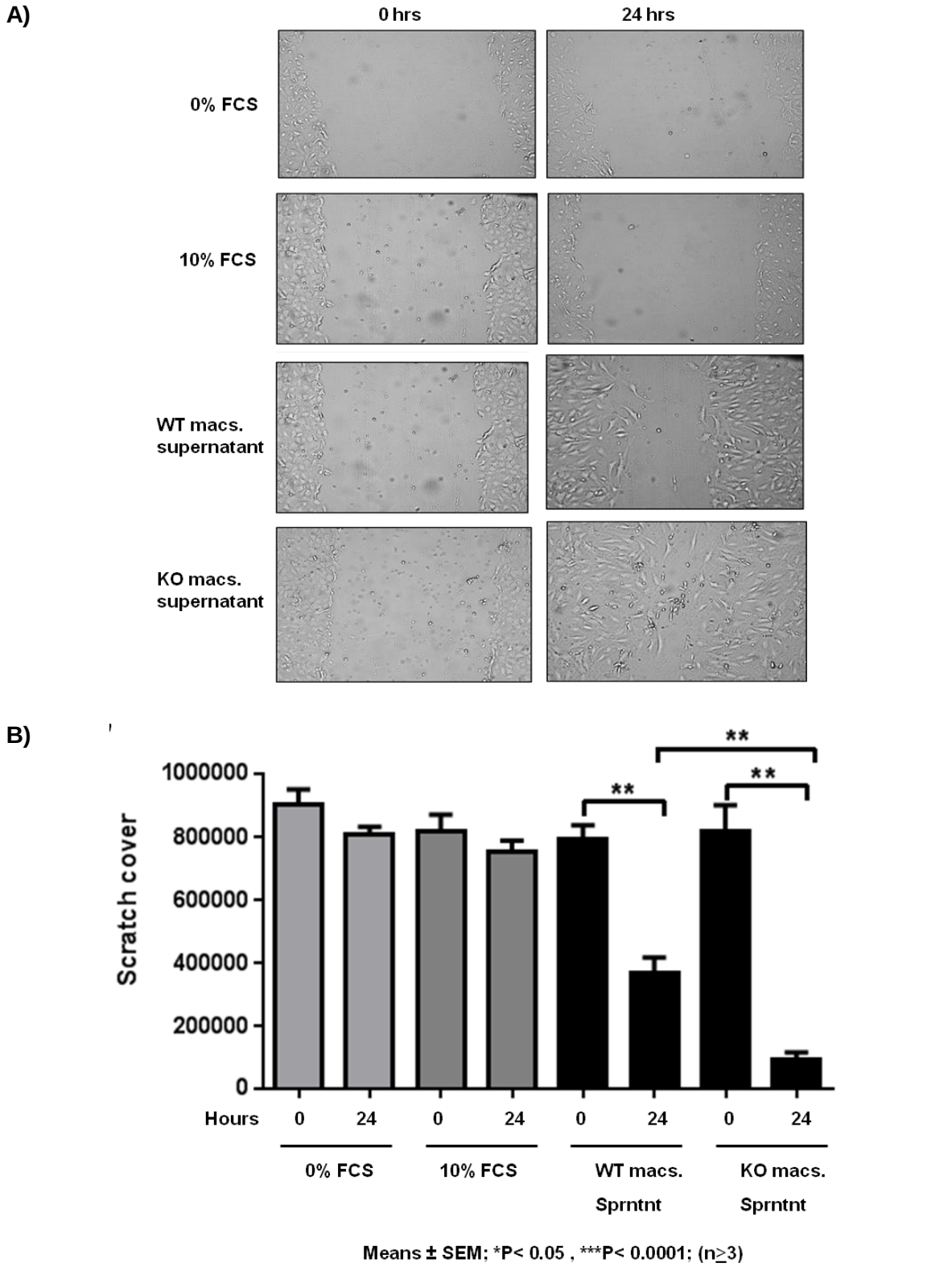


**Figure 4.27: Stamp2-KO macrophage supernatant causes significantly higher mouse PASMCs migration compared to WT macrophage supernatant**

*The FCS controls showed minimal migration of PASMCs after 24 hour, supernatant from both WT and Stamp2-KO macrophages induced migration but the Stamp2-KO macrophages induced significantly higher migration as shown by scratch area covered by PASMCs after 24 hours of incubation. In Fig A) the migration of cells can be visually seen and Fig B) shows the quantitative values based graph.*

## 4.9 Impact of Stamp2 on the cytokine profile

In order to get an insight into the factors present in the Stamp2-KO supernatant which may be responsible for the higher PASMC migration rate, a cytokine profiling experiment was performed. Supernatant samples from WT and Stamp2-KO macrophage were used to identify the expressed cytokines.

A number of cytokines were detected which were differentially expressed in the macrophages supernatant from both genotypes. Among the differentially expressed cytokines, MCP-1 and CXCL12 showed a remarkable difference, with substantially higher levels in supernatant from Stamp2 deficient cells (Figure 4.28).

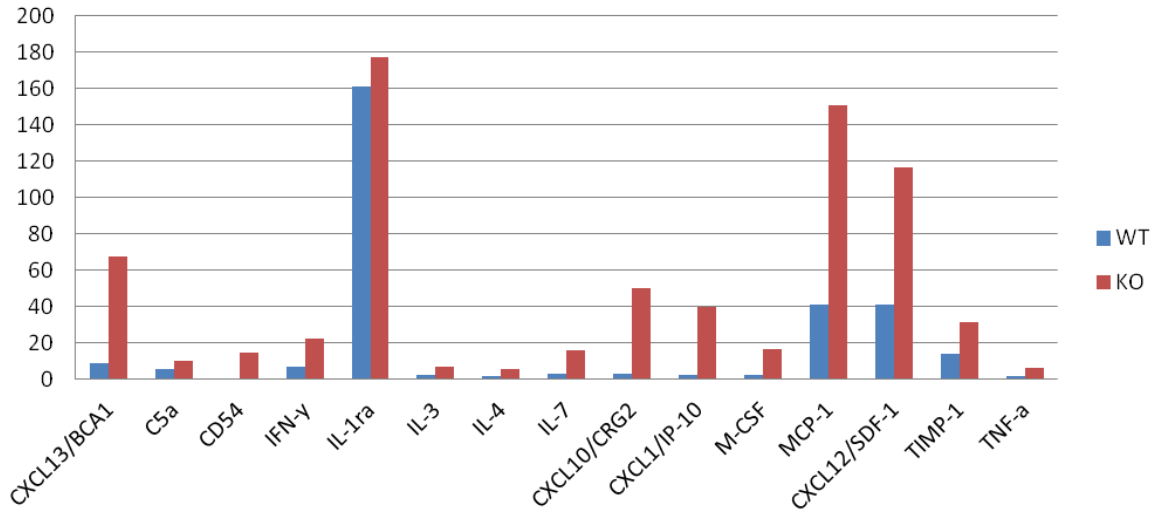


**Figure 4.28: Mouse cytokine array of macrophage supernatant from WT and Stamp2-KO mice**

*Supernatant from WT and Stamp2-KO macrophages was screened for differentially expressed cytokines via cytokine profiling. MCP-1 and CXCL12 along with other cytokines showed a significant difference among genotypes.*

### 4.9.1 Expression of CXCL12 in absence of Stamp2

Earlier we looked at differential expression of various cytokines in the lungs of WT and Stamp2-KO mice. It was shown that absence of Stamp2 leads to higher inflammation and thus higher expression of cytokines including IL-6, IL-1β, MCP-1, TNF-α and ET-1.

The cytokine array then revealed that CXCL12 was highly present in the supernatant of Stamp2-deficient mice. We therefore specifically studied the impact of Stamp2 deficiency on CXCL12 expression in lung tissue. Lungs from WT and Stamp2-KO mice kept under hypoxic (three days and three weeks) or normoxic conditions were used to perform qPCR analysis and analyze CXCL12 expression. Intriguingly, these data showed that CXCL12 expression – although similar under normoxia – was significantly higher in absence of Stamp2 for both time points of hypoxia exposure, with only minimal changes in WT (Figure 4.29).

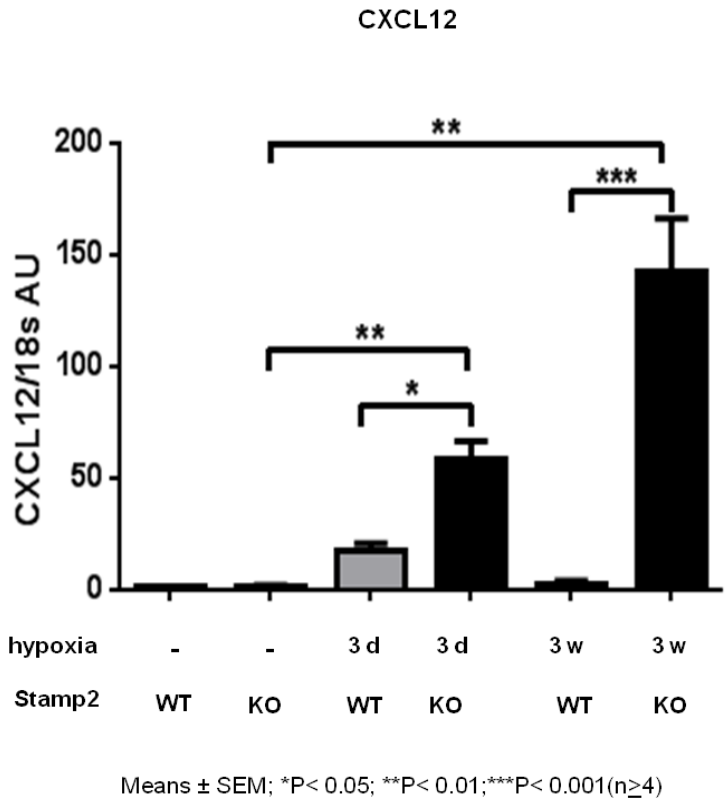


**Figure 4.29: Stamp2 deficiency leads to higher CXCL12 expression under hypoxia**

*RNA from Stamp2-KO and WT mouse lungs from (hypoxia and normoxia exposed) mice were used for qPCR; the Stamp2-KO mouse lung showed significantly higher mRNA expression of CXCL12.*

## 4.10 Effect of cytokines on PASMCs migration

Since supernatant from Stamp2-KO macrophages induced a more pronounced PASMC migration when compared to WT, and a number of cytokines were identified in the cytokine array, we next aimed at exploring the biological relevance of distinct cytokines in this context. Therefore, we evaluated how each of these cytokines individually and collectively affects the migration rate of PASMCs. A series of experiments was thus performed using mouse PASMCs and treating these with individual and combined cytokines (IL-6, MCP-1 and CXCL12). Conditioned media with cytokines along with respective cytokine neutralizing antibodies was also used. All the experiments were performed within 24 hours of incubation. Respective control

conditions with starvation and normal growth medium were also included.

### 4.10.1 **Effect of IL-6 on mouse PASMCs migration**

Migration of mouse PASMCs was measured by performing a scratch assay. IL-6 induced considerable migration of mouse PASMCs which was visually observed and photographed (Figure 4.30A).

The quantitative values were recorded after measuring the scratch area before and after incubation with IL-6, and neutralizing antibody. These data confirm the significantly higher migration of mouse PASMCs in the presence of IL-6; whereas the use of IL-6 neutralizing antibody effectively prevented migration (Figure 4.30B). While conducting the experiments, 0 and 10% FCS were used as negative and positive controls.

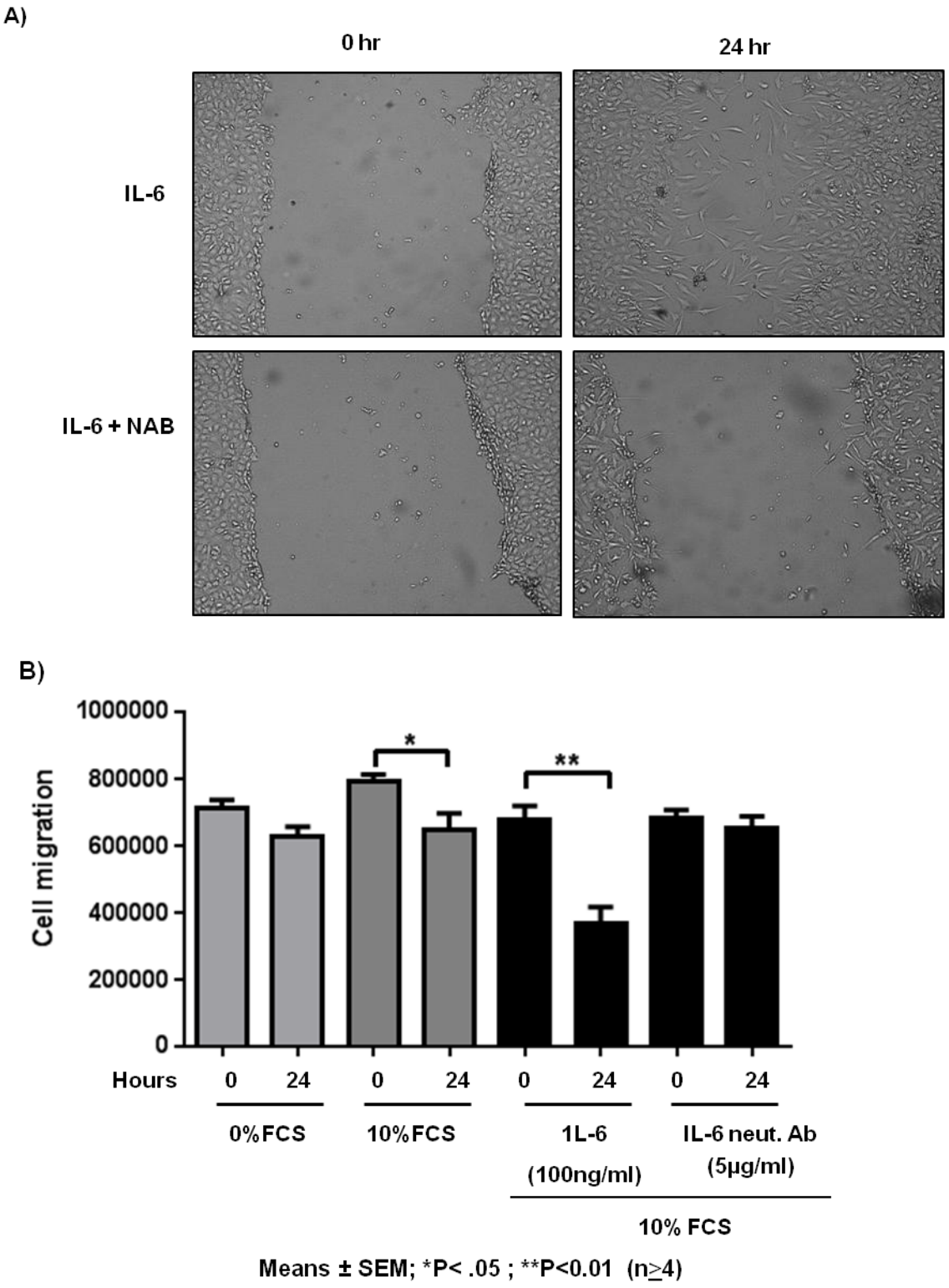


**Figure 4.30: IL-6 induces migration in mouse PASMCS**

*(A) Figure shows cells moving to cover the scratch in individual wells. (B) Scratch covered area values shown in graph for individual incubation conditions. IL-6 leads to significantly higher PASMCs migration.*

### 4.10.2 **Effect of CXCL12 on mouse PASMCs migration**

Migration of mouse PASMCs was measured by performing a scratch assay. Like IL-6, CXCL12 also induced considerable migration of mouse PASMCs (Figure 4.31A).

The quantitative values after calculating the scratch area confirm significantly higher migration of mouse PASMCs in the presence of CXCL12, which was reversed by neutralizing antibody and appeared more pronounced in comparison to IL-6 (Figure 4.31B). This shows individual cytokines have varying degree of effects on these cellular actions. While conducting the experiments 0 and 10% FCS were used as negative and positive controls.

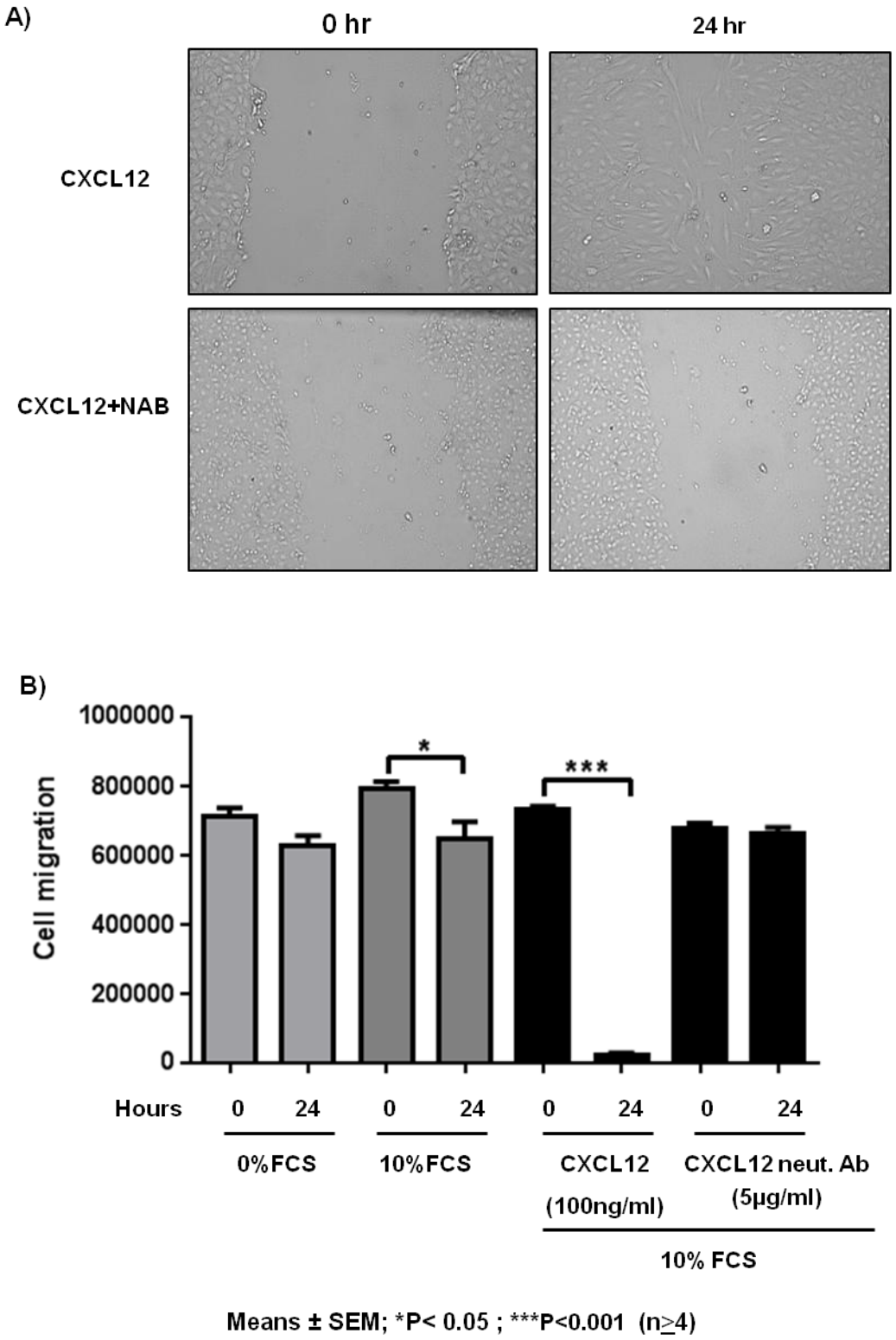


**Figure 4.31: CXCL12 induces migration in mouse PASMCs**

*The PASMCs showed significant scratch cover after 24 hours of CXCL12 induction. The migration was effectively prevented by using CXCL12 neutralizing antibody. Figure A) shows cells moving to cover the scratch in individual wells; Figure B) shows Quantitative values for Scratch covered area*

### 4.10.3 **Effect of MCP-1 on mouse PASMCs migration**

Migration of mouse PASMCs was again measured by performing a scratch assay. As shown in Figure 4.32, MCP-1 also induced considerable migration of mouse PASMCs, which appeared of similar extent as the CXCL12 response. While conducting the experiments, 0 and 10% FCS were used as negative and positive controls.

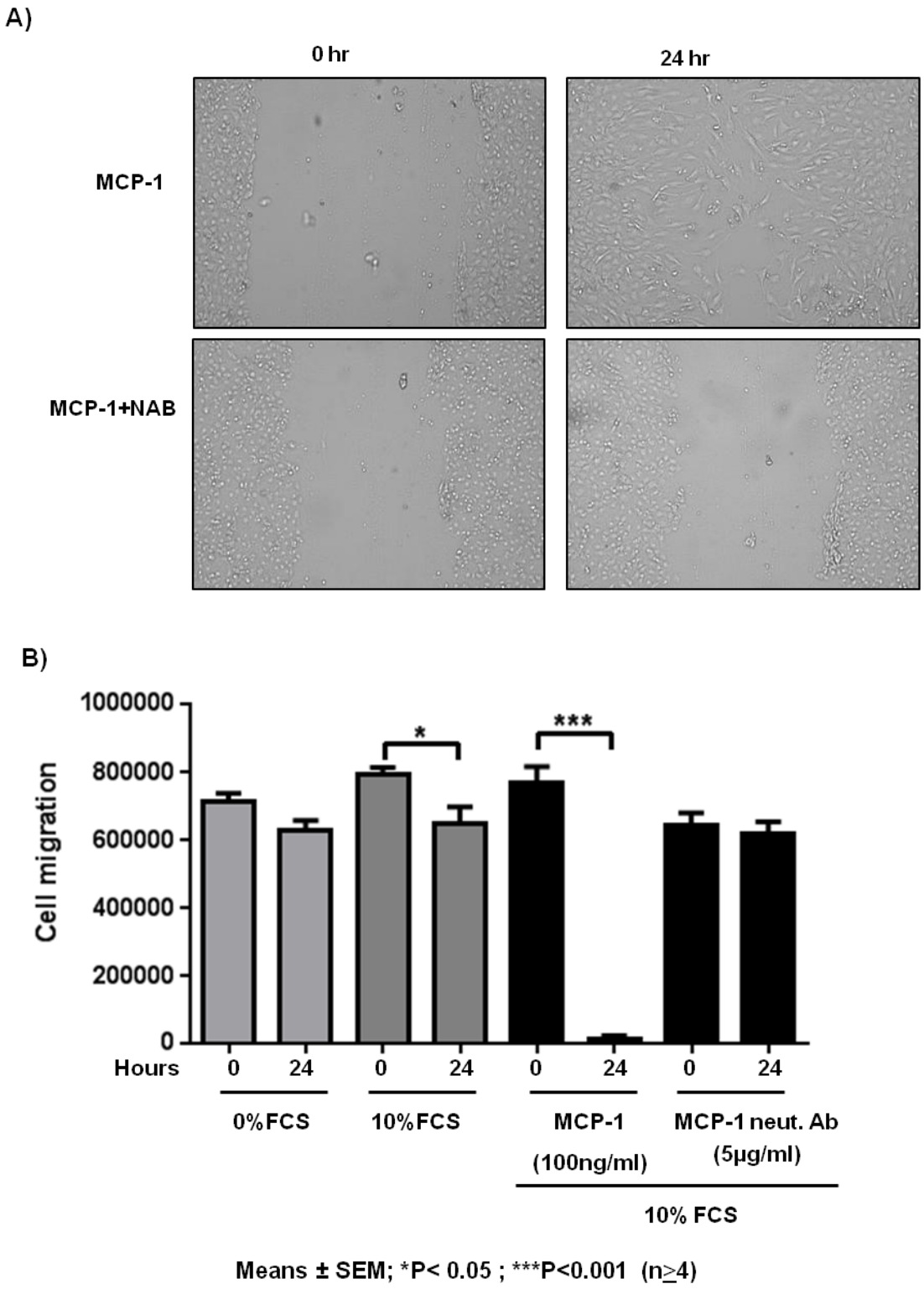


**Figure 4.32: MCP-1 induces migration in mouse PASMCs**

*The PASMCs showed significant scratch cover after 24 hours of MCP-1 induction. The migration was effectively prevented by using MCP-1 neutralizing antibody. Figure A) shows cells moving to cover the scratch in individual wells; Figure B) shows Quantitative values for Scratch covered area*

### 4.10.4 Effect of all cytokines combined on mouse PASMCs migration

Since effective migration of mouse PASMCs was measured by performing scratch assays using cytokines individually, we next evaluated their combined effect.

A cytokine cocktail containing all three cytokines (MCP-1, CXCL12 and IL-6) combined was used, which induced very robust migration of mouse PASMCs which was completely reversed by a mixture of neutralizing antibodies (Figure 4.33). While conducting the experiments, 0 and 10% FCS were used as negative and positive controls.

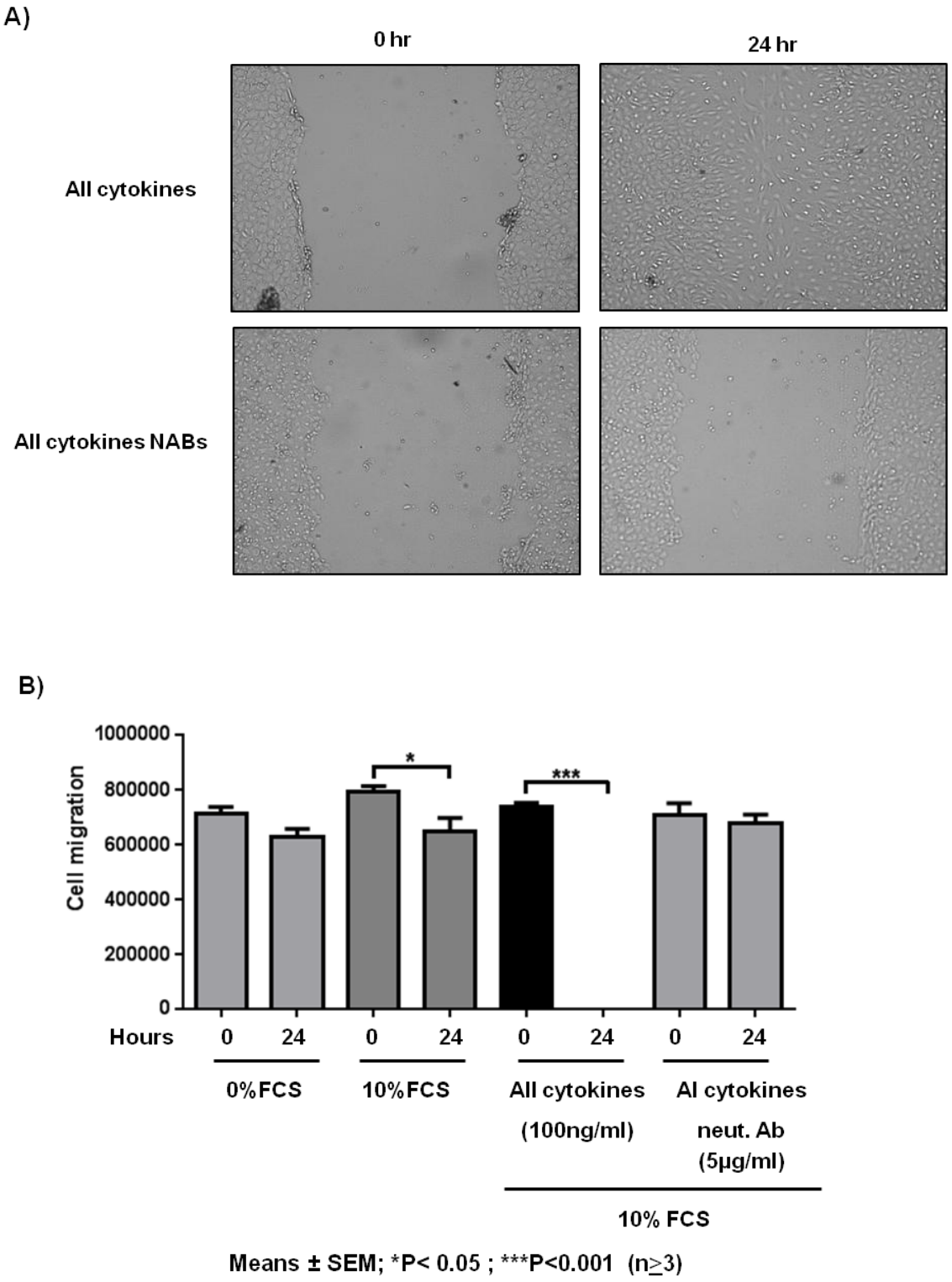


**Figure 4.33: Combined cytokines induce migration in mouse PASMCs**

*The PASMCs showed highly significant scratch cover after 24 hours of all cytokines combined (MCP-1+CXCL12+IL-6) induction. The migration was effectively prevented by using neutralizing antibodies combined for all the respective cytokines. Figure A) shows cells moving to cover the scratch in individual wells; Figure B) shows Quantitative values for Scratch covered area*

## 4.11 Effect of all cytokines neutralizing antibodies combined on macrophage mediated mouse PASMCs migration

Once all cytokines individually and collectively exhibited strong migration of PASMCs which was effectively prevented using their respective neutralizing antibodies, we tested the effect of these neutralizing antibodies on the macrophage supernatant from WT and Stamp2-KO mice. As shown already in Fig 4.27 the supernatant from both WT and Stamp2-KO macrophages induced PASMCs migration, we decided to test these antibodies against the macrophage supernatant

As demonstrated in Figure 4.34, the combination of neutralizing antibodies against MCP-1, CXCL12 and IL-6 largely prevented PASMCs migration upon macrophage supernatant stimulation from both genotypes. Hence, these data indicate that the identified cytokines are indeed few of the main mediators of macrophage supernatant induced PASMC migration.

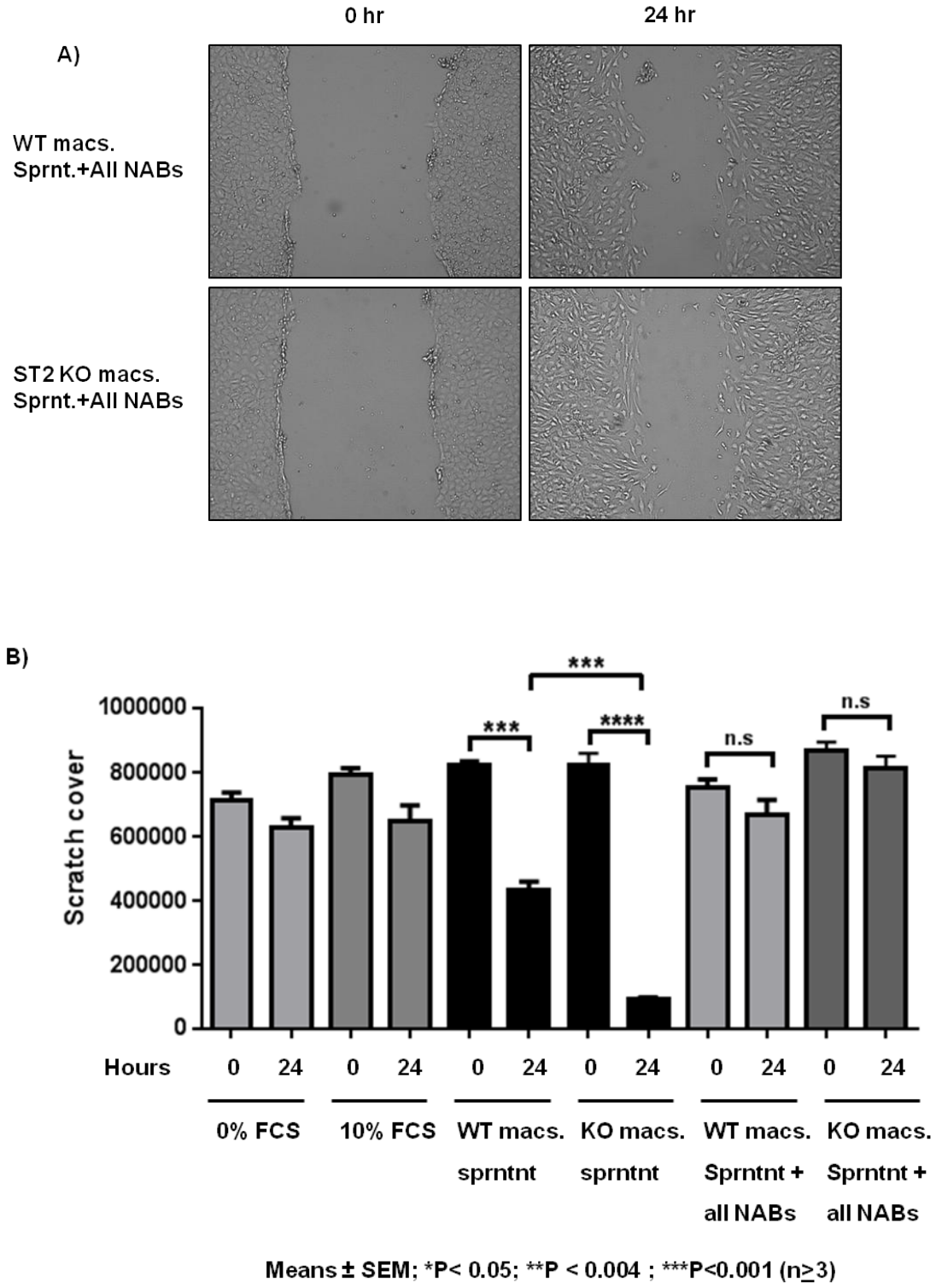


**Figure 4.34: combined cytokines neutralizing antibodies prevent migration in mouse PASMCs**

*The PASMCs showed significant prevention of scratch cover after 24 hours of combined cytokines (MCP-1+CXCL12+IL-6) neutralizing antibodies with WT and Stamp2-KO supernatant induction. Figure A) shows photos of cells and the scratch in individual wells. In Figure B) Scratch covered area values are shown in graph for individual incubation conditions. NAB=neutralizing antibody*

When interpreting the results of the scratch assays, it is important to note that all scratch assays were performed along with control conditions to ensure no other factors apart from chosen inducers imparted any effect.

The cells were cultured with starvation medium and normal medium to ensure how presence of growth factors affects the migration of cells. PASMCs were cultured with and without the control antibody to confirm that its presence has no effect on pattern of cell migration in both starvation medium and growth medium condition. Cells cultured in starvation medium showed quiet low cell migration in comparison to normal growth medium. These control conditions are shown in Figure 4.35.

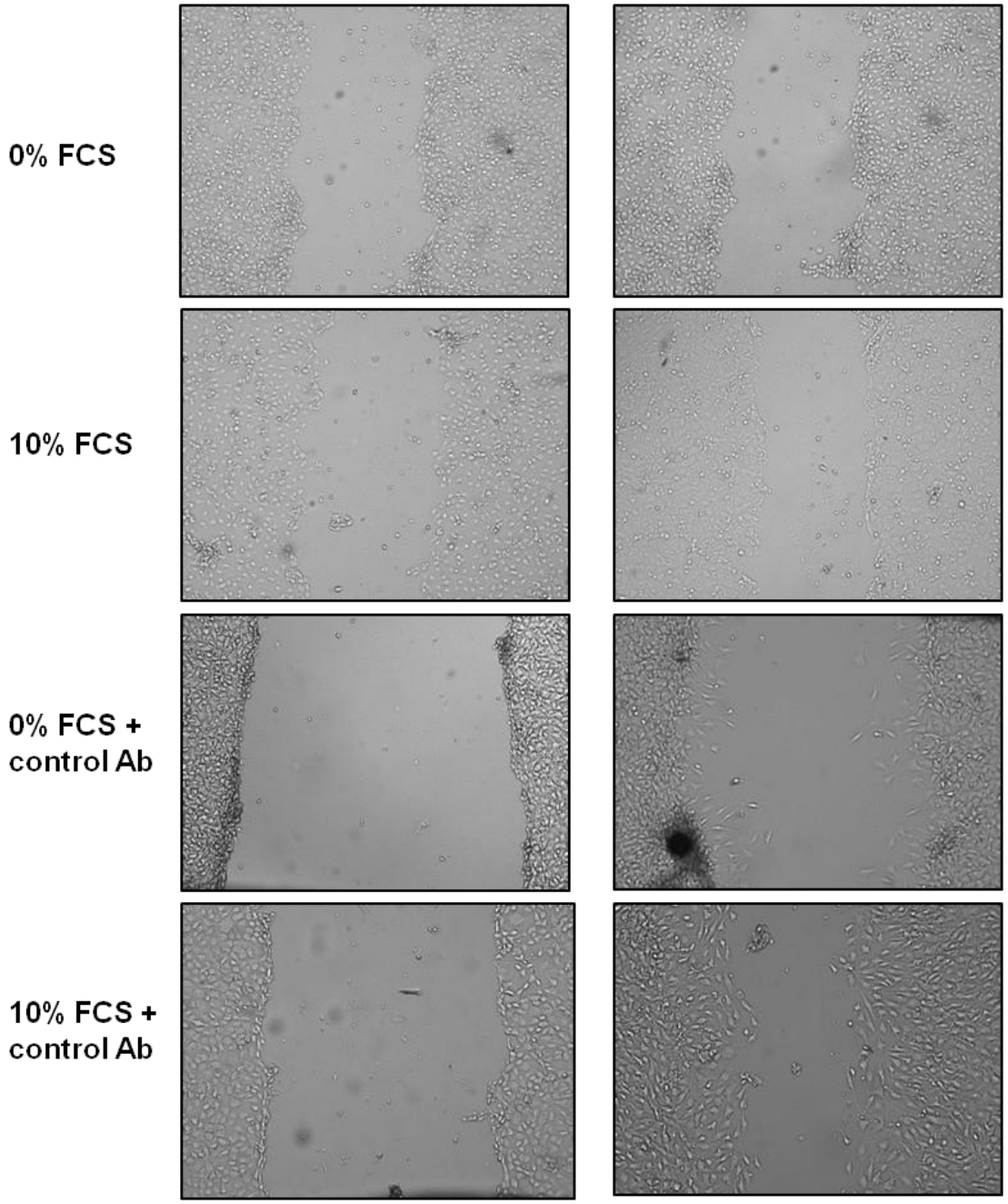


**Figure 4.35: Control conditions for scratch assays**

*All scratch assays were performed along with control conditions of 0%FCS and 10%FCS, also both FCS concentrations were used with and without control antibody.*

## 4.12 **Effect of WT and Stamp2-KO macrophage supernatant on mouse PASMCs proliferation**

As PASMC proliferation along with migration is an important cellular action imparting vascular remodelling, we also assessed the impact of supernatant from Stamp2-KO or WT macrophages on this cellular response. To this end, BrdU incorporation assays were performed. PASMCs show significantly higher proliferation in the presence of Stamp2-KO macrophage supernatant as compared to WT macrophage supernatant, both under normoxic and hypoxic conditions (Figure 4.36).

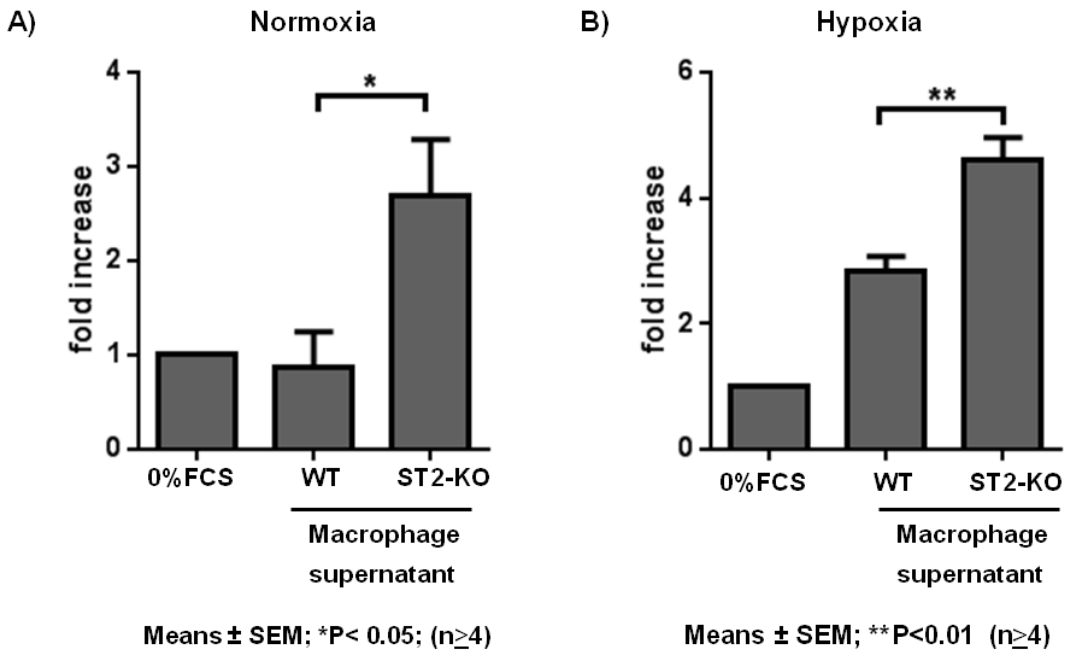


**Figure 4.36: Effect of WT and Stamp2-KO macrophage supernatant on PASMCs proliferation**

*Mouse PASMCs showed significantly higher proliferation in the presence of supernatant collected from Stamp2-KO macrophages under both normoxic (A) and hypoxic (B) conditions. The 0% and 10% FCS were used as negative and posative controls.*

## 4.13 Effect of cytokines on PASMCs Proliferation

After studying the effects of individual and combined cytokines on PASMCs migration, the same conditions were used to study PASMCs proliferation.

### 4.13.1 Effect of IL-6 on PASMCs proliferation

IL-6 previously showed effective PASMCs migration. Contrary to these results, IL-6 did not show any significant effect on PASMCs proliferation under normoxic conditions, and only a mild trend under hypoxia (Figure 4.37).

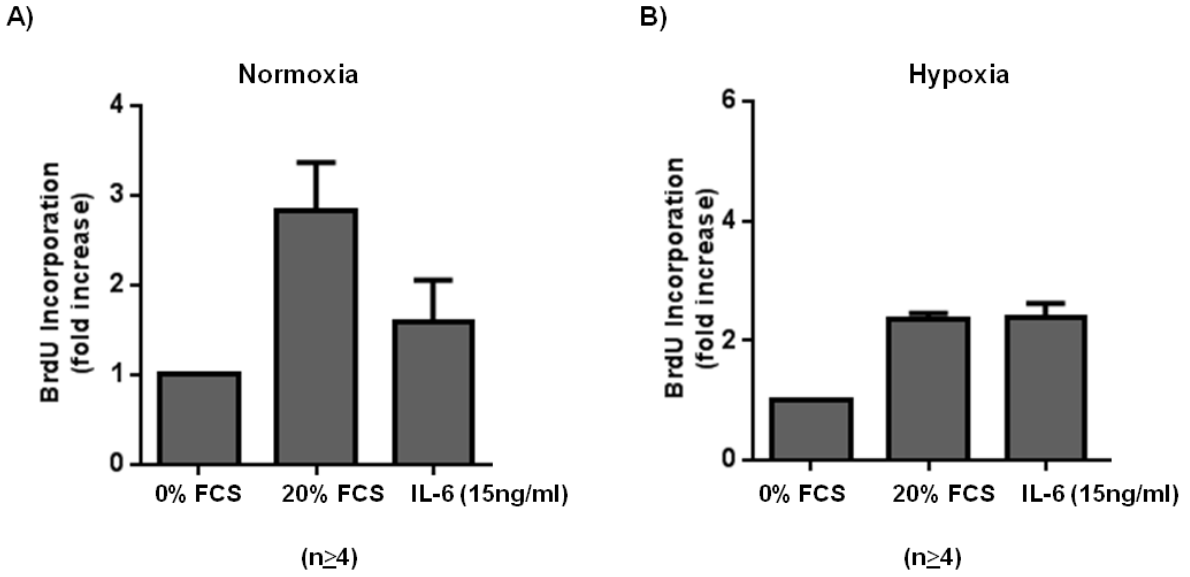


**Figure 4.37: Effect IL-6 on PASMCs proliferation**

*Mouse PASMCs showed no significantly higher proliferation in the presence of IL-6 under both normoxia (A) and hypoxia (B) conditions*

### 4.13.2 Effect of combined cytokines and respective neutralizing antibodies on mouse PASMCs proliferation

The combination of cytokines and their respective neutralizing antibodies were also used for studying mouse PASMCs proliferation. All similar cytokines used for studying migration behaviour of the PASMCs were used to study proliferation. As shown earlier, IL-6 induced effective cell migration in PASMCs but failed to do so regarding proliferation. In order to create an even more effective IL-6 action hypoxia conditions were also established along with the cytokine induction but even that failed to cause significant increase in proliferation, indicating that IL-6 has more pronounced effects on PASMCs migration rather than proliferation.

Since IL-6 did not induce an effective proliferation, we focussed on the combination of MCP-1 and CXCL12 and did not include IL-6. These cytokines used individually as well as in combination were found to magnify the proliferation in PASMCs under normoxic conditions, which was partly rescued by adding the respective neutralizing antibodies (Figure 4.38). These results are similar to the high proliferation rate which was observed by using WT and Stamp2-KO macrophages supernatant.

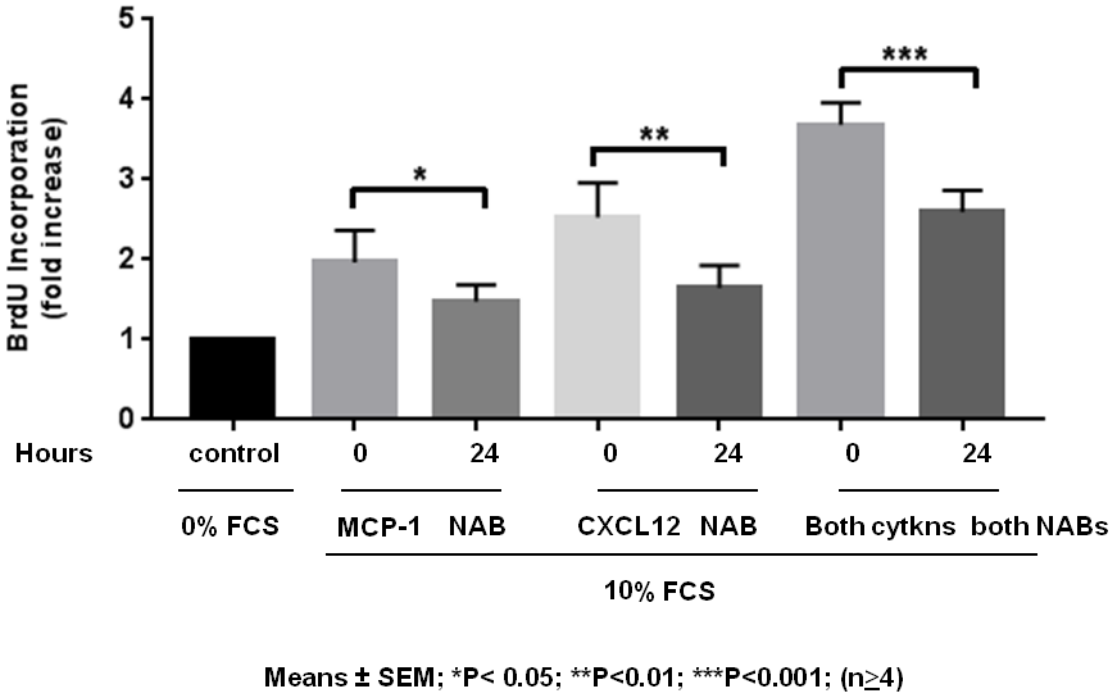


**Figure 4.38: Mouse PASMCs proliferation in the presence of MCP-1 and CXCL12 and their respective neutralizing antibodies**

*Individual and combination usage of MCP-1 and CXCL12 (100 ng/ml) caused higher proliferation in mouse PASMCs; the high proliferation was significantly reduced by using respective neutralizing antibodies (5 µg/ml), NAB=neutralizing antibody.*

## 4.14 Effect of selected neutralizing antibodies on mouse macrophage mediated mouse PASMCs proliferation

Once it was established that MCP-1 and CXCL12 were inducing PASMC proliferation similar to Stamp2-KO macrophage supernatant, neutralizing antibodies against MCP-1 and CXCL12 along with macrophage supernatant from WT and Stamp2-KO mice were tested. The neutralizing antibodies did suppress supernatant-induced PASMC proliferation, and this suppression was stronger when the neutralizing antibodies were applied in combination rather than individually (Figure 4.39). This effect was observed for both WT and Stamp2 KO macrophages supernatant induced proliferation.

The MCP-1 and CXCL12 neutralizing antibodies alone did not show a significant reduction in WT macrophage supernatant induced proliferation, whereas a combination of both caused a significant suppression of proliferation. For Stamp2-KO macrophage supernatant, MCP-1 neutralizing antibody did not suppress PASMCs proliferation, but the neutralization of CXCL12 caused significant suppression in proliferation. Similar effect was observed by using a combination of both neutralizing antibodies. These findings create a link between macrophage supernatant induced proliferation and the role of these particular cytokines along with other chemokines responsible for these effects.

It is interesting to note that the cellular actions responsible for morphological changes in the vasculature are regulated by these cytokines which appear to be regulated by Stamp2 and hypoxia, and this suggests a link between inflammatory cells and the vascular wall. These changes appear to be relevant for development as well as the progression of PAH, and thus are an important finding in developing a broader understanding of the pathobiology of the disease and treatment strategies.

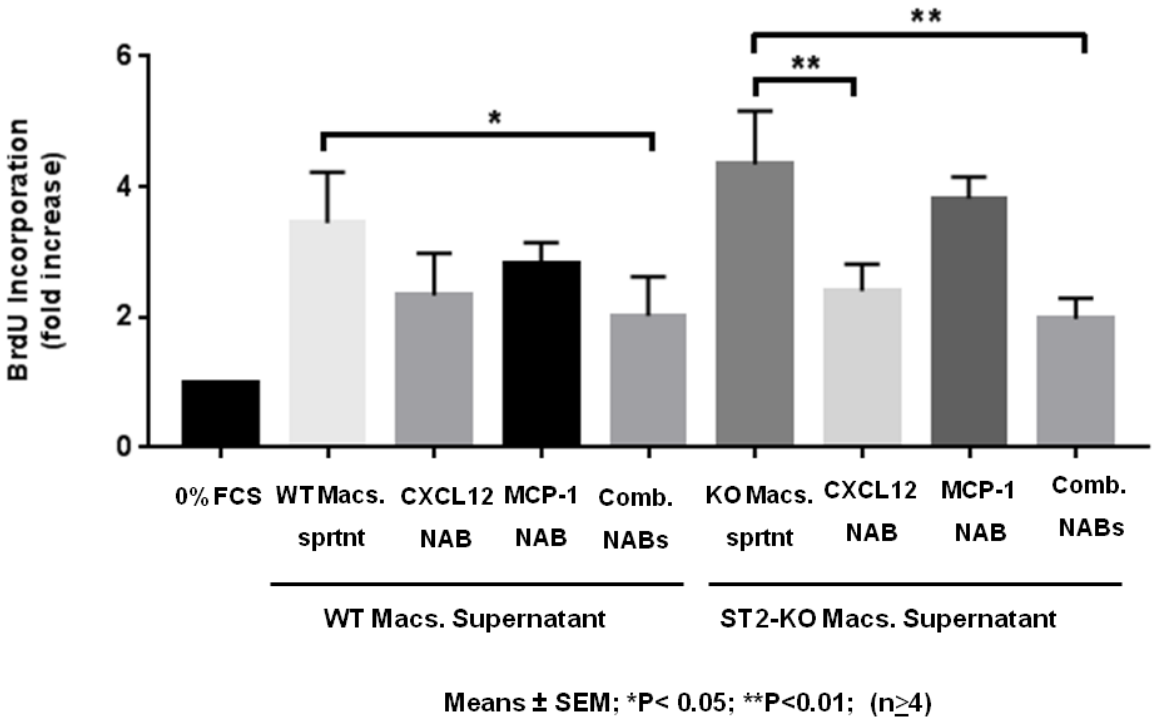


**Figure 4.39: Effect of selected neutralizing antibodies on WT and Stamp2-KO macrophages supernatant induced mouse PASMCs proliferation**

*The neutralizing antibodies for MCP-1 and CXCL12 suppressed the proliferation in mouse PASMCs and this suppression was stronger when antibodies were used in combination, NAB= neutralizing antibody.*

# 5. Discussion

# 5 Discussion

This study demonstrates that Stamp2 exerts anti-inflammatory properties, which are linked to a protective role against PH in animal model and human disease. Due its ability to be regulated by an imbalance in inflammation, Stamp2 can mark the onset and progression of disease.

Our results published already (Batool et al. 2020) demonstrate that Stamp2 expression is downregulated in pulmonary vascular cells under hypoxic conditions *in vitro*. Also we were able to select some active chemokines up-regulated upon Stamp2 downregulation and/or absence and this is in line with previous findings where along with IL-6 and TNF-α, MCP-1 and CXCL12 have been shown to play a role in development of vascular remodelling and human PH (McCullagh et al. 2015, Schlosser et al. 2017, Sikkeland et al. 2012). In our study, lack of Stamp2 promoted the development of PH in mice and its expression was diminished upon progression of disease in both experimental and human PAH. This observation coupled with the finding that Stamp2 expression increases upon exposure to inflammatory cytokines thereby connecting it to inflammation and immune responses (Scarl et al. 2017). This suggests a connection between the inflammatory profile and disease development coupled with Stamp2 regulation and puts forward a protective role of Stamp2 against the advancement of PH.

## 5.1 Stamp2 absence results in overt inflammatory response

Stamp2 absence has been associated with enhanced inflammation, whereas its presence appears to be required for a balanced inflammatory profile. Many diseases and aggravated disease states have been connected to absence of Stamp2 (Sikkeland et al. 2016, Waki and Tontonoz 2007). In our study, we were able to further

confirm and elaborate these findings. We found that absence of Stamp2 causes high expression of a number of inflammatory mediators, such as MCP-1, IL-1β, IL-6, TNF-α, CXCL12 and ET-1. All these cytokines are implicated in vascular remodeling (Grudzinska et al. 2013), (Knobloch et al. 2016, Steiner et al. 2009, Kherbeck et al. 2013, Yang et al. 2014). In patients with IPAH, elevated circulating levels of IL-6, TNF-α and MCP-1 have been reported (Itoh et al. 2006). ET-1 is a known vasoconstrictor, has also been shown to promote cell proliferation and vascular remodeling, and has been associated with various forms of cardiovascular disease and PH in particular (Sikkeland et al. 2012, Sanchez et al. 2014, Schiffrin 2001).

The results reported herein put Stamp2 in a critical perspective of balancing and affecting immune regulation, thereby tailoring procedures which are in turn affected by immune dysregulation. It is known that development and progression of a number of cardiovascular diseases is not only worsened but also preceded by elevated inflammation. Studies have proven that cells from pulmonary vasculature and inflammatory cells are the prime sources of cytokines and inflammation (Rabinovitch et al. 2014). Keeping in view this background, in our study the expression of cytokines was assessed at the mRNA level using qPCR, as protein expression for the cytokines in the lung tissue was too low to be detected by western blotting, using the available antibodies. We also quantified expression of IL-6 and ET-1 in serum from hypoxia and normoxia exposed mice from WT or Stamp2-KO genotypes. These findings show significantly higher ET-1 expression in serum of hypoxic Stamp2-KO animals, while IL-6 showed a trend towards higher expression which was however, not significant. IL-6 is also a pro-inflammatory cytokine with an active role in PH. High expression of IL-6 in lungs along with other cytokines is known to promote the

development of PH (Savale et al. 2009). High serum IL-6 levels in PAH patients has also been reported. Blocking the IL-6 receptor helped resolve hypoxia induced PH in a mouse model, indicating that IL-6 is important in PH (Hashimoto-Kataoka et al. 2015).

CXCL12 and MCP-1 both showed highly pronounced expression in the supernatant from macrophages in the cytokine array, which was even higher in supernatant from Stamp2-KO macrophage cells. Recent studies have shown that the pro-inflammatory and pro-angiogenic cytokine CXCL12 has an important role in PH pathogenesis. High CXCL12 levels have been recorded in the plasma of PAH patients and these higher CXCL12 levels were related with reduced survival in these patients (Wei et al. 2015). Another study has shown a three to four fold higher CXCL12 protein expression in lungs of idiopathic PAH patients as compared with healthy subjects. Higher circulating levels as well as higher protein expression of CXL12 in the lungs of animal models with established PH (SuHx and MCT) were also observed and CXCL12 neutralization using neutraligands not only improved the hemodynamic parameters but also improved the lung and cardiac structure in the PH animal models (Bordenave et al. 2020). These findings are consistent with the higher CXCL12 expression we observed in Stamp2-KO mouse lungs under hypoxia and point towards a role of CXCL12 in PH with respect to Stamp2 deficiency.

These findings showing higher inflammatory cytokine expression in absence of Stamp2 along with the already established knowledge that CXCL12 is responsible for recruitment of macrophages (Sánchez-Martín et al. 2011) relates to the high CD68+ staining we observed in lungs of hypoxia-exposed Stamp2-KO mice as well. The CD68+ stained cells observed in the hypoxia-induced Stamp2-KO lungs appeared to be of monocytic origin, and we know that MCP-1 causes recruitment of monocytes. We found MCP-1 along with other

cytokines was highly expressed in Stamp2-KO mouse lungs. The cell type was further confirmed by performing dual staining to separate SMCs from CD68+ stained cells. Recruitment of monocytes along with elevated inflammation is critical in paving the path for hypoxia-dependent PH, and actually acts as a precursor to disease development (Vergadi et al. 2011). It has been found that Stamp2 expression is associated with the CD68+ expression in the adipose tissue, which is an active site for inflammatory action leading to obesity (Moreno-Navarrete et al. 2011). These findings explain the high CD68+ cell recruitment we observed in Stamp2 deficient mouse lungs under the influence of hypoxia and ultimate PH development. Our findings thus indicate a link between absence of Stamp2 and enhanced inflammation along with development of PH.

## 5.2 Stamp2 absence leads to development of PH

Genetic ablation of Stamp2 led to enhanced hypoxia-induced PH in the mouse model as compared to WT. Hypoxia-induced PH was successively achieved in WT and Stamp2-KO mouse model, both showing a significantly higher RVSP as compared to their normoxic controls. Stamp2-KO mice had significantly higher RVSP as compared to WT under hypoxia. Although significantly different, these values showed a humble difference. This modest difference may explain the lack of more pronounced RV hypertrophy in Stamp2-KO mice compared to WT. Stamp2 is already linked with disease like obesity, insulin resistance, cancer and metabolic disorders and has a protective role in obese and genetic diabetic mouse models showing its relevance to high inflammation based diseases (Sikkeland et al. 2019). According to a recent study, overexpression of Stamp2 attenuated adipose tissue angiogenesis and insulin resistance; it is interesting to note that the major actions regulating angiogenesis in the adipose tissue include inflammation and tissue hypoxia, and the

adipose tissue vasculature is the key site involved in the nutritional furbishing and inflammatory profile regulation of the adipose tissue (Wang et al. 2017). This carries similarity with disease prognosis of PH where, hypoxia and inflammation play a key role and also the vasculature acts as the site of recruiting inflammatory cells and cytokines. Our results show a pattern of diminished Stamp2 expression in PH subjects similar to what has been observed in obese subjects, where Stamp2 expression was found to be significantly and inversely associated with the obesity phenotype measurements including systemic blood pressure (Moreno-Navarrete et al. 2011).

Taken together, our data may suggest that absence of Stamp2 has a more direct effect on vascular cell function along with higher inflammation which promotes progression of the disease.

## 5.3 Stamp2 is downregulated in experimental and human PH

In addition to interference with Stamp2 signalling, the correlation between disease development per se and Stamp2 regulation was an important aspect to be looked at. Earlier studies which focused on Stamp2 regulation in human disease have primarily looked at insulin resistance and angiogenesis of adipose tissue leading to obesity which cause diseases like high fat liver disease and diabetes (Arner et al. 2008, Kim et al. 2015). The findings in these existing studies can be helpful in the context of our study since these diseases, like PH, are inflammation driven as well. Thus, the function of Stamp2 can be considered in this setting using existing knowledge regarding its regulation in the presence or absence of overt inflammation, an important feature of PH.

Here, we found that Stamp2 expression in lung tissue was significantly downregulated during disease development of

experimental PH (hypoxia mouse model, Su/Hx rat model), and in samples from patients with PAH. In context with our data on loss of Stamp2 and its effect on inflammation and PH progression, this suggests that Stamp2 acts a protective factor against disease progression, and its downregulation during PH development allows other factors to more effectively elicit their pathogenic signals. Moreover, Stamp2 expression may be used as a marker to flag disease onset, and restoration of Stamp2 expression may provide a therapeutic strategy. It has also been shown previously that Stamp2 is one of the top ten markers which are differentially expressed in the RV under conditions of RV dysfunction (di Salvo et al. 2015). These findings confirm the earlier evidence showing Stamp2 as a critical player in maintaining systemic homeostasis and regulating inflammatory responses. Stamp2 is essential to regulate inflammation and to avoid excessive inflammation, thus its deficiency sufficiently causes many features of metabolic syndrome which primarily includes inflammation. Lack of Stamp2 has been found to induce inflammation and insulin resistance (IR) in healthy lean mice and its dysregulated expression has been observed in obese mice and humans (Moreno-Navarrete et al. 2011)

## 5.4 **Pulmonary vasculature and Stamp2 expression**

It is known that Stamp2 is expressed in many human tissues and is relatively highly expressed in heart, lung, placenta and adipose tissue (Yoo et al. 2014). We found Stamp2 expression in basically all cells involved in forming the pulmonary vasculature and relatively higher expression at mRNA levels was observed in coronary ECs and microvascular ECs. Such high expression at the mRNA levels may be explained by various post-transcriptional factors in these particular cell types as compared to other vascular cells. Post-translational modifications of mRNA can lead to relatively lower protein output as

compared to higher mRNA level. Factors like protein half-life, protein degradation/damage and experimental factors could play a role as well. At the protein level, Stamp2 expression was similar for most cells except for monocytes where expression was too little to be visually observed as a protein band but was present at the mRNA level. The same monocytes when differentiated into macrophages showed a substantial increase in protein and mRNA expression of Stamp2, which appears to be relevant for disease progression.

## 5.5 Stamp2 regulation in vitro

It is already known that nutritional components can regulate Stamp2 expression in both in-vivo and in-vitro settings (Wellen et al. 2007) and inflammatory stimuli are also known to induce Stamp2 expression (Moreno-Navarrete et al. 2011). SMCs, monocytes, macrophages and ECs drive cellular functions contributing to disease development. Hence, we studied how Stamp2 is regulated in the distinct cell types when exposed to hypoxia to imitate disease like conditions in vitro.

Human and murine PASMCs showed a significant downregulation of Stamp2 expression when exposed to hypoxia. This is in line with previous findings where Stamp2 expression decreased in lungs of WT mice after exposure to hypoxia, in Su/Hx-exposed rat lungs and the lungs of PAH patients. ECs, also play a prominent role in PH development (Amiri et al. 2004). Human microvascular ECs also showed downregulation of Stamp2 expression after hypoxia, indicating a role in PH development.

With regard to inflammatory cells, mouse macrophages also showed significant downregulation of Stamp2 expression when exposed to hypoxia. As numerous studies have indicated early recruitment of macrophages in lungs of mice under hypoxia and the importance of

pulmonary macrophages in the pathogenesis of PH (Pugliese et al. 2017), and we observed accumulation of CD68+ cells in lungs of Stamp2 deficient mice under hypoxia, these findings are likely relevant and point towards an important role of these cells in connecting lack of Stamp2 and disease pathogenesis.

## 5.6 Stamp2 absence modestly affects cellular actions

Hypertension is characterized by vascular remodelling coupled with heightened resistance which is due to pronounced proliferation, apoptosis and migration of vascular smooth muscle cells (VSMCs). The smooth muscle cells are a dominant building bock of the medial layer of arteries and thus have a very important function in ensuring healthy vasculature. Various studies have shown that metabolism of smooth muscle cells is related to the progression of many vascular diseases such as systemic and pulmonary hypertension and atherosclerosis (Shi et al. 2020). Since the smooth muscle cells play a major role in maintaining functional blood vessel tone, blood stream and pressure, it was important to study the function of these cells in regard to our study.

To assess how absence of Stamp2 may affect the cellular actions of vascular cells, we compared cellular responses in WT and Stamp2-KO cells under normoxic and/or hypoxic conditions. It is known that PASMCs carry hypoxia sensor and thus can have altered functions in accordance with exposure and placement of cells in the vasculature (Madden et al. 1992). WT and Stamp2-KO PASMCs were assessed in proliferation assays. While under normoxic conditions there was no difference between both genotypes under basal conditions, upon stimulation with IL-6 or growth medium, but under hypoxic conditions Stamp2-KO PASMCs showed a significantly higher proliferation rate only in the presence of growth medium and provided a modest effect. This result makes sense since in presence of hypoxia PASMCs are

known to perform a central role in developing constricted arteries to ensure oxygen uptake. Thus, hypoxia is considered as one of the major determinants of PH development, and is also attributed to other lung disorders such as interstitial lung disease (Sylvester et al. 2012).

Along with SMCs, other key cell types that play an important role in the development of vascular disease and PH include endothelial cells (ECs). It is already known that ECs can regulate the function of underlying SMCs by releasing various bioactive factors, thus contributing to pulmonary vascular homeostasis and remodeling (Gao et al. 2016). So it was natural to study the cellular actions of ECs next. As we were unable to isolate microvascular ECs from WT or Stamp2-KO mice, we utilized commercially available human microvascular ECs and siRNA of Stamp2 to mimic the WT and Stamp2-KO genotypes. Viability assays were performed to evaluate a potential role of cell death for Stamp2-dependent impact on vascular remodeling. Stamp2 siRNA treated HMVECs vs. untreated control HMVECs yielded comparable values of viability. To understand the role of ECs further, apoptosis assays were also conducted, again showing no significant differences. When interpreting these results, one has to keep in mind that HMVECs are fragile cells requiring ultimate care and sensitive handling to ensure proper experimental conditions. Stamp2 siRNA treatment tends to be harsh where cells are starved and then kept in siRNA along with starvation medium mix for more than 48 hours, which may also affect cellular integrity and function.

Endothelial dysfunction plays a role in smooth muscle cell mediated vasoconstriction connected to hypertension. Dysfunction in ECs can be an important hallmark in the development of PH, since ECs affect the cellular actions of SMCs by inducing proliferation, vascular remodelling and by releasing vasodilator and vasoconstrictor factors

(Shi et al. 2020). In light of these studies it was an important finding that overall, lack of Stamp2 did not show a meaningful effect on the cellular actions of these cell types which could explain an impact on the development of PH, so that additional factors including cellular cross-talk via inflammatory mediators must be taken into consideration.

## 5.7 Stamp2 absence in macrophages promotes PASMCs proliferation and migration

Several mechanisms may indirectly affect cellular functions under pathogenic conditions. For instance, it has been shown that hypoxia derives increased PDGF signalling in the pulmonary vasculature which in turn causes enhanced proliferation and migration of PASMCs, both of which are leading factors in developing PH. Notably, this occurred without affecting expression levels, but due to downregulation of PDGFR-deactivating protein tyrosine phosphatases (ten Freyhaus et al. 2011).

Here, we interestingly found that Stamp2-KO mouse PASMCs showed significantly higher proliferation only under hypoxia and under the influence of growth medium. Thus, lack of Stamp2 in PASMCs alone was not sufficient to promote proliferation. Therefore, we decided to evaluate factors present in the surroundings of pulmonary vasculature which might have an impact. To this end, we used supernatant from macrophages extracted from WT and Stamp2-KO mice and compared their potency to induce proliferation and migration in WT PASMCs. The results showed that macrophage supernatant from Stamp2-KO but not WT mice caused significantly higher proliferation of PASMCs, which was similar for both normoxia and hypoxia. Thus, even without the additional trigger of hypoxia, the

lack of Stamp2 in macrophage supernatant is enough to cause significantly enhanced proliferation.

Inflammation is known to further averse the phenomena causing PH, which we have already observed in the hypoxia treated lungs from Stamp2-KO mice. The higher PASMCs proliferation rate under the influence of Stamp2 deficient macrophages may also explain the higher muscularization that we observed in the small vessels of Stamp2-KO mouse lungs as compared to WT. In a similar fashion, supernatant from WT and Stamp2-KO macrophages was used to induce PASMC migration. Supernatant from both genotypes induced PASMC migration, but significantly higher migration was induced by supernatant from Stamp2-KO macrophages.

Although the cytokine array of macrophages supernatant showed a number of active cytokines the selection of cytokines namely CXCL12, MCP-1 and IL-6, we made was backed by literature review and earlier scientific findings (Park et al. 2014, Wei et al. 2015). We selected the cytokines which showed high expression and which are known to have an active role in vascular remodeling and cardiovascular inflammation in particular (Bordenave et al. 2020, Yang et al. 2014, Sikkeland et al. 2012). These cytokines and their respective neutralizing antibodies were then further used to study cellular actions.

CXCL12 and its receptor CXCR4 is known to help develop hypoxia induced PH and vascular remodeling; it also regulates cell cycle progression and proliferation in PASMCs. It has been found that inhibiting CXCL12/CXCR4 decreases cell cycle progression and also causes lower expression of cell cycle progression proteins (Wei et al. 2015). CXCL12 has also been reported to be elevated in PH patients, and associated with outcome (Yang et al. 2014, Bordenave et al. 2020). CXCL12 has shown to impart vascular remodeling and induce

proliferation of PASMCs (McCullagh et al. 2015). It is established already that hypoxia induces the expression of the CXCL12 receptor (CXCR4) in PASMCs and the pulmonary arteries of rats upon hypoxia exposure, and silencing CXCL12/CXCR4 blocks hypoxia induced cell viability and proliferation (Wei et al. 2015). Keeping in view this scientific knowledge, it made sense to indulge this cytokine in our study.

MCP-1 plays an important role in development of cardiovascular diseases owing to its inflammation supporting characteristics. It has been reported that MCP-1 has a central role in the development of atherosclerosis since monocytes and macrophages cause growth of other inflammatory cells and cytokines within atherosclerotic plaques. MCP-1 causes monocytes accumulation which leads to fatty streak formation leading to atherosclerotic plaque formation (Niu and Kolattukudy 2009, Lin et al. 2014). Atherogenesis includes monocytes maturing into macrophages which causes increased cytokine expression and growth of other inflammatory cells as well (Lin et al. 2014). Higher plasma levels of MCP-1 have been reported in patients of IPAH, this implies MCP-1 has a role in the development of pulmonary hypertension (Itoh et al. 2006). Mechanical stress and PH provide stimuli leading to vascular remodeling of pulmonary arteries which is in part mediated by MCP-1 release (Park et al. 2014). Advancement of many disease conditions is mainly caused by migration and adhesion of inflammatory cells, and MCP-1 is known to cause the pathogenesis of inflammatory disease by promoting these functions by facilitating monocytes migration and attracting other inflammatory cells to the sub-endothelium. It is already established that endothelial dysfunction is correlated to several inflammatory conditions such as diabetes and hypertension. MCP-1 affects the endothelium which subsequently leads to cellular adhesion,

proliferation of smooth muscle cells and inflammation of vessel wall thus worsening the disease conditions (Singh et al. 2021).

Many members of the scientific community have affirmed the role of IL-6 in PH. In mouse model, it was reported that overexpression of IL-6 caused formation of pulmonary vascular lesions and mice which were IL-6 deficient were protected. IL-6 neutralization has also shown disease compensation effects, where neutralizing IL-6 receptor lead to ameliorated development of experimental PH (Toshner and Rothman 2020). The finding that upon inflammatory stimuli PASMCs show higher concentration of IL-6 in comparison to the endothelial cells confirms that PASMCs might be a source of IL-6 (Davies et al. 2012). This demonstration thus naturally points towards studying how PASMCs behave towards IL-6 exposure in context of Stamp2 absence and PH for our study.

In light of this aforementioned scientific information we thus, selected these cytokines as we wanted to keep focus on this particular trail following vascular remodelling and PH.

Along with proliferation, migration of cells of vasculature also plays an important role in aggravating the process of vascular remodeling. We utilized scratch assays to evaluate cell migration, which best mimics the in vivo environment and thus, is a preferred way of studying cell migration (Liang et al. 2007). In order to ensure that the phenomena under study was purely migration and not proliferation, we inhibited cell proliferation during scratch assay by starving the cells for a period of 24 hours (Glenn et al. 2016).

The cytokines CXCL12, MCP-1 and IL-6 individually as well as in combination, as a cytokines cocktail, induced effective PASMCs migration. CXCL12 and MCP-1 individually and in combination induced effective PASMCs proliferation. Interestingly, IL-6 did not induce any proliferation in PASMCs, but was very effective in

inducing migration. These results are in line with previous studies regarding IL-6 preferably contributing to PASMCs proliferation rather than migration (Maston et al. 2017, Savale et al. 2009). Our data also shows that many cytokines have dual effect of proliferation and migration, and some act for either of the actions and a collective effect of many chemokines contributes to the overall pathophysiolgy of disease.

To confirm the active role of these cytokines in the macrophage supernatant, we applied these individually and in combination to assess their impact on proliferation and migration of PASMCs. These experiments confirmed their biological relevance, where cellular responses were even more pronounced when a combination of cytokines was used, and this effect was prevented by using neutralizing antibodies against the respective cytokines.

The neutralizing antibodies against MCP-1, CXCL12 and IL-6 even more effectively prevented PASMCs proliferation and migration induced by Stamp2-KO macrophage supernatant, further confirming the link to Stamp2 in their active role for PASMCs responses contributing to vascular remodeling.

When viewed together, our results presented herein propose a relevant role of Stamp2 acting as a negative regulator and preventive mediator from PAH. The results are consistent with the pictorial illustration in the following figure. Loss of Stamp2 during disease progression allows a change in the inflammatory milieu and pathogenic cellular responses of vascular cells, collectively promoting pulmonary vascular remodeling and PH.

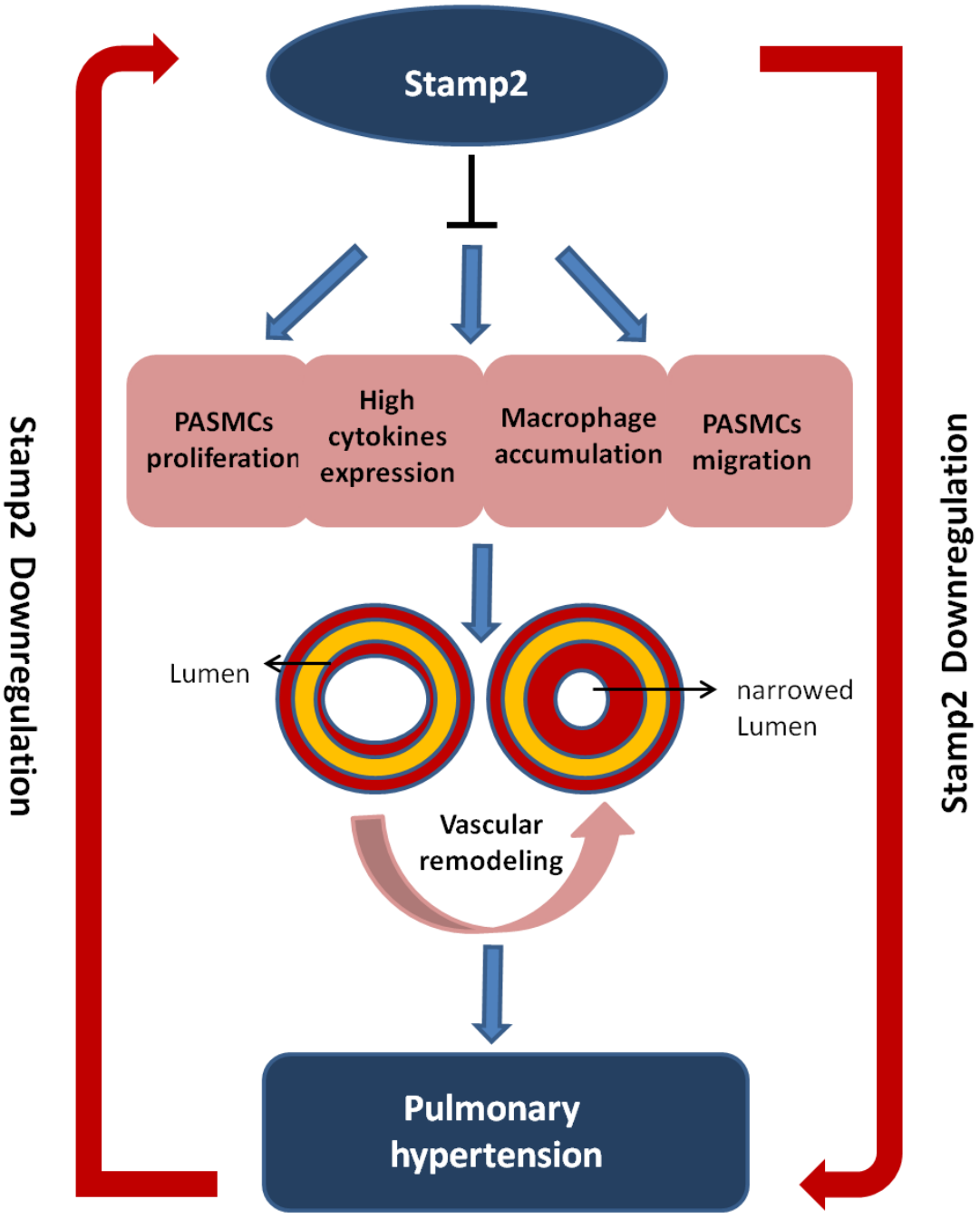


**Figure 5.1: Lack of Stamp2 leads to development of PH**

*Schematic diagram summarizing the findings of this thesis and indicating the proposed protective role of Stamp2 against the development of PH*

.

## 5.8 Limitations of the study

In this study, we primarily utilized the hypoxia induced PH mouse model. It is important to consider that despite many similarities, the mouse model for PH can not exactly replicate human disease. A number of anatomical, physical and physiological differences lie between the two systems. Hypoxia based PH of mouse model is also not as intense as human PH disease, the latter presenting with more pronounced vascular remodeling and narrowing of vessels in particular. Alternative PH animal model such as the MCT (monocrotaline) or Su/Hx rat models are considered better because of more prominent vascular remodeling and pathology. However, development of genetically altered animals, their maintenance and experimental design is rather more workable with a smaller animal model such as mouse. So a compromise had to be reached in order to have an effective and feasible experimental design. In this study, we observed PASMCs actively participated in the pathophysiolgy of the disease via actions of proliferation and migration but no such finding was associated with ECs. In another study a similar finding has been reported where no significant EC proliferation was observed in hypoxia exposed mouse PH (Voelkel and Tuder 2000), whereas in human PAH, ECs contribute a great deal to vascular remodeling by forming plexiform lesions. Nonetheless, a genetically modified mouse model still proves to be a good way to study the molecular and functional basis of the disease to understand it further.

## 5.9 Conclusions

In this study we were able to successfully show that absence of Stamp2 enhances the development of PH in mice under hypoxia. We showed that Stamp2 expression is present in the cells of vasculature

and is directly affected by hypoxia both in-vivo and in-vitro. The lung tissue shows downregulated Stamp2 for both mouse and rat PH model as well as for human disease. Similarly, SMCs, ECs and macrophages show Stamp2 downregulation upon hypoxia exposure. Higher inflammation in the lungs and serum was also found in the absence of Stamp2 through high expression of cytokines and CD68+ cells accumulation in the Stamp2-KO lungs. The macrophages supernatant from Stamp2-KO mouse acted as a strong driving agent for higher degrees of inflammation along with proliferation and migration of SMCs. Thus, it may be concluded that (i) Stamp2 acts as a negative and protective mediator against PH which is downregulated during disease progression and (ii) elevated inflammation along with macrophage mediated higher migration and proliferation of PASMCs play an active role in promoting PH in the absence of Stamp2.

## 5.10 **Future prospects**

Stamp2 and its relation to inflammation have been explained along with its association in a number of metabolic diseases. Stamp2 has been shown to play a critical role in regulation of inflammation and nutritional signals with respect to metabolism, it acts via adipocytes and macrophages and plays its role in maintaining a balanced metabolic homeostasis (ten Freyhaus et al. 2012). It has also been shown that stamp2 expression itself is regulated by inflammatory signals and its deficiency causes deposition of fat and insulin resistance, both of these diseased states are fuelled by enhanced inflammation (Wellen et al. 2007). Stamp2 has been shown to be downregulated in the livers of non-alcoholic fatty liver disease (NAFLD) patients (Kim et al. 2015), in obese patients (Chen et al. 2010) and also in obese patients with type 2 diabetes (Moreno-Navarrete et al. 2011). Stamp2 prevents from hepatic steatosis by

decreasing the hepatitis B protein induced insulin resistance and fat accumulation (Kim et al. 2012) and suppresses atherosclerosis (Wang et al. 2014). A recent study showed how Stamp2 helps in increased Akt-phosphorylation in hepatic tissue and thus rescues against insulin development and hepatic steatosis (Park et al. 2020).

In light of animal studies where Stamp2 overexpression helped attenuate the diseased states and showed tremendous effects of disease prevention, it can be considered as cure-tool in future pharmacological interventions. These studies included findings where adenoviral constructs were used to impose Stamp2 overexpression in the liver and this helped attenuate insulin resistance and hepatic steatosis in high fat diet fed mice (Hye Y Kim et al. 2015). It has been shown that overexpression can help attenuate the adipose tissue angiogenesis which is one of the most lethal obesity related pathological disorder (F. Wang et al. 2017) and this overexpression also prevented insulin resistance in diabetic mice (Han et al. 2013). Also, even atherosclerosis was suppressed along with stabilization of plaques in diabetic mice via Stamp2 overexpression (J. Wang et al. 2014).

As the next step in this study to further understand how Stamp2 regulates the occurrence and development of disease and how preventive its presence in terms of over-expression can be, a Stamp2 over-expressing mouse model might be developed. If this model is prevented against development of hypoxia based PH and overt inflammation; it would further confirm and elaborate its protective role against the disease.

In a recent study, the phosphodiesterase-3 inhibitor Cilostazol was found to enhance the hepatic expression of Stamp2 through AMP-activated protein kinase (AMPK) in vivo and in vitro. This enhanced Stamp2 expression prevented hepatic steatosis in mouse model of

non alcoholic fatty liver (NAFLD) disease (Oh et al. 2018). Hence, this data points towards possible strategies of maintaining Stamp2 expression in diseased states and prevent its downregulation thus, using the protective role of Stamp2 against inflammation and disease progression. In future studies, Cilostazol can be studied for its therapeutic tendencies in experimental models of PH and if proven successful might be used in pharmacological interventions targeting human disease.

# 6. Summary

# 6 Summary

**Background:** Pulmonary hypertension (PH) is a grave disease affecting people around the globe from all walks of life and young to older age groups. The disease is characterised by high pulmonary artery pressure and pulmonary vascular resistance, along with vascular remodeling. Ultimately, PH leads to right ventricular failure and death. The cells in the pulmonary vasculature play a pivotal role in developing the underlying vascular remodeling, where increased proliferation and migration is orchestrated in the presence of inflammation which promotes pathogenic cellular responses.

**Aim:** The aim of this study was to define the role of Stamp2 in the development of PH and to study how the presence or absence of Stamp2 affects disease progression. The prior knowledge that Stamp2 absence leads to elevated inflammation and has a role in inflammatory and cardiovascular diseases paved way for developing our hypothesis which is; Stamp2 protects against PH

**Results:** Lung tissue from hypoxia exposed mice, Sugen-hypoxia exposed rats and PAH patients showed significant downregulation of Stamp2 as compared to control animals and healthy patients, showing that disease is associated with low levels of Stamp2. A causal relationship was further solidified with Stamp2-KO mice showing significantly higher muscularization in the small pulmonary arteries and significantly higher right ventricular systolic pressure (RVSP) as measured by invasive hemodynamic assessment characterizing PH, as compared to WT control. Based on these in-vivo findings we characterized Stamp2 regulation in-vitro in human and mouse pulmonary arterial smooth muscle cells (PASMCs) and human microvascular endothelial cells (HMVECs) under hypoxia and

normoxia conditions. Similar to the in-vivo findings, downregulation of Stamp2 under hypoxia was observed for both cell types.

The relationship between lack of Stamp2 and PH was further solidified with enhancement of pulmonary inflammation in hypoxia-exposed mouse lungs as compared to control. High mRNA expression of inflammatory cytokines in hypoxia exposed Stamp2-KO mouse lungs and serum along with high CD68+ staining in the lung tissue was found.

PASMCs showed significantly higher proliferation and migration rates when treated with macrophage supernatant from Stamp2-KO mice as compared to the WT control, which likely contributes to developing pulmonary vascular remodelling. MCP-1, CXCL12 and IL-6 were found to be few of the active cytokines causing these cross-talks between macrophages and PASMCs, as their inhibition effectively prevented these actions mediated by macrophage supernatant.

**Conclusions:** These results show that Stamp2 acts as a protective factor against PH development in both human and mouse. PH progression is associated with Stamp2 downregulation, and lack of Stamp2 promotes pathogenic cellular responses and results in enhanced development of PH. Hence, low expression of Stamp2 may mark the presence of disease, and strategies to upregulate or maintain Stamp2 expression may represent a novel therapeutic intervention.

# 7. Zusammenfassung

# 7 Zusammenfassung

**Hintergrund:** Pulmonale Hypertonie (PH) ist eine schwerwiegende Erkrankung, von der weltweit Menschen aus allen Gesellschaftsschichten und Altersgruppen betroffen sind. Die Erkrankung ist gekennzeichnet durch einen hohen Druck in der Lungenarterie und einen hohen pulmonalen Gefäßwiderstand, verbunden mit einem Gefäßumbau. Letztlich führt die PH zum Versagen des rechten Ventrikels und zum Tod. Die Zellen des pulmonalen Gefäßsystem spielen eine zentrale Rolle bei der Entstehung des zugrunde liegenden Gefäßumbaus, im Rahmen dessen es zu einer verstärkten Proliferation und Migration kommt, welche durch inflammtorische Prozesse begünstigt wird.

**Ziel:** Ziel dieser Studie war es, die Rolle von Stamp2 bei der Entwicklung der PH zu definieren und zu untersuchen, wie die Anwesenheit oder Defizienz von Stamp2 die Progression der Erkrankung beeinflusst. Basiend auf bereits publizierten Daten, die zeigen, dass Stamp2 Defizienz zu einer erhöhten Infammation führt und eine Rolle bei inflammatorischen sowie kardiovaskulären Erkrankungen spielt, wurde die Hypthese generiert, dass Stamp2 vor PH schützt.

**Ergebnisse:** Lungengewebe von Mäusen, die Hypoxie- und Ratten, die Sugen-Hypoxie ausgesetzt waren, sowie von PAH-Patienten zeigte eine signifikante Herabregulierung von Stamp2 im Vergleich zu Kontrolltieren und gesunden Patienten, was zeigt, dass die Erkrankung mit reduzierten Stamp2 Leveln assozieiert ist. Ein kausaler Zusammenhang konnte mittels Stamp2-KO-Mäusen gezeigt werden, welche im Vergleich zu WT-Kontrolltieren nach Hypoxie Exposition eine signifikant stärkere Muskularisierung der kleinen Lungenarterien aufwiesen und bei denen im Rahmen der invasiven

hämodynamischen Untersuchungen zur Charakterisierung der PH ein signifikant höherer rechtsventrikulärer systolischer Druck (RVSP) gemessen wurde.

Basierend aus diesen in-vivo Ergebnissen haben wir die Stamp2-Regulation in vitro in humanen und murinen pulmonal-arteriellen glatten Muskelzellen (PASMCs) und humanen mikrovaskulären Endothelzellen (HMVECs) unter hypoxischen und normoxischen Bedingungen untersucht. In Übereinstimmung mit den in-vivo Ergebnissen wurde in beiden Zelltypen eine Herunterregulierung von Stamp2 unter Hypoxie beobachtet.

Der Zusammenhang zwischen Stamp2 Defizienz und PH wurde außerdem bekräfigt durch eine Verstärkung der Inflammation in Lungen von Hypoxie-exponierten Mäusen im Vergleich zu Kontrollen. So konnte eine erhöhte mRNA-Expression inflammatorischer Zytokine in Lungenhomogenaten und Seren von Hypoxie-exponierten Stamp2 KO-Mäusen gezeigt werden als auch eine intensive Färbung des Markophagenmarkers CD68+- in Lungengewebesschnitten. Außerdem reagierten PASMCs mit einer signifikant höheren Proliferation und Migration, wenn sie mit Makrophagenüberständen aus Stamp2 KO- verus WT Mäusen behandelt wurden, was mit hoher Wahrscheinlichkeit zum pulmonalen Gefäßumbaus beiträgt. Darüberhinaus konnte gezeigt werden, dass unteranderem die Zytokine MCP-1, CXCL12 und IL-6 diese Wechselwirkungen zwischen Makrophagen und PASMCs begünstigen, da deren Inhibition die, durch den Makrophagenüberstand vermittelten Effekte verhindert.

**Schlussfolgerungen:** Diese Ergebnisse zeigen, dass Stamp2 sowohl bei Menschen als auch im murinen Modell protektiv gegen die Entstehung einer PH wirkt. Die Progression der PH ist assoziiert mit einer Herunterregulierung von Stamp2. Eine Stamp2 Defizienz fördert pathologische zelluläre Reaktionen, welche zur Entstehung einer PH beitragen können. Eine reduzierte Stamp2 Expression könnte daher

als prognostischer Marker für eine PH fungieren. Außerdem könnten Strategien zur Erhöhung oder Aufrechterhaltung der Stamp2-Expression eine neue therapeutische Option darstellen

# 8. References

# 8 References

Amiri, Farhad, Agostino Virdis, Mario Fritsch Neves, Marc Iglarz, Nabil G Seidah, Rhian M Touyz, Timothy L Reudelhuber, and Ernesto L Schiffrin. 2004. “Endothelium-Restricted Overexpression of Human Endothelin-1 Causes Vascular Remodeling and Endothelial Dysfunction.” *Circulation* 110 (15): 2233–40. https://doi.org/10.1161/01.CIR.0000144462.08345.B9.

Arner, Peter, Britta M Stenson, Elisabeth Dungner, Erik Naslund, Johan Hoffstedt, Mikael Ryden, and Ingrid Dahlman. 2008. “Expression of Six Transmembrane Protein of Prostate 2 in Human Adipose Tissue Associates with Adiposity and Insulin Resistance.” *The Journal of Clinical Endocrinology and Metabolism* 93 (6): 2249–54. https://doi.org/10.1210/jc.2008-0206.

Batool, Mehreen, Eva M Berghausen, Mario Zierden, Marius Vantler, Ralph T Schermuly, Stephan Baldus, Stephan Rosenkranz, and Henrik ten Freyhaus. 2020. “The Six-Transmembrane Protein Stamp2 Ameliorates Pulmonary Vascular Remodeling and Pulmonary Hypertension in Mice.” *Basic Research in Cardiology* 115 (6): 68. https://doi.org/10.1007/s00395-020-00826-8.

Bhatnagar, Akshay, Jonathan Wiesen, Raed Dweik, and Neal F Chaisson. 2018. “Evaluating Suspected Pulmonary Hypertension: A Structured Approach.” *Cleveland Clinic Journal of Medicine* 85 (6): 468–80. https://doi.org/10.3949/ccjm.85a.17065.

Bordenave, Jennifer, Raphaël Thuillet, Ly Tu, Carole Phan, Amélie Cumont, Claire Marsol, Alice Huertas, et al. 2020. “Neutralization of CXCL12 Attenuates Established Pulmonary Hypertension in Rats.” *Cardiovascular Research* 116 (3): 686–97. https://doi.org/10.1093/cvr/cvz153.

Catalan, Victoria, Javier Gomez-Ambrosi, Amaia Rodriguez, Beatriz Ramirez, Fernando Rotellar, Victor Valenti, Camilo Silva, Maria J Gil, Javier Salvador, and Gema Fruhbeck. 2013. “Six-Transmembrane Epithelial Antigen of Prostate 4 and Neutrophil Gelatinase-Associated Lipocalin Expression in Visceral Adipose Tissue Is Related to Iron Status and Inflammation in Human Obesity.” *European Journal of Nutrition* 52 (6): 1587–95. https://doi.org/10.1007/s00394-012-0464-8.

Chen, Xiaohui, Chun Zhu, Chenbo Ji, Yaping Zhao, Chunmei Zhang, Fukun Chen, Chunlin Gao, Jingai Zhu, Lingmei Qian, and Xirong Guo. 2010. “STEAP4, a Gene Associated with Insulin Sensitivity, Is Regulated by Several Adipokines in Human Adipocytes.” *International Journal of Molecular Medicine* 25 (3): 361–67.

Chinali, Marcello, Richard B Devereux, Barbara V Howard, Mary J Roman, Jonathan N Bella, Jennifer E Liu, Helaine E Resnick, Elisa T Lee, Lyle G Best, and Giovanni de Simone. 2004. “Comparison of Cardiac Structure and Function in American Indians with and without the Metabolic Syndrome (the Strong Heart Study).” *The American Journal of Cardiology* 93 (1): 40–44.

Chuang, Chao-Tang, Jinn-Yuh Guh, Chi-Yu Lu, Yeng-Tseng Wang, Hung-Chun Chen, and Lea-Yea Chuang. 2015. “Steap4 Attenuates High Glucose and S100B-Induced Effects in Mesangial Cells.” *Journal of Cellular and Molecular Medicine* 19 (6): 1234–44. https://doi.org/10.1111/jcmm.12472.

Davies, Rachel J, Alan M Holmes, John Deighton, Lu Long, Xudong Yang, Lucy Barker, Christoph Walker, David C Budd, Paul D Upton, and Nicholas W Morrell. 2012. “BMP Type II Receptor Deficiency Confers Resistance to Growth Inhibition by TGF-β in Pulmonary Artery Smooth Muscle Cells: Role of Proinflammatory Cytokines.” *American Journal of Physiology. Lung Cellular and Molecular Physiology* 302 (6): L604-15. https://doi.org/10.1152/ajplung.00309.2011.

Fishman, Alfred P. 2001. “Clinical Classification of Pulmonary Hypertension.” *Clinics in Chest Medicine* 22 (3): 385–91, vii. https://doi.org/10.1016/S0272-5231(05)70278-1.

Freyhaus, Henrik ten, Ediz S Calay, Abdullah Yalcin, Sara N Vallerie, Ling Yang, Zerrin Z Calay, Fahri Saatcioglu, and Gokhan S Hotamisligil. 2012. “Stamp2 Controls Macrophage Inflammation through Nicotinamide Adenine Dinucleotide Phosphate Homeostasis and Protects against Atherosclerosis.” *Cell Metabolism* 16 (1): 81–89. https://doi.org/10.1016/j.cmet.2012.05.009.

Freyhaus, Henrik ten, Markus Dagnell, Maike Leuchs, Marius Vantler, Eva M Berghausen, Evren Caglayan, Norbert Weissmann, et al. 2011. “Hypoxia Enhances Platelet-Derived Growth Factor Signaling in the Pulmonary Vasculature by down-Regulation of Protein Tyrosine Phosphatases.” *American Journal of Respiratory and Critical Care Medicine* 183 (8): 1092–1102. https://doi.org/10.1164/rccm.200911-1663OC.

Frid, Maria G, Jacqueline A Brunetti, Danielle L Burke, Todd C Carpenter, Neil J Davie, John T Reeves, Mark T Roedersheimer, Nico van Rooijen, and Kurt R Stenmark. 2006. “Hypoxia-Induced Pulmonary Vascular Remodeling Requires Recruitment of Circulating Mesenchymal Precursors of a Monocyte/Macrophage Lineage.” *The American Journal of Pathology* 168 (2): 659–69. https://doi.org/10.2353/ajpath.2006.050599.

Galiè, Nazzareno, Vallerie V McLaughlin, Lewis J Rubin, and Gerald Simonneau. 2019. “An Overview of the 6th World Symposium on Pulmonary Hypertension.” *European Respiratory Journal* 53 (1): 1802148. https://doi.org/10.1183/13993003.02148-2018.

Gao, Yuansheng, Tianji Chen, and Usha Raj. 2016. “Endothelial and Smooth Muscle Cell Interactions in the Pathobiology of Pulmonary Hypertension.” *American Journal of Respiratory Cell and Molecular Biology* 54 (4): 451–60. https://doi.org/10.1165/rcmb.2015-0323TR.

Glenn, Honor, Jacob Messner, and Deirdre R Meldrum. 2016. “A Simple Non-Perturbing Cell Migration Assay Insensitive to Proliferation Effects.” *Scientific Reports* 6 (August): 31694. https://doi.org/10.1038/srep31694.

Golembeski, Scott, James West, Yuji Tada, and Karen A Fagan. 2005. “Interleukin-6

Causes Mild Pulmonary Hypertension and Augments Hypoxia-Induced Pulmonary Hypertension in Mice." *Chest* 128 (6 Suppl): 572S-573S. https://doi.org/10.1378/chest.128.6_suppl.572S-a.

Gordeuk, Victor, Oswaldo L Castro, and Roberto F Machado. 2016. "Pathophysiology and Treatment of Pulmonary Hypertension in Sickle Cell Disease." *Blood* 127 (7): 820–28. https://doi.org/10.1182/blood-2015-08-618561.

Grudzinska, Monika K, Ewa Kurzejamska, Krzysztof Bojakowski, Joanna Soin, Michael H Lehmann, Hans Reinecke, Charles E Murry, Cecilia Soderberg-Naucler, and Piotr Religa. 2013. "Monocyte Chemoattractant Protein 1-Mediated Migration of Mesenchymal Stem Cells Is a Source of Intimal Hyperplasia." *Arteriosclerosis, Thrombosis, and Vascular Biology* 33 (6): 1271–79. https://doi.org/10.1161/ATVBAHA.112.300773.

Han, Lu, Meng-Xiong Tang, Yun Ti, Zhi-Hao Wang, Jia Wang, Wen-Yuan Ding, Hua Wang, Yun Zhang, Wei Zhang, and Ming Zhong. 2013. "Overexpressing STAMP2 Improves Insulin Resistance in Diabetic ApoE(-)/(-)/LDLR(-)/(-) Mice via Macrophage Polarization Shift in Adipose Tissues." *PloS One* 8 (11): e78903. https://doi.org/10.1371/journal.pone.0078903.

Hashimoto-Kataoka, Takahiro, Naoki Hosen, Takashi Sonobe, Yoh Arita, Taku Yasui, Takeshi Masaki, Masato Minami, et al. 2015. "Interleukin-6/Interleukin-21 Signaling Axis Is Critical in the Pathogenesis of Pulmonary Arterial Hypertension." *Proceedings of the National Academy of Sciences of the United States of America* 112 (20): E2677-86. https://doi.org/10.1073/pnas.1424774112.

Hoeper, Marius, Harm Jan Bogaard, Robin Condliffe, Robert Frantz, Dinesh Khanna, Marcin Kurzyna, David Langleben, et al. 2013. "Definitions and Diagnosis of Pulmonary Hypertension." *Journal of the American College of Cardiology* 62 (25 Suppl): D42-50. https://doi.org/10.1016/j.jacc.2013.10.032.

Hoeper, Marius, Tilmann Kramer, Zixuan Pan, Christina A Eichstaedt, Jens Spiesshoefer, Nicola Benjamin, Karen M Olsson, et al. 2017. "Mortality in Pulmonary Arterial Hypertension: Prediction by the 2015 European Pulmonary Hypertension Guidelines Risk Stratification Model." *The European Respiratory Journal* 50 (2). https://doi.org/10.1183/13993003.00740-2017.

Huertas, Alice, Frederic Perros, Ly Tu, Sylvia Cohen-Kaminsky, David Montani, Peter Dorfmuller, Christophe Guignabert, and Marc Humbert. 2014. "Immune Dysregulation and Endothelial Dysfunction in Pulmonary Arterial Hypertension: A Complex Interplay." *Circulation* 129 (12): 1332–40. https://doi.org/10.1161/CIRCULATIONAHA.113.004555.

Humbert, Yaici, Sztrymf, and Montani. 2004. "[Pulmonary hypertension: from genetics to treatments]." *Revue de pneumologie clinique* 60 (4): 196–201.

Humbert, Marc, Olivier Sitbon, Ari Chaouat, Michele Bertocchi, Gilbert Habib, Virginie Gressin, Azzedine Yaici, et al. 2010. "Survival in Patients with Idiopathic, Familial, and Anorexigen-Associated Pulmonary Arterial Hypertension in the

Modern Management Era." *Circulation* 122 (2): 156–63. https://doi.org/10.1161/CIRCULATIONAHA.109.911818.

Hurdman, Judith, Robin Condliffe, Charlie A. Elliot, Christine Davies, Catherine Hill, Jim M. Wild, Dale Capener, et al. 2012. "ASPIRE Registry: Assessing the Spectrum of Pulmonary Hypertension Identified at a REferral Centre." *The European Respiratory Journal* 39 (4): 945–55. https://doi.org/10.1183/09031936.00078411.

Inoue, Asuka, Isao Matsumoto, Yoko Tanaka, Keiichi Iwanami, Akihiro Kanamori, Naoyuki Ochiai, Daisuke Goto, Satoshi Ito, and Takayuki Sumida. 2009. "Tumor Necrosis Factor Alpha-Induced Adipose-Related Protein Expression in Experimental Arthritis and in Rheumatoid Arthritis." *Arthritis Research & Therapy* 11 (4): R118. https://doi.org/10.1186/ar2779.

Itoh, Takefumi, Noritoshi Nagaya, Hatsue Ishibashi-Ueda, Shingo Kyotani, Hideo Oya, Fumio Sakamaki, Hiroshi Kimura, and Norifumi Nakanishi. 2006. "Increased Plasma Monocyte Chemoattractant Protein-1 Level in Idiopathic Pulmonary Arterial Hypertension." *Respirology (Carlton, Vic.)* 11 (2): 158–63. https://doi.org/10.1111/j.1440-1843.2006.00821.x.

Jesus, Perez, Vinicio A de. 2016. "Molecular Pathogenesis and Current Pathology of Pulmonary Hypertension." *Heart Failure Reviews* 21 (3): 239–57. https://doi.org/10.1007/s10741-015-9519-2.

Kherbeck, Nada, Mathieu C Tamby, Guillaume Bussone, Hanadi Dib, Frederic Perros, Marc Humbert, and Luc Mouthon. 2013. "The Role of Inflammation and Autoimmunity in the Pathophysiology of Pulmonary Arterial Hypertension." *Clinical Reviews in Allergy & Immunology* 44 (1): 31–38. https://doi.org/10.1007/s12016-011-8265-z.

Kim, Hye, So Y Park, Mi H Lee, Jee H Rho, Yoo J Oh, Hye U Jung, Seung H Yoo, et al. 2015. "Hepatic STAMP2 Alleviates High Fat Diet-Induced Hepatic Steatosis and Insulin Resistance." *Journal of Hepatology* 63 (2): 477–85. https://doi.org/10.1016/j.jhep.2015.01.025.

Kim, Hye Young, Hyun Kook Cho, Seong Keun Yoo, and Jae Hun Cheong. 2012. "Hepatic STAMP2 Decreases Hepatitis B Virus X Protein-Associated Metabolic Deregulation." *Experimental & Molecular Medicine* 44 (10): 622–32. https://doi.org/10.3858/emm.2012.44.10.071.

Knobloch, Jurgen, Sarah Derya Yanik, Sandra Korber, Erich Stoelben, David Jungck, and Andrea Koch. 2016. "TNFalpha-Induced Airway Smooth Muscle Cell Proliferation Depends on Endothelin Receptor Signaling, GM-CSF and IL-6." *Biochemical Pharmacology* 116 (September): 188–99. https://doi.org/10.1016/j.bcp.2016.07.008.

Korkmaz, Ceren, Kemal S Korkmaz, Piotr Kurys, Cem Elbi, Ling Wang, Tove I Klokk, Clara Hammarstrom, et al. 2005. "Molecular Cloning and Characterization of STAMP2, an Androgen-Regulated Six Transmembrane Protein That Is Overexpressed in Prostate Cancer." *Oncogene* 24 (31): 4934–45.

https://doi.org/10.1038/sj.onc.1208677.

Korkmaz, Kemal, Korkmaz, Ragnhildstveit, Pretlow, and Saatcioglu. 2000. “An Efficient Procedure for Cloning Hormone-Responsive Genes from a Specific Tissue.” *DNA and Cell Biology* 19 (8): 499–506. https://doi.org/10.1089/10445490050128421.

Korkmaz, Kemal, Cem Elbi, Ceren G Korkmaz, Massimo Loda, Gordon L Hager, and Fahri Saatcioglu. 2002. “Molecular Cloning and Characterization of STAMP1, a Highly Prostate-Specific Six Transmembrane Protein That Is Overexpressed in Prostate Cancer.” *The Journal of Biological Chemistry* 277 (39): 36689–96. https://doi.org/10.1074/jbc.M202414200.

Kralisch, Susan, Grit Sommer, Sebastian Weise, Jana Lipfert, Ulrike Lossner, Manja Kamprad, Kathleen Schrock, Matthias Bluher, Michael Stumvoll, and Mathias Fasshauer. 2009. “Interleukin-1beta Is a Positive Regulator of TIARP/STAMP2 Gene and Protein Expression in Adipocytes in Vitro.” *FEBS Letters* 583 (7): 1196–1200. https://doi.org/10.1016/j.febslet.2009.03.015.

Kylhammar, David, Barbro Kjellström, Clara Hjalmarsson, Kjell Jansson, Magnus Nisell, Stefan Söderberg, Gerhard Wikström, and Göran Rådegran. 2018. “A Comprehensive Risk Stratification at Early Follow-up Determines Prognosis in Pulmonary Arterial Hypertension.” *European Heart Journal* 39 (47): 4175–81. https://doi.org/10.1093/eurheartj/ehx257.

Liang, Chun-Chi, Ann Y Park, and Jun-Lin Guan. 2007. “In Vitro Scratch Assay: A Convenient and Inexpensive Method for Analysis of Cell Migration in Vitro.” *Nature Protocols* 2 (2): 329–33. https://doi.org/10.1038/nprot.2007.30.

Lin, Juntang, Vijay Kakkar, and Xinjie Lu. 2014. “Impact of MCP-1 in Atherosclerosis.” *Current Pharmaceutical Design* 20 (28): 4580–88. https://doi.org/10.2174/1381612820666140522115801.

Madden, Jane , Maya S Vadula, and Viswanath P Kurup. 1992. “Effects of Hypoxia and Other Vasoactive Agents on Pulmonary and Cerebral Artery Smooth Muscle Cells.” *The American Journal of Physiology* 263 (3 Pt 1): L384-93. https://doi.org/10.1152/ajplung.1992.263.3.L384.

Maston, Levi D, David T Jones, Wieslawa Giermakowska, Thomas C Resta, and Laura Gonzalez Bosc. 2017. “Interleukin-6 Trans-Signaling Contributes to Chronic Hypoxia-Induced Pulmonary Hypertension.” *The FASEB Journal* 31 (1 Supplement): 1016.20-1016.20. http://www.fasebj.org/content/31/1_Supplement/1016.20.abstract.

McCullagh, Brian N, Christine M Costello, Lili Li, Caroline O’Connell, Mary Codd, Allan Lawrie, Allison Morton, et al. 2015. “Elevated Plasma CXCL12alpha Is Associated with a Poorer Prognosis in Pulmonary Arterial Hypertension.” *PloS One* 10 (4): e0123709. https://doi.org/10.1371/journal.pone.0123709.

McGoon, Michael D, Raymond L Benza, Pilar Escribano-Subias, Xin Jiang, Dave P Miller, Andrew J Peacock, Joanna Pepke-Zaba, et al. 2013. “Pulmonary Arterial Hypertension: Epidemiology and Registries.” *Journal of the American College of*

*Cardiology* 62 (25 Suppl): D51-9. https://doi.org/10.1016/j.jacc.2013.10.023.

McMillen, Marvin and Sumpio Bauer . 1995. “Endothelins: Polyfunctional Cytokines.” *Journal of the American College of Surgeons* 180 (5): 621–37. https://pubmed.ncbi.nlm.nih.gov/7749544/

Montani, David, Sven Gunther, Peter Dorfmuller, Frederic Perros, Barbara Girerd, Gilles Garcia, Xavier Jais, et al. 2013. “Pulmonary Arterial Hypertension.” *Orphanet Journal of Rare Diseases* 8 (July): 97. https://doi.org/10.1186/1750-1172-8-97.

Moreno-Navarrete, Jose Maria, Francisco Ortega, Marta Serrano, Rafael Perez-Perez, Monica Sabater, Wifredo Ricart, Francisco Tinahones, Belen Peral, and Jose Manuel Fernandez-Real. 2011. “Decreased STAMP2 Expression in Association with Visceral Adipose Tissue Dysfunction.” *The Journal of Clinical Endocrinology and Metabolism* 96 (11): E1816-25. https://doi.org/10.1210/jc.2011-0310.

Murali, Srinivas, and Raymond L Benza. 2012. “Pulmonary Hypertension.” *Heart Failure Clinics*. United States. https://doi.org/10.1016/j.hfc.2012.05.001.

Naeije, Robert, and Kelly Chin. 2019. “Differentiating Precapillary From Postcapillary Pulmonary Hypertension.” *Circulation* 140 (9): 712–14. https://doi.org/10.1161/CIRCULATIONAHA.119.040295.

Nanfang, Li, Guo Yanying, Wang Hongmei, Yan Zhitao, Zhang Juhong, Zhou Ling, and Luo Wenli. 2010. “Variations of Six Transmembrane Epithelial Antigen of Prostate 4 (STEAP4) Gene Are Associated with Metabolic Syndrome in a Female Uygur General Population.” *Archives of Medical Research* 41 (6): 449–56. https://doi.org/10.1016/j.arcmed.2010.08.006.

Niu, Jianli, and Pappachan E Kolattukudy. 2009. “Role of MCP-1 in Cardiovascular Disease: Molecular Mechanisms and Clinical Implications.” *Clinical Science (London, England : 1979)* 117 (3): 95–109. https://doi.org/10.1042/CS20080581.

Oh, Yoo Jin, Hye Young Kim, Mi Hwa Lee, Sung Hwan Suh, Yongmun Choi, Tae-Gyu Nam, Woo Young Kwon, Sang Yeob Lee, and Young Hyun Yoo. 2018. “Cilostazol Improves HFD-Induced Hepatic Steatosis by Upregulating Hepatic STAMP2 Expression through AMPK.” *Molecular Pharmacology* 94 (6): 1401–11. https://doi.org/10.1124/mol.118.113217.

Ohgami, Robert, Dean R Campagna, Alice McDonald, and Mark D Fleming. 2006. “The Steap Proteins Are Metalloreductases.” *Blood* 108 (4): 1388–94. https://doi.org/10.1182/blood-2006-02-003681.

Örem, Cihan. 2017. “Epidemiology of Pulmonary Hypertension in the Elderly.” Edited by Ebru Ozpelit. *Journal of Geriatric Cardiology : JGC* 14 (1): 11–16. https://doi.org/10.11909/j.issn.1671-5411.2017.01.001.

Park, Ji-Eun, Yeon Jae Jeong, Hye Young Kim, Young Hyun Yoo, Kwang Sik Lee, Won Tae Yang, Doh Hoon Kim, and Jong-Min Kim. 2020. “Hepatic Steatosis Alleviated in Diabetic Mice upon Dietary Exposure to Fibroin via Transgenic

Rice: Potential STAMP2 Involvement in Hepatocytes." *Development & Reproduction* 24 (3): 231—239. https://doi.org/10.12717/dr.2020.24.3.231.

Park, John, Alexander R Lyon, Dongmin Shao, Lauren R Hector, Hua Xu, Peter O'Gara, Liao Pinhu, Rachel C Chambers, S John Wort, and Mark J D Griffiths. 2014. "Pulmonary Venous Hypertension and Mechanical Strain Stimulate Monocyte Chemoattractant Protein-1 Release and Structural Remodelling of the Lung in Human and Rodent Chronic Heart Failure Models." *Thorax* 69 (12): 1120–27. https://doi.org/10.1136/thoraxjnl-2013-204190.

Patel, Pavankumar, and Nicola Abate. 2013. "Body Fat Distribution and Insulin Resistance." *Nutrients* 5 (6): 2019–27. https://doi.org/10.3390/nu5062019.

Phang James M. 1985. "The Regulatory Functions of Proline and Pyrroline-5-Carboxylic Acid." *Current Topics in Cellular Regulation* 25: 91–132. https://doi.org/10.1016/B978-0-12-152825-6.50008-4.

Preis, Sarah R, Joseph M Massaro, Sander J Robins, Udo Hoffmann, Ramachandran S Vasan, Thomas Irlbeck, James B Meigs, et al. 2010. "Abdominal Subcutaneous and Visceral Adipose Tissue and Insulin Resistance in the Framingham Heart Study." *Obesity (Silver Spring, Md.)* 18 (11): 2191–98. https://doi.org/10.1038/oby.2010.59.

Pugliese, Steven C, Sushil Kumar, William J Janssen, Brian B Graham, Maria G Frid, Suzette R Riddle, Karim C El Kasmi, and Kurt R Stenmark. 2017. "A Time- and Compartment-Specific Activation of Lung Macrophages in Hypoxic Pulmonary Hypertension." *Journal of Immunology (Baltimore, Md. : 1950)* 198 (12): 4802–12. https://doi.org/10.4049/jimmunol.1601692.

Pullamsetti, Soni Savai, Ralph Schermuly, Ardeschir Ghofrani, Norbert Weissmann, Friedrich Grimminger, and Werner Seeger. 2014. "Novel and Emerging Therapies for Pulmonary Hypertension." *American Journal of Respiratory and Critical Care Medicine* 189 (4): 394–400. https://doi.org/10.1164/rccm.201308-1543PP.

Rabinovitch, Marlene. 2012. "Molecular Pathogenesis of Pulmonary Arterial Hypertension." *The Journal of Clinical Investigation* 122 (12): 4306–13. https://doi.org/10.1172/JCI60658.

Rabinovitch, Marlene, Christophe Guignabert, Marc Humbert, and Mark R Nicolls. 2014. "Inflammation and Immunity in the Pathogenesis of Pulmonary Arterial Hypertension." *Circulation Research* 115 (1): 165–75. https://doi.org/10.1161/CIRCRESAHA.113.301141.

Rosenkranz, Stephan. 2015. "Pulmonary Hypertension 2015: Current Definitions, Terminology, and Novel Treatment Options." *Clinical Research in Cardiology : Official Journal of the German Cardiac Society* 104 (3): 197–207. https://doi.org/10.1007/s00392-014-0765-4.

Rosenkranz, Stephan, and Ioana R Preston. 2015. "Right Heart Catheterisation: Best Practice and Pitfalls in Pulmonary Hypertension." *European Respiratory Review* 24 (138): 642 LP – 652. https://doi.org/10.1183/16000617.0062-2015.

Rubin, Lewis. 1997. “Primary Pulmonary Hypertension.” *The New England Journal of Medicine* 336 (2): 111–17. https://doi.org/10.1056/NEJM199701093360207.

Salvo, Thomas G di, Kai-Chien Yang, Evan Brittain, Tarek Absi, Simon Maltais, and Anna Hemnes. 2015. “Right Ventricular Myocardial Biomarkers in Human Heart Failure.” *Journal of Cardiac Failure* 21 (5): 398–411. https://doi.org/10.1016/j.cardfail.2015.02.005.

Sánchez-Martín, Lorena, Ana Estecha, Rafael Samaniego, Silvia Sánchez-Ramón, Miguel Ángel Vega, and Paloma Sánchez-Mateos. 2011. “The Chemokine CXCL12 Regulates Monocyte-Macrophage Differentiation and RUNX3 Expression.” *Blood* 117 (1): 88–97. https://doi.org/10.1182/blood-2009-12-258186.

Sanchez, Martinez, Munoz, Benedito, Garcia-Sacristan, Hernandez, and Prieto. 2014. “Endothelin-1 Contributes to Endothelial Dysfunction and Enhanced Vasoconstriction through Augmented Superoxide Production in Penile Arteries from Insulin-Resistant Obese Rats: Role of ET(A) and ET(B) Receptors.” *British Journal of Pharmacology* 171 (24): 5682–95. https://doi.org/10.1111/bph.12870.

Savale, Laurent, Ly Tu, Dominique Rideau, Mohamed Izziki, Bernard Maitre, Serge Adnot, and Saadia Eddahibi. 2009. “Impact of Interleukin-6 on Hypoxia-Induced Pulmonary Hypertension and Lung Inflammation in Mice.” *Respiratory Research* 10 (January): 6. https://doi.org/10.1186/1465-9921-10-6.

Scarl, Rachel T, C Martin Lawrence, Hannah M Gordon, and Craig S Nunemaker. 2017. “STEAP4: Its Emerging Role in Metabolism and Homeostasis of Cellular Iron and Copper.” *The Journal of Endocrinology* 234 (3): R123–34. https://doi.org/10.1530/JOE-16-0594.

Schiffrin, Ernesto L. 1995. “Endothelin: Potential Role in Hypertension and Vascular Hypertrophy. ” *Hypertension (Dallas, Tex. : 1979)* 25 (6): 1135–43. https://doi.org/10.1161/01.HYP.25.6.1135.

Schiffrin, Ernesto L. 2001. “Role of Endothelin-1 in Hypertension and Vascular Disease.” *American Journal of Hypertension* 14 (6 Pt 2): 83S-89S. https://doi.org/10.1016/S0895-7061(01)02074-X.

Schlosser, Kenny, Mohamad Taha, Yupu Deng, Baohua Jiang, Lauralyn A McIntyre, Shirley Hj Mei, and Duncan J Stewart. 2017. “Lack of Elevation in Plasma Levels of Pro-Inflammatory Cytokines in Common Rodent Models of Pulmonary Arterial Hypertension: Questions of Construct Validity for Human Patients.” *Pulmonary Circulation* 7 (2): 476–85. https://doi.org/10.1177/2045893217705878.

Shi, Jia, Yi Yang, Anying Cheng, Gang Xu, and Fan He. 2020. “Metabolism of Vascular Smooth Muscle Cells in Vascular Diseases.” *American Journal of Physiology. Heart and Circulatory Physiology* 319 (3): H613–31. https://doi.org/10.1152/ajpheart.00220.2020.

Sikkeland, Jorgen, Torstein Lindstad, Hatice Zeynep Nenseth, Xavier Dezitter, Su Qu, Ridhwan M Muhumed, Meric Erikci Ertunc, Margaret F Gregor, and Fahri Saatcioglu. 2019. “Inflammation and ER Stress Differentially Regulate STAMP2

Expression and Localization in Adipocytes." *Metabolism: Clinical and Experimental* 93 (April): 75–85. https://doi.org/10.1016/j.metabol.2019.01.014.

Sikkeland, Jorgen, and Fahri Saatcioglu. 2013. "Differential Expression and Function of Stamp Family Proteins in Adipocyte Differentiation." *PloS One* 8 (7): e68249. https://doi.org/10.1371/journal.pone.0068249.

Sikkeland, Jorgen, Xia Sheng, Yang Jin, and Fahri Saatcioglu. 2016. "STAMPing at the Crossroads of Normal Physiology and Disease States." *Molecular and Cellular Endocrinology* 425 (April): 26–36. https://doi.org/10.1016/j.mce.2016.02.013.

Sikkeland, Jorgen, Liv I Bjoner, Christen P Dahl, Thor Ueland, Arne K Andreassen, Einar Gude, Thor Edvardsen, Torbjorn Holm, et al. 2012. "Increased Levels of Inflammatory Cytokines and Endothelin-1 in Alveolar Macrophages from Patients with Chronic Heart Failure." *PloS One* 7 (5): e36815. https://doi.org/10.1371/journal.pone.0036815.

Simonneau, Gerald, Michael A Gatzoulis, Ian Adatia, David Celermajer, Chris Denton, Ardeschir Ghofrani, Miguel Angel Gomez Sanchez, et al. 2014. "[Updated clinical classification of pulmonary hypertension]." *Turk Kardiyoloji Dernegi arsivi : Turk Kardiyoloji Derneginin yayin organidir* 42 Suppl 1 (October): 45–54.

Simonneau, Gerald, David Montani, David S Celermajer, Christopher P Denton, Michael A Gatzoulis, Michael Krowka, Paul G Williams, and Rogerio Souza. 2019. "Haemodynamic Definitions and Updated Clinical Classification of Pulmonary Hypertension." *The European Respiratory Journal* 53 (1): 1801913. https://doi.org/10.1183/13993003.01913-2018.

Singh Sanjiv, Dixit Anshita, and velyuthem Ravichandiran. 2021. "MCP-1: Function, Regulation, and Involvement in Disease." *International Immunopharmacology* 101 (Pt B): 107598. https://doi.org/10.1016/j.intimp.2021.107598.

Steiner, Kathryn, Olga L Syrkina, Narasaish Kolliputi, Eugene J Mark, Charles A Hales, and Aaron B Waxman. 2009. "Interleukin-6 Overexpression Induces Pulmonary Hypertension." *Circulation Research* 104 (2): 236–44, 28p following 244. https://doi.org/10.1161/CIRCRESAHA.108.182014.

Shuichi, Hatano, and Toma Strasser. 1975. "Primary Pulmonary Hypertension : Report on a WHO Meeting, Geneva, 15-17 October 1973." In . Geneva; [Albany, N.Y.]: World Health Organization ; [Distributed by Q Corp.].

Sylvester Jimmie, Larissa A Shimoda, Philip I Aaronson, and Jeremy P T Ward. 2012. "Hypoxic Pulmonary Vasoconstriction." *Physiological Reviews* 92 (1): 367–520. https://doi.org/10.1152/physrev.00041.2010.

Toshner, Mark, and Alex Rothman. 2020. "IL-6 in Pulmonary Hypertension: Why Novel Is Not Always Best." *The European Respiratory Journal*. England. https://doi.org/10.1183/13993003.00314-2020.

Vergadi, Eleni, Mun Seog Chang, Changjin Lee, Olin D Liang, Xianlan Liu, Angeles

Fernandez-Gonzalez, S Alex Mitsialis, and Stella Kourembanas. 2011. “Early Macrophage Recruitment and Alternative Activation Are Critical for the Later Development of Hypoxia-Induced Pulmonary Hypertension.” *Circulation* 123 (18): 1986–95. https://doi.org/10.1161/CIRCULATIONAHA.110.978627.

Viray, Michael C, Eric L Bonno, Nicholas D Gabrielle, Bradley A Maron, Jessica Atkins, Nicholas S Amoroso, Valerian L C Fernandes, et al. 2020. “Role of Pulmonary Artery Wedge Pressure Saturation During Right Heart Catheterization: A Prospective Study.” *Circulation. Heart Failure*. https://doi.org/10.1161/CIRCHEARTFAILURE.120.007981.

Voelkel, Norbert and Tuder Rubin. 2000. “Hypoxia-Induced Pulmonary Vascular Remodeling: A Model for What Human Disease?” *The Journal of Clinical Investigation* 106 (6): 733–38. https://doi.org/10.1172/JCI11144.

Wagenvoort, Cornelius Adrian. 1970. “The Pathology of Primary Pulmonary Hypertension.” *The Journal of Pathology* 101 (4): Pi. https://doi.org/10.1002/path.1711010408.

Waki, Hironori, and Peter Tontonoz. 2007. “STAMPing out Inflammation.” *Cell* 129 (3): 451–52. https://doi.org/10.1016/j.cell.2007.04.022.

Wang, Feng, Lu Han, Ran-Ran Qin, Yao-Yuan Zhang, Di Wang, Zhi-Hao Wang, Meng-Xiong Tang, Yun Zhang, Ming Zhong, and Wei Zhang. 2017. “Overexpressing STAMP2 Attenuates Adipose Tissue Angiogenesis and Insulin Resistance in Diabetic ApoE(-/-) /LDLR(-/-) Mouse via a PPARgamma/CD36 Pathway.” *Journal of Cellular and Molecular Medicine* 21 (12): 3298–3308. https://doi.org/10.1111/jcmm.13233.

Wang, Jia, Lu Han, Zhi-hao Wang, Wen-yuan Ding, Yuan-yuan Shang, Meng-xiong Tang, Wen-bo Li, Yun Zhang, Wei Zhang, and Ming Zhong. 2014. “Overexpression of STAMP2 Suppresses Atherosclerosis and Stabilizes Plaques in Diabetic Mice.” *Journal of Cellular and Molecular Medicine* 18 (4): 735–48. https://doi.org/10.1111/jcmm.12222.

Wang, Zhi-Hao, Wei Zhang, Hui-Ping Gong, Zhong-Xiu Guo, Jing Zhao, Yuan-Yuan Shang, Jin-Bo Feng, Yun Zhang, and Ming Zhong. 2010. “Expression of STAMP2 in Monocytes Associates with Cardiovascular Alterations.” *European Journal of Clinical Investigation* 40 (6): 490–96. https://doi.org/10.1111/j.1365-2362.2010.02288.x.

Warkentin, Mamat, Sordel-Klippert, Wicke,Thauer, Iwata, Iwata, Ermler, and Shima. 2001. “Structures of F420H2:NADP+ Oxidoreductase with and without Its Substrates Bound.” *The EMBO Journal* 20 (23): 6561–69. https://doi.org/10.1093/emboj/20.23.6561.

Wei, Liuping, Bo Zhang, Weiwei Cao, Hao Xing, Xiufeng Yu, and Daling Zhu. 2015. “Inhibition of CXCL12/CXCR4 Suppresses Pulmonary Arterial Smooth Muscle Cell Proliferation and Cell Cycle Progression via PI3K/Akt Pathway under Hypoxia.” *Journal of Receptor and Signal Transduction Research* 35 (4): 329–39. https://doi.org/10.3109/10799893.2014.984308.

Wellen, Kathryn E, Raquel Fucho, Margaret F Gregor, Masato Furuhashi, Carlos Morgan, Torstein Lindstad, Eric Vaillancourt, Cem Z Gorgun, Fahri Saatcioglu, and Gokhan S Hotamisligil. 2007. “Coordinated Regulation of Nutrient and Inflammatory Responses by STAMP2 Is Essential for Metabolic Homeostasis.” *Cell* 129 (3): 537–48. https://doi.org/10.1016/j.cell.2007.02.049.

Yang, Tao, Zhen-Nan Li, Guo Chen, Qing Gu, Xin-Hai Ni, Zhi-Hui Zhao, Jue Ye, et al. 2014. “Increased Levels of Plasma CXC-Chemokine Ligand 10, 12 and 16 Are Associated with Right Ventricular Function in Patients with Idiopathic Pulmonary Arterial Hypertension.” *Heart & Lung : The Journal of Critical Care* 43 (4): 322–27. https://doi.org/10.1016/j.hrtlng.2014.04.016.

Yoo, Seong Keun, JaeHun Cheong, and Hye Young Kim. 2014. “STAMPing into Mitochondria.” *International Journal of Biological Sciences* 10 (3): 321–26. https://doi.org/10.7150/ijbs.8456.

Zeller, John L, Denise M Goodman, Cassio Lynm, and Edward H Livingston. 2012. “JAMA Patient Page. Pulmonary Hypertension.” *JAMA*. United States. https://doi.org/10.1001/2012.jama.11701.

# 9. Supplementary

# 9 Supplemmentary

## 9.1 Acknowledgment

I owe gratitude to Prof. Dr. Stephan Rosenkranz for providing me with a platform to pursue my doctoral degree, which has been a lifelong dream. I also owe thanks to Dr. Henrik tenFreyhaus for supervising my research work. I am in gratitude of my lab fellows for their scientific input and co-operation along with a welcoming environment which was highly appreciated being an international student. My senior lab fellow Eva Berghausen deserves a special mention here since she helped me with conducting hemodynamic measurements and the rather difficult and technical tasks of catheter insertion and pressure curve recording. I also want to acknowledge the help extended by Dr. Stephan Baldus's lab by letting me share their equipment such as hypoxia chamber and incubators without which most of my crucial experiments would not have been possible. I would also like to extend my very special and profound thanks to Dr. Debora Grosskopf-Kroiher for always lending a listening ear and providing me with the much needed emotional support in low times.

This journey would never have been possible without my family and friends. I am grateful to the unconditional support and help extended by my friend Aaradhita, also a fellow PhD scholar at ZMMK. I am indebted to the love and belief showed by my Parents Ikram and Shagufta, throughout my life and this PhD journey. I can never thank them enough for their continuous prayers and wishes. I am most thankful to my daughter Areena for making me smile through the hardest of times. Last but not the least I would like to mention that I am most thankful to Allah almighty for bringing this experience in my life and making me able to accomplish this amazing endeavour which shall mark a new path in my life.

## 9.2 **Declaration**

Ich versichere, dass ich die von mir vorgelegte Dissertation selbstständig angefertigt, die benutzten Quellen und Hilfsmittel vollständig angegeben und die Stellen der Arbeit -einschließlich Tabellen, Karten und Abbildungen -, die anderen Werken im Wortlaut oder dem Sinn nach entnommen sind, in jedem Einzelfall als Entlehnung kenntlich gemacht habe; dass diese Dissertation noch keiner anderen Fakultät oder Universität zur Prüfung vorgelegen hat; dass sie - abgesehen von unten angegebenen Teilpublikationen - noch nicht veröffentlicht worden ist sowie, dass ich eine solche Veröffentlichung vor Abschluss des Promotionsverfahrens nicht vornehmen werde. Die Bestimmungen dieser Promotionsordnung sind mir bekannt. Die von mir vorgelegte Dissertation ist von Prof. Dr. Stephan Rosenkranz betreut worden.

Ich versichere, dass ich alle Angaben wahrheitsgemäß nach bestem Wissen und Gewissen gemacht habe und verpflichte mich, jedmögliche, die obigen Angaben betreffenden Veränderungen, dem Promotionsausschuss unverzüglich mitzuteilen.

Datum: 08-03-2024 Unterschrift: Mehreen Batool